



BLOCK EROSION OF UNLINED ROCK SPILLWAY CANALS

David Saiang

Musa Adebayo Idris

Erling Nordlund

Cover photo by David Saiang.
Place: Case Study I Spillway Canal.

Block erosion of unlined rock spillway canals

Blockerosion av utskov i berg

David Saiang, Luleå University of Technology

Musa Adebayo Idris, Luleå University of Technology

Erling Nordlund, Luleå University of Technology

PREFACE

This block erosion study focuses on hydropower dam spillway canals in Sweden and their rock mass or geological conditions. Some observations may not be relevant to observations in the other places due to the differences in geological factors. However, the Swedish experience are comparable to the arctic region countries, that have similar geological conditions.

Another factor is the time history of the Swedish hydropower dams. Many of these dams are approaching either 100 years or have exceeded 100 years. During this long period design methodologies have evolved with better understanding of hydrological and geological conditions and even more so, the adaption of risk-consequence based design methodologies. Therefore, these dams face unique challenges not only related to geological conditions, but also the need to improve them to meet the current standards in dam safety that did not exist when they were constructed and commissioned.

This report does not dwell on the design issues of the dams, but it focuses on rock conditions of the spillway canals. Many of the Swedish hydropower dams have and are seeing erosion in the spillway channels, which in the long term will affect the safety of these dams. The report focuses on the geological conditions and mechanisms that promote block erosion. The term “block erosion” is used here because the majority (if not all) of the Swedish hydro-power dams are constructed on hard rock masses. And therefore, the occurrence of erosion involves rock blocks.

Although there are well over 1000 hydro-power dams in Sweden this field inventory or field investigation only involved two hydropower dams. Both hydropower dams are among the largest in Sweden. The geological conditions of these two dams are uniquely different and thus provide a contrasting observation of block erosion and the mechanisms involved. It is observed that majority of the dams in Sweden may fall within the characteristics of these two dams with respect to block erosion or scouring of the discharge canals and tunnels.

The research was conducted at Luleå University of Technology by the Mining and Rock Engineering research group at the Division of Mining and Geotechnology Engineering. The research was led by David Saiang and assisted by Idris Musa, Erling Nordlund and Jonny Sjöberg. The research project was supported by a reference group consisted of Anders Isander (Uniper), Peter Viklander (Vattenfall), Eva Hakami (Geosigma), Fredrik Johansson (KTH) and Per Tengborg (BeFo).

Financial support was provided by BeFo and Energiforsk.

Stockholm, 2022

Per Tengborg

FÖRORD

Denna studie om blockerosion fokuserar på utskov kring vattenkraftsdammar i Sverige och den bergmassa och de geologiska förhållanden som finns. Vissa observationer kan vara irrelevanta i områden med andra geologiska förhållanden. Dock kan de svenska observationerna jämföras med andra länder inom den arktiska regionen med liknande geologiska förhållanden.

En annan faktor är åldern av svenska vattenkraftsdammar. Många dammar närmar sig 100 år eller är ännu äldre. Under det senaste seklet har designmetodik utvecklats med en bättre förståelse för hydrauliska och geologiska förhållanden, speciellt också anpassat med riskmedveten designmetodik.

Denna rapport tar inte upp frågeställningar kring design, utan fokuserar på utskovens bergförhållanden. Många av Sveriges vattenkraftsdammar har upplevt och upplever erosion i utskoven, som i längden utgör en risk för dessa dammar. Rapporten fokuserar på geologiska förhållanden och mekanismer som bidrar till blockerosion. Termen "block erosion" används eftersom att majoriteten, om inte alla, av de svenska vattenkraftsdammarna är grundlagda på hårt berg. Därför medverkar bergblock i erosionsprocessen på utskov och utskovskanaler.

Trots att det finns över 100 vattenkraftsdammar i Sverige, involverar denna utredning endast två vattenkraftsdammar. De båda dammarna är bland de största i Sverige. De geologiska förhållandena vid de två dammarna är unika och ger därför två helt olika observationer av blockerosion och involverande mekanismer. Observera att majoriteten av alla dammar i Sverige kan falla mellan dess två dammars egenskaper när det gäller blockerosion eller yterosion av utskovskanaler och tunnlar.

Forskningen utfördes på Luleå Tekniska Universitet av Gruv- och berganläggningstekniska forskningsgruppen på Avdelningen för geoteknologi. Forskningsprojektet utfördes av projektledare David Saiang och assisterades av Idris Musa, Erling Nordlund och Jonny Sjöberg. En referensgrupp har varit knuten till forskningsprojektet och bestod av Anders Isander (Uniper), Peter Viklander (Vattenfall), Eva Hakami (Geosigma), Fredrik Johansson (KTH) och Per Tengborg (BeFo).

Forskningsprojektet finansierades av Stiftelsen Bergteknisk Forskning (BeFo) och Energiforsk.

Stockholm, 2022

Per Tengborg

SUMMARY

Canals and tunnels in hydropower plants must be able to receive high shock-like flows without damaging either the dam or the rock foundation. Although the canals often consist of rock, erosion can occur when water is released. The natural riverbeds and lakes in Sweden usually run along large faults and other zones of weakness in the rock. This is because the water could more easily erode its way along these weakness zones. Spillways of hydropower dams are generally unlined thereby exposing the bedrock to erosion during floods.

This study focuses on block erosion mechanisms and characteristics in unlined spillway canals that comprises hard rock mass systems. Two hydropower dam spillway canals were investigated as case studies; identified as Dam 1 and Dam 2. The spillway canals of these two dams have uniquely different bed rock characteristics. At Dam 1 the rock mass is very blocky with visually estimated GSI classification in the range of 50 to 70, while Dam 2 is composed of massive rock mass with visually assessed GSI classification of 70 to 90.

The erosion characteristics observed in these two spillway canals are uniquely different. The rock mass is obviously the principal factor contributing to these observations. However, there are also other factors, namely the hydraulic factors, as well as the geometrical factors of the canals. In this report these factors have been described in detail.

Three main mechanisms of block erosion were observed, (i) removal or plucking of rock blocks, (ii) fracturing of intact rock blocks and (iii) abrasion. At Dam 1 spillway canal all three mechanisms were observed to be significantly evident. At Dam 2, abrasion is the dominant mechanism of erosion. Hydraulic parameters, water pressure and velocity, affect the criticality of the erosion.

Numerical simulations of the spillway canals were conducted using 3DEC. These simulations show that block displacements greater than 10 m are experienced within 1 to 2 minutes of flow. This observation is consistent with observations made during an actual discharge from a dam. Numerical simulations indicated that blocks with sizes less than 1 m³ would easily be plucked and transported downstream. If they are intact and with unfavourable geometry, they can be easily fractured by the spill water loads. Field investigations support these observations.

Remedial measures would first require classification of a spillway canal into erosion domains based on erosion vulnerability. For example, the upstream sections of the channels are typically vulnerable to high intensity erosion. Hydraulic jumps, plunge pools, stilling basins, etc, have been typically used to break up the energy before the water flows downstream. However, erosion still occurs further down since the energy is still very large. Reinforcing the bedrock with artificial supports such as rock bolting, widening and levelling of canals, diverting the flow to less vulnerable areas of the canal, etc, have been some means to reduce block erosion.

This study concludes that, remedial measures must start with identifying the mechanisms of block erosion, three of which have been described above. Domaining of the channels into erosion critically domains may also assist in monitoring and application of remedial measures. Empirical methods, such as Pells (2016) can be applied in each domain to identify their erosion potential.

This study also concludes that the hydraulic pressure and displacements that occur around a rock block needs to be further investigated, either by field measurements in a spillway or by using physical models. In this way, it will be possible to better understand the conditions around blocks in a spillway and erosion mechanisms during a discharge.

Note that this report is also available in .pdf format on Stiftelsen Bergteknisk Forskning's website. The report can easily be opened in Acrobat Reader and images can be enlarged. <https://www.befoonline.org> - Publikationer, BeFo report No. 230.

Keywords: Block erosion, scouring, spillway channels/canals, hydropower dams

SAMMANFATTNING

Kanaler och tunnlar i vattenkraftverk måste hålla för plötsliga och kraftiga flöden utan skador på dammen eller berggrunden. Trots att utskoven ofta består av berg kan erosion förekomma när vatten släpps på. Floder och sjöar i Sverige sträcker sig ofta längs stora förkastningar och svaghetszoner i berggrunden. Det beror på att vattnet enklast kunnat erodera sin väg längs dessa svaga områden i berggrunden. Vattenkraftsdammarnas utskov utgörs normalt av blottat berg, d v s de är inte ingjutna vilket utsätter berggrunden för erosion när vatten strömmar över bergytan.

Den här studien fokuserar på mekanismer för bergerosion och egenskaper i oingjutna utskov i hårt berg. Två utskov har studerats genom fallstudier, identifierade som Dam 1 och Dam 2. De två dammarnas utskovskanaler har helt olika karaktär på bergmassan. Vid Dam 1 är bergmassan mycket blockig med en visuellt bedömd GSI-klassificering mellan 50 och 70, medan Dam 2 består av massiv bergmassa med en visuellt bedömd GSI-klassificering mellan 70 och 90.

Erosionen som observerats i dessa utskov är av helt olika typ. Bergmassan är uppenbarligen den huvudsakliga bidragande faktorn till dessa observationer. Det finns dock andra faktorer, nämligen de hydrauliska faktorerna, såväl som de geometriska faktorerna av utskoven. I denna rapport har dessa faktorer beskrivits i detalj.

Tre huvudsakliga mekanismer av blockerosion observerades, (i) borttagning av stenblock, (ii) sönderbrytning av intakta stenblock och (iii) nedslipning. Vid Dam 1 utskov visade observationer att alla tre mekanismer var betydelsefulla. Vid Dam 2 är nedslipning den dominanta mekanismen för erosion. Hydrauliska parametrar, vattentryck och hastighet, påverkar hur allvarlig erosion är.

Numerisk modellering av utskoven gjordes i 3DEC. Modelleringen visar en blockförflyttning större än 10 m inom 1 till 2 minuters flöde. Resultaten överensstämmer med observationer gjorda under en avbördning från ett utskov i en damm. Numerisk modellering indikerar att bergblock av storlek mindre än 1 m³ lätt kan lossgöras och transporteras nedströms. Om blocken är hela och har en ogynnsam geometrisk form så kan de lätt brytas sönder av krafterna från vattenflödet. Fältstudier stödjer dessa observationer.

Avhjälpande åtgärder kräver först en klassificering av erosion i utskovskanalen baserat på känslighet för erosion. Exempelvis är områden uppström i kanalerna typiskt sårbara för erosion. Hydrauliska hopp, ”plunge pools”, bassänger för att bromsa vattenhastigheten, etc, har använts för att bryta ner energi innan vattnet rör sig nedström. Trots detta sker erosion då energin fortfarande är stor. Förstärkning av berggrund med artificiell support såsom bergbultning, breddande och utjämnande av kanaler, avledande av flödet till mindre utsatta områden i kanalen, etc, är några åtgärder för att reducera blockerosion.

Slutsatsen av denna studie är att avhjälpande åtgärder måste börja med identifieringen av mekanismerna för blockerosion, varav tre har beskrivits ovan. Uppdelning av kanaler i domäner avseende erosionskänslighet kan också underlätta övervakning och tillämpning av lämpliga åtgärder. Empiriska metoder såsom Pells (2016) kan appliceras i varje domän för att identifiera dess erosionspotential.

En ytterligare slutsats av denna studie är att hydrauliskt tryck och förflyttningar som sker kring ett bergblock behöver studeras ytterligare, antingen via fältmätning i ett utskov eller fysisk modell. Endast då möjliggörs förståelsen av förhållanden och erosionsmekanismer kring ett bergblock vid tömning.

Notera att denna rapport även finns tillgänglig som pdf på Stiftelsen Bergteknisk Forsknings hemsida. Rapporten kan enkelt öppnas i Acrobat Reader och där kan bilder förstoras. <https://www.befoonline.org> - Publikationer, BeFo rapport nr 230.

Nyckelord: Blockerosion, yterrosion, utskov, vattenkraftsdamm.

CONTENTS

PREFACE	i
FÖRORD	iii
SUMMARY	v
SAMMANFATTNING.....	vii
1. INTRODUCTION.....	1
1.1 Background.....	1
1.2 Objectives and scope	2
1.3 Methodology.....	2
1.4 Limitations	3
2. LITERATURE.....	5
2.1 Mechanism of rock erosion.....	5
2.2 Factors affecting block erosion in spillway canals	8
2.3 Methods for erosion assessment	10
3. FIELD INVESTIGATIONS.....	21
3.1 Dam 1.....	22
3.2 Dam 2.....	34
3.3 Laboratory tests.....	50
4. EMPIRICAL ANALYSES	51
4.1 Hydraulic Parameters	51
4.2 Rock mass erodibility	55
5. NUMERICAL ANALYSES	61
5.1 Modelling approach	61
5.2 Rock mass inputs	61
5.3 In-situ stresses	63
5.4 Water pressure	63
5.5 Shear velocity.....	64
5.6 Modelling approach	65

5.7	Assumptions	66
5.8	3DEC Modelling.....	66
5.9	Single block models	67
5.10	Dam 1 spillway model.....	81
5.11	Dam 2 spillway model.....	89
6.	Discussions and conclusions	97
6.1	Literature.....	97
6.2	Field investigations.....	97
6.3	Empirical Analyses	98
6.4	Numerical modelling	99
7.	Recommendations.....	101
7.1	Further study	101
7.2	Remedial measures	101
7.3	In-situ measurement of pore pressures and block displacements.....	103
7.4	Physical model to study block erosion	104
7.5	Investigation of fracture apertures.....	104
8.	REFERENCES	109

1. INTRODUCTION

1.1 Background

Canals and tunnels in hydropower plants must be able to receive high shock-like flows without damaging either the dam or the rock foundation. Although the canals often consist of rocks, erosion can occur when water is released. The natural riverbeds and lakes in Sweden usually run along large faults and other zones of weakness in the rock. This is because the water could more easily erode its way along these weakness zones. Spillways of hydropower dams are generally unlined thereby exposing the bedrock to erosion during floods.

Glacial induced slabbing in rocks is a very common phenomenon in Sweden and therefore large parts of the rock mass, including many rock channels, contain shallow sub-horizontal cracks. This slabbing or banking resulted from tensile fracturing due to stress release during isostatic uplift after glaciation. Although the phenomenon appears to be very common in Sweden irrespective of rock types, it is very pronounced in igneous hard rocks (Bauer and Andersson 2020).

Block erosion is a type of erosion that involves dislodging and transportation of rock blocks, where water pressure and water flow loosen entire rock boulders and blocks. This erosion does not occur gradually and continuously but rather as sudden incidents when large blocks are moved (Woodward 1992). The blocks can then be transported with the water along the channel extent and end up in unsuitable places. For example, blocks can lie against existing articulated walls and contribute to their overwashing. This can lead to soil erosion behind the walls. The loose blocks can also cause concrete damage and change the flow in the channel. In the worst case, the erosion can go upstream and thus risk dam failure.

As the current climate situation appears to give an increased amount of precipitation in Sweden, new guidelines on design flood calculations for flows have been established by The Swedish Committee for Design Flood Determination (Flödeskommitten 2007). This means that most of today's dams must be dimensioned to withstand higher flows than in the past. A larger flow also means that the spillways are exposed to more water. In many of the larger dams' outflow channels, block erosion is observed in the spillways. The spillways have generally not been long-lasting, but damage to blocks that have been moved and changes in the channel's geometry have been detected.

The same type of problem arises in the tunnels that are part of a hydropower plant and that have high flows of water. As a result of water pressure that can be pulsed, blocks can be detached from the walls of the tunnel. The more uneven the surface of the tunnel, the more turbulent the water flow can become. This can contribute to local pressure differences and that, blocks are fractured or forced loose (in the crack) from the tunnel boundary.

The problem of rock erosion has also attracted international attention, but there are relatively few extensive studies done. Most are based on empirical relationships, while the underlying mechanisms have not been studied to the same extent. To quote Richard Goodman (Professor Emeritus at Berkeley): "It is one of the remaining great problems in rock mechanics"

The Fluid Mechanics Research Group at Luleå University of Technology has for a number of years conducted research on the effect of rock surface roughness on the flow in hydropower tunnels (Andersson et al. 2016; Andersson et al. 2014a; Andersson et al. 2014b; Andersson et al. 2012; Andersson 2013). These researchers have focused on the technical aspects of flow, such as the

pressure variation over the rock surface. The research has included laboratory tests and numerical analyses. The rough surfaces for the laboratory experiments have been created by scaling down 1:10 of laser-scanned real rock surfaces from tunnels driven by drilling-blasting. Computer simulations have been used to study flow over rough rock surfaces in regulated rivers, in which fish migrate, design of overflows (spillways) and flow over rough surfaces in tunnels and natural canals. Numerical simulations have been applied at one hydropower plant, also in northern Sweden, with regard to fish migration. Field measurements were performed to validate the simulations. A significant part of the work has dealt with the models' sensitivity to the resolution of the roughness. Analyses with different simplified geometries were performed and compared.

1.2 Objectives and scope

The main objectives of these research are to:

- investigate how block erosion occurs in spillway canals,
- investigate the mechanisms or governing factors involved in the block erosion, and
- make recommendations to optimize the design of canals as well as corrective measures.

The general scope of work involved field investigations and numerical analysis to:

- Identify the different types of blocks erosion that occurs in spillways with have high flow rates,
- Identify what is required for the process to be progressive,
- Identify the main factors that cause block erosion in relation to factors such as fractures in the spillway bedrock and flow direction, mechanical properties of fractures, and water pressure variation,
- Examine the methods (e.g., any type of reinforcement) that can be used to secure the rock against block erosion.

1.3 Methodology

The research method involved the following logical steps:

- Literature study of block erosion mechanisms and factors, as well as methods to assess or study block erosion and erosion potential in hydropower spillway canals.
- Field investigations were conducted at the spillway canals of two hydro-power dams; one located in northern Sweden (Dam 1), and another located in central Sweden (Dam 2). Data gathering was conducted in two phases. The first phase involved manual data collection and visual assessment of the spillway canals. The second phase involved the use of unmanned aerial vehicle (UAV) to digitally map the spillway canals. Rock samples were also collected for laboratory testing. Significant amounts of photographs were taken of the observation.
- Spillway characterisation and domaining can be considered part of field investigation, but importantly for the understanding block erosions characteristics and flow behaviour. Furthermore, the spillway channel characterisation also involved characterisation of canal rock mass of both spillways.
- Empirical analysis – which involved applying commonly used methods of assessing block erosion potential. In this study, three methods; Kirsten (1982,1988), Annandale (1995) and Pells (2016) were utilized.
- Numerical modelling was conducted using 3DEC software (Itasca 2019) and was split into parts. Part 1 involved a single block modelling exercise, which was a form of parameter study to investigate the effects of water velocity, block size, water column height and

channel slope on block displacement. Part 2 of the 3DEC modelling involved the simulation of two spillway channels or canals with actual canal geometries. The mapped joints were added into the model and actual topographic profiles of canals captured by the drone were used in the model.

- Numerical analysis was mainly three dimensional and performed using 3DEC. This was because early literature study revealed that, block erosion is three-dimensional problem (e.g., George 2015). Inputs for the models were obtained from field investigations and also from publications from studies conducted earlier in these dam sites.

1.4 Limitations

Due to time limitations, discharge tunnels were not investigated. Furthermore, detailed analyses of remediations measure were also not conducted. Another limitation is that 3DEC is not a fully dynamic fluid model and therefore additional models and assumptions were utilized.

2. LITERATURE

2.1 Mechanism of rock erosion

Rock erosion of an unlined spillway is a complex process, which depends mainly on the geological characteristics of the rock mass such as the rock types, discontinuity characteristics, rock mass quality, and hydraulic parameters. The mechanism of the rock erosion has been studied by many researchers (e.g., Akhmedov 1988; Annandale 1995; Sklar and Dietrich 2004; Whipple et al. 2000; George 2015; Pells 2016). From the numerous studies the major mechanism of the rock erosion may include abrasion, fracture of intact rock and removal of individual rock blocks, also known as plucking.

In Sweden block erosion studies have been conducted by for example Lorig (2002), Mörén (2005), Mörén & Sjöberg (2007) and various studies sponsored by Energiforsk, as well as internal studies conducted by the power companies. In some cases, studies were conducted utilizing both physical and numerical models (e.g., Billstein 2002; Billstein et al 2003). These studies were aimed at understanding the block erosion mechanisms to assist in the remedial works of spillway channels.

The following sub-sections will describe some of these mechanisms.

2.1.1 Abrasion mechanism

Abrasion is the process by which the rock surface is gradually grinding away over an extended period of time due to the repeated impact from sediment particles. These particles may be carried in suspension or as bed load or suspended load, or both (Richardson and Carling 2005). The impacts of the abrasion may lead to the disintegration of intact rock into small fragments (Sklar and Dietrich 2014). The rate of the abrasion is a function of the flood velocity, the quantity and grain size composition of the particles or sediments and the hardness contrast between the particles and the bedrock. Abrasion dominates where the rock surfaces are smooth and polished and where ripples and potholes are developed without any significant exhumed joint planes (Whipple et al. 2000). Abrasion is not always the dominant erosion process of a spillway channel in a granitic jointed bedrock, as in the case of the two dams studied herein. However, there could be a combination of abrasion with other erosion mechanisms, or it can be a precursor to other erosion processes (Whipple et al. 2000). Karlsson (2013) observed that the gently rounded rock surfaces downstream at the Dam 2 could have been because of abrasion and grinding by the water over an extended period.

2.1.2 Fracture of intact rock

Fracture of intact rock occurs when close-ended joints in a rock mass beneath a spillway is subjected to a turbulence hydraulic pressure thereby leading to the propagation of the joints. The propagation of the joints depends on the intensity of the pressure, the tensile strength of the rock and the toughness of the fracture (Bollaert 2002; Li et al. 2016). Bollaert (2002) observed that this mechanism of rock erosion is prominent at a depth in plunge pools where resonance condition can lead to the amplification of the pressure within the rock joint.

Depending on the magnitude of the pressure, the rock may fail instantaneously by brittle failure or overtime by fatigue (George and Sitar 2012). According to Annandale (2005) the brittle failure of the intact rock occurs when the stress intensity at the tip of close-ended joint as a result of turbulent

hydraulic pressures is more than the fracture toughness of the intact rock. However, when the fracture toughness at the tip of joint is more than the stress intensity that develops within the joint fatigue failure will occur as a result of the repeated fluctuating stress intensity, over a period of time, at the tip of the close-ended joint. Figure 1 illustrates the mechanisms for the rock block when subjected to fluctuating hydraulic pressures. This mechanism of rock erosion is dominant in the moderately jointed rock mass with non-persistence and widely spaced joints where rock blocks cannot form without the fracture of the intact rock.

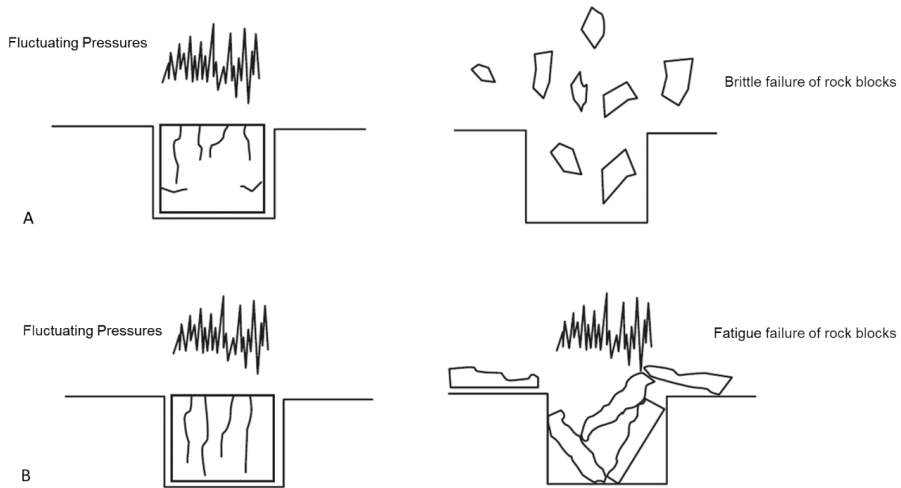


Figure 1. Mechanics of a rock block subjected to fluctuating hydraulic pressures (A) Brittle failure (B) Fatigue failure (Adapted from Annandale 2005).

2.1.3 Removal of Individual Rock Blocks or Plucking

Plucking is one of the mechanisms responsible for the block erosion. It usually occurs to sub-meter rock blocks in a bedrock channel or spillways (Li et al. 2016). For the block erosion to occur all the discontinuities (joints, bed planes, etc.) surrounding the block must be fully connected to isolate the block. The propagation of partially connected fractures could lead to the creation of isolated blocks that have kinematic freedom to displace though it often takes time to occur (Figure 2) hence fracture propagation due to turbulent water flow could be a precursor to plucking mechanism (Li et al. 2016). The plucking mechanism is dominant in a jointed and blocky rock mass with closely spaced joint sets. The discontinuities bounding the blocks allow the transmission of transient water pressures beneath the blocks resulting in the displacement of the isolated blocks (George 2015). The displacement of the block depends on the magnitude of the instantaneous difference between the shear forces and resulting forces, the mass of the isolated block and the time during which the shear forces exceed the resisting forces (Billstein et al. 2003). According to Annandale (2006) the ejection or removal of the isolated block will occur over a period of time when the pressure within the bounding joints caused by the transient flow within the joints exceed the water pressure overlying the rock, as well as the weight of the submerged rock block and the

shear forces on the sides of the block. Using Figure 2, the condition for the removal the isolated block can be expressed with Equation 1 (Annandale 2006).

$$F_{up} > F_{down} + W_g + F_{s1} + F_{s2} \quad 1$$

where F_{up} and F_{down} are the total upward forces caused by the transient pressure in the joint and the total downward forces caused by the fluctuating pressure on the top of the block of rock, respectively. F_{s1} and F_{s2} are the instantaneous shear forces on the sides of the block and the submerged weight of the block of rock is W_g . The shear strength of the lateral joints (τ) resisting the lateral displacements of the rock block can be determined according to the Mohr-coulomb's law as follows:

$$\tau = c + \sigma'_n \tan \theta \quad 2$$

Where c is the cohesion, σ'_n is the effective stress acting normal to the lateral joints minus the water pressure in the joint and θ is the joint friction angle.

The mechanism for vertical movement of the block can be accumulative when under cyclic loadings due to water pressure fluctuation, the rock block experiences upward oscillating movement, which can lead to plastic upward displacement (George and Sitar 2012; Li et al. 2016). The frictional forces on the sides of the rock block are majorly responsible for the plastic upward displacement of the block. The frictional forces hinder the return of the downward displacement (Pan et al. 2014).

Aside the fluctuating water pressure, stagnation pressure can also be responsible for the uplift of the block of rocks (Frizell 2007). Stagnation pressure often occur in spillways or rock channels influenced with strong flow when the surface of the rock blocks is uneven, or the rock block protrudes relative to its neighbouring blocks (Reinius 1986; Frizell 2007).

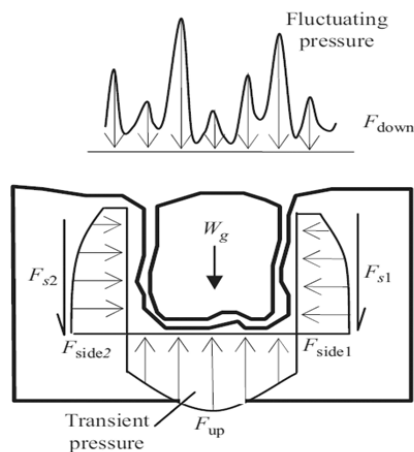


Figure 2. Forces acting on a submerged isolated rock block (Annandale 2006)

2.2 Factors affecting block erosion in spillway canals

The erosion of rock block in a spillway channel is a complex process that are influenced by many factors. The factors can be grouped into geotechnical, geometry and hydraulic. All these factors are interrelated with combined effects on the erosion process.

2.2.1 Geotechnical factors

The resistant of a rock mass to block erosion is majorly determined by its geotechnical parameters. Rock mass is comprised of intact rock separated by discontinuities such as joints, bedding planes, folds, sheared zone and fault.

The property of the intact rock is described with parameters, which includes the density, strength (compressive and tensile), hardness, deformability, etc. The failure of the intact rock along micro cracks either by brittle fracture or fatigue during the erosion process is majorly influenced by the strength of the rock. The hardness of the rock will determine the rate of abrasion and grinding of the surface of the rock during the erosion process. The effect of the strength of intact rock is well pronounced when considering the erosion of soft rock and it has a very limited influence on the erosion of jointed rock mass, which primarily involves unravelling of blocks of rock along natural discontinuities rather than the fracturing of the intact rock (Pells 2016).

Many studies (e.g., Woodward,1985; Cameron et al. 1986; Pitsiou 1990; George et al. 2015; Pells 2016) have emphasised the significant effect of the joint/fracture and its properties on the erosion of jointed rock mass subject to variety of flow conditions. The most important properties of the joints in these regards include number of the joint sets, joint spacing, orientation, joint wall roughness, aperture and infill materials.

The number of the joint sets and the joint spacing within the rock mass determine the block size number while the block size depends on the joint spacing. A rock mass with small rock blocks is more susceptible to erosion because the blocks could be easily lifted and transported by the flow water. In addition to the size, the shape of the block has significant effect on the rate and extent of the erosion. Elongated rock block will be more difficult to be eroded by plucking than equal-sided blocks of rock (Annandale 2006).

Joint wall roughness is one of the factors that influence the shear strength of joint especially when the joint is unfilled. Very rough surface will have higher shear strength and consequently greater resistance to the erosion process than the joint with smooth surface. In addition, a rock mass with numerous widely open joint (i.e., aperture) is prone to erosion than the rock mass with tight joint walls. In a situation when the joint is filled with material such as calcite, chlorite, clay, etc., the infill material influences the shear strength of the joint. However, the infill materials could be easily eroded making the joint to be opened and make it prone to erosion.

Depending on the direction of the water flow, joint orientation (dip and dip direction) affects the rate and extent of erosion. A rock mass with joints that strike about normal to the direction of the flow and dip steeply upstream (Figure 3a) will be less resistant and facilitate less block erosion than a rock mass that has joints that dip downstream (Figure 3b) (Woodward 1985; Annandale 2006).

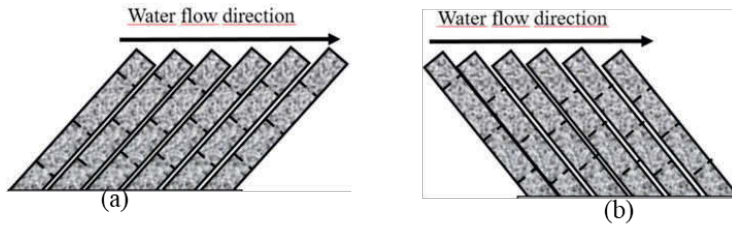


Figure 3. Joints orientation relative to the flow direction (Woodward 1985).

2.2.1 Geometry of the spillway

The physical characteristics of the spillway geometry, which influences the rate and extent of block erosion includes the channel width, the length, the slope, the knickpoint, which is the part of the channel where there is a sharp change in the slope and the curvature of the spillway. These characteristics will have effect on the flow velocity and consequently the stream power of the flow as well as the flow path. The velocity profile, for example, varies with the width and the depth of the channel. The narrower the channel, the higher velocity and the greater the erosion.

2.2.1 Hydraulic factor

The hydraulic parameters which affect the rate and extent of block erosion include the discharge capacity of the dam, the velocity of flow, the flow depth, duration of the flow and the roughness of the spillway surface.

The discharge capacity is a function of the length of the dam crest or the width of the water section, the height of water flow section and the discharge coefficient. The coefficient depends on many factors, which includes upstream flow conditions, the spillway layout and outlet configuration for the overflow spillway or submerged bottom outlet, respectively (Yang et al. 2019). The discharge capacity (Q) can be expressed as:

$$Q = C \times \sqrt{H_h} \times L \times H_f \quad 3$$

where C is the discharge coefficient, L is the length of the crest, H_h is the head over the crest and H_f is the height of water flow section. For a submerged bottom outlet, $L \times H_f = A$, where A is the outlet total area (Yang et al 2019). Equation 3 is applied for partially opened spillway gate but when the gate is fully opened $H_f = H_h = H$ and Equation 3 becomes:

$$Q = C \times H^{3/2} \times L \quad 4$$

The magnitude of the flow velocity is very crucial to the erosion rates, and it depends on the quantity of discharge. As the magnitude of the velocity increases the shear stress increases geometrically (i.e., shear stress is proportional to the square of the flow velocity) and leads to erosion of the rock within the region where the shear stress is greater than the shear strength of the rock.

The roughness of the surface of the unlined spillway is not only influenced by the rock structure but by the possible blasting damage during the excavation. The roughness of the channel has a significant effect on the head lost and the velocity of the flow. The roughness of the surface is

responsible for the flow pressures and stress fluctuation (Pitsiou 1990). The higher roughness surface results in stronger turbulent boundary layer – between the flow and the channel surface. Surface roughness is characterized with roughness height – a length measure of roughness or Manning roughness coefficient.

2.3 Methods for erosion assessment

Several methods have been proposed since 1930s for the prediction or assessment of erosion in the rock and soil formations. These methods can be categorized into physical hydraulic model studies, rigorous constitutive model and empirical methods (Sawadogo 2010). The constitutive model is based on Keyblock Theory (Goodman and Shi 1985), which can be used to solve the problems involving the removability of block from rock mass. The analytical approach is proposed by many researchers such as Temple and Moore (1994), Van Schalkwyk et al. (1995), Kirsten et al. (1996), Annandale (1995) and Pells (2016). The approach is based on field observations and laboratory tests, and they provide a correlation between the hydraulic power generated by the flowing water and the geo-mechanical properties of the rock mass. Many researchers have used the approach for the assessment of erosion in spillways most especially the Annandale’s method and Pells’ method (e.g., Hahn and Drain 2010; Mörén and Sjöberg 2007; Pells et al. 2017). Therefore, in the following sub-section the method proposed by Annandale (1995) and Pells (2016) are briefly explained.

2.3.1 Analytical Approach

2.3.1.1 Annandale’s Method

Annandale’s method, which is also known as Erodibility Index Method (EIM) was proposed by Annandale (1995) based on field observations of spillways performances and published data regarding erosion process. The EIM is a semi-empirical method for evaluating erosion of rock masses. The method is based on the correlation between the relative magnitude of the erosive power of water and the earth material (e.g., rock mass) resistance.

2.3.1.2 Erodibility Index (Annandale’s method)

The erodibility index is based on a rippability index developed by Kirsten (1982, 1988). It was modified from Barton’s Q-system (Barton et al. 1974). The erodibility index, K_r is calculated as the product of four parameters (Annandale, 1995):

$$K_r = M_s K_b K_d J_s \quad 5$$

The M_s is the material strength number based on the rock unconfined compressive strength (UCS). The value of M_s is the product of the UCS and its unit weight relative to a standard of 27 kN/m³ (Wyllie 1999). For example, a rock with UCS of 60 MPa and a unit weight of 25 kN/m³ will have an M_s value of approximately 56, i.e., $60 \times \frac{25}{27}$.

The block size number (K_b) can be estimated from the ratio of the rock quality designation (RQD) to the number of joint set number (J_n). The K_d is the discontinuity shear strength number based on the ratio of the joint roughness number (J_r) to the joint alteration number (J_a). The original ratings for J_n by Barton et al. (1974) were modified by Kirsten (1982) for the Kirsten index (Rock mass erodibility index) as shown in Table 1. The Barton’s rating tables for J_r and J_a were simplified by Kirsten (1982) to be relevant to rock mass erodibility and they are shown in Table 2 and Table 3, respectively.

The relative ground structure number (J_s) represents the effective dip of the least favourable discontinuity, set with respect to the flow, and account for the shape of the blocks of the rock and ease with which the stream can penetrate the rock surface and dislodge blocks (Wyllie, 1999). Rock masses are more resistant to scour if they are slabby rather than blocky, and if the slabs dip upstream rather than downstream (Wyllie, 1999). Table 5 contains values of the relative ground structure number for various ratios of joint spacing.

Table 1. Modified joint set number, J_n (Kirsten 1982)

Joint sets	Joint set number (J_n)
Intact, no or few joints	1.00
One joint set	1.22
One joint set plus random	1.50
Two joint sets	1.83
Two joint sets plus random	2.24
Three joint sets	2.73
Three joint sets plus random	3.34
Four joint sets	4.09
More than four joint sets	5.00

Table 2. Modified Joint roughness number, J_r (Kirsten 1982)

Joint separation	Joint Roughness Condition	J_r
Joints are tight or become closed during hydraulic flow	Discontinuous joint; stepped	4.0
	Rough/irregular: undulating (e.g., tension joints, rough sheeting joints, rough/bedding)	3.0
	Smooth; undulating (e.g., smooth sheeting, non-planar foliation, and bedding)	2.0
	Slickensided; undulating	15
	Rough/irregular; planar	15
	Smooth; planar (e.g., planar sheeting joints, planar foliation, and bedding)	1.0
	Slickensided; planar	0.5
Joints are open and remain open during hydraulic flow	Joints are either open or contain relatively soft gouge of sufficient thickness to prevent wall contact during hydraulic flow	1.0
	Joints contain swelling clays	1.0

Table 3. Modified Joint alteration number, *Ja* (Kirsten 1982)

Description of Gouge (Infilling)	<i>Ja</i> for Aperture Width, mm		
	< 1.01	1.0– 5.02	> 5.03
Tightly healed, hard, non-softening impermeable filling.	0.75	-	-
Unaltered joint walls, surface staining only	1.0	-	-
Slightly altered non-softening, non-cohesive rock material or crushed rock filling.	2.0	4.0	6.0
Non-softening, slightly clayey non-cohesive filling.	3.0*4	6.0*	10.0*
Non-softening strongly over-consolidated clay mineral filling, with or without crushed rock.	3.0	6.0	10.0
Softening or low friction clay mineral coatings and small quantities of swellings clays.	4.0	8.0	13.0
Softening moderately over-consolidated clay mineral filling, with or without crushed rock.	4.0*	8.0*	13.0*
Shattered or micro-shattered (swelling) clay gouge, with or without crushed rock.	5.0*	10.0	18.0
Note: 1. Joint walls effectively in contact 2. Joint walls come into contact after approximately 100 mm shear 3. Joint walls do not come into contact at all upon shear 4. Values asterisked added to Barton's data			

Table 4. Relative ground structure number, J_s (Kirsten 1982)

Dip direction of closer spaced joints (degree)	Dip direction of closer spaced joints (degree)	Ratio of joint spacing, r			
		1:1	1:2	1:4	1:8
180/0	90	1.00	1.00	1.00	1.00
In direction of stream flow	85	0.72	0.67	0.62	0.56
	80	0.63	0.57	0.50	0.45
	70	0.52	0.45	0.41	0.38
	60	0.49	0.44	0.41	0.37
	50	0.49	0.46	0.43	0.40
	40	0.53	0.49	0.46	0.44
	30	0.63	0.59	0.55	0.53
	20	0.84	0.77	0.71	0.68
	10	1.22	1.10	0.99	0.93
	5	1.33	1.20	1.09	1.03
0/180	0	1.00	1.00	1.00	1.00
Against direction of stream flow	5	0.72	0.81	0.86	0.90
	10	0.63	0.70	0.76	0.81
	20	0.52	0.57	0.63	0.67
	30	0.49	0.53	0.57	0.59
	40	0.49	0.52	0.54	0.56
	50	0.53	0.56	0.58	0.60
	60	0.63	0.67	0.71	0.73
	70	0.84	0.91	0.97	1.01
	80	1.22	1.32	1.40	1.46
	85	1.33	1.39	1.45	1.50
	90	1.00	1.00	1.00	1.00
Note: For intact material take $J_s = 1.00$. For values of r less than 1:8, take J_s as for $r = 1.8$					

2.3.1.3 Stream Power (Annandale's method)

The stream power is the rate of energy dissipation against the bedrock and the bank of the river. The energy dissipation is related to turbulence such that an increase in the intensity of the turbulence will result in the increase rates of energy dissipation and the magnitude of fluctuating pressures (Annandale 1995; 2006). According to Annandale (2006) the rate of energy dissipation per unit area in an open channel flow is:

$$P = \gamma q \Delta E$$

where P is the unit stream power dissipation (kW/m^2), γ is the unit weight of water (9.81 kN/m^3), q is the unit discharge ($\text{m}^3/\text{s} \cdot \text{m}$) and ΔE is the energy loss in terms of head per unit length of flow (m/m).

The open channel flow is uniform when the characteristics of the flow such as slope, roughness and cross-section are constant along the channel and in such condition; the flow velocity will be constant and ΔE will be the same as the slope of the channel. However, the open channel flow is non-uniform or varied flow when the flow characteristics are not constant along the channel. Non-uniform flow is further classified into gradually varied or rapidly varied flow (Akan 2011). As shown in Figure 4, the flow is gradually varied between sections 1–2 and 2–3, rapidly varied in section 3–4 and the flow is uniform in section 4–5. Rapidly varied flow usually occurs where depth abruptly changes due to hydraulic drop or a hydraulic jump (Chow 1959). The change in energy during rapidly varied flow is dominated by turbulent mixing hence the rate of energy dissipation (i.e., stream power) developed by a hydraulic jump can be determined by first calculating the energy loss over the hydraulic jump (Annandale 2006) and the energy loss over the jump can be estimated from the equation proposed by Henderson (1966):

$$\Delta E = y_1 + \frac{q^2}{2gy_1^2} - \frac{y_1}{2} \left(\sqrt{1 + 8F_r^2} - 1 \right) - \frac{4q^2}{2gy_1^2 \left(\sqrt{1 + 8F_r^2} - 1 \right)^2} \quad 7$$

where y_1 is the depth of the water before the hydraulic jump and can be determined from the ratio of the unit discharge (q) and the mean flow velocity (V) i.e., $y_1 = \frac{q}{V}$, g is acceleration due to gravity, F_r is the Froude number, which is the ratio of the mean flow velocity to wave speed hence $F_r = \frac{V}{\sqrt{g \times y_1}}$ when F_r equals 1 the condition of the flow is critical, it super critical when it greater than 1 and subcritical when it is less than 1.

Having calculated the energy loss over the hydraulic jump, the average stream power per unit area underneath a wide hydraulic jump can be determined thus (Annandale 2006):

$$P = \gamma q \frac{\Delta E}{L} = \gamma \frac{q}{L} \left(y_1 + \frac{q^2}{2gy_1^2} - \frac{y_1}{2} \left(\sqrt{1 + 8F_r^2} - 1 \right) - \frac{4q^2}{2gy_1^2 \left(\sqrt{1 + 8F_r^2} - 1 \right)^2} \right) \quad 8$$

where L is the effective length of the hydraulic jump over which the energy is dissipated. Annandale (2006) recommended that L should be 1 m due to the absence of reliable data however Pells (2016) observed that the recommendation overestimates the average stream power. Henderson (1966) has proposed an empirical relationship of $L = 6y_2$ for the flow whose F_r ranges between 4.5 and 13. The depth of water after the hydraulic jump (y_2) can be calculated using the relationship proposed by Henderson (1966):

$$y_2 = 0.5 \times y_1 \left(\sqrt{1 + 8F_r^2} \right) \quad 9$$

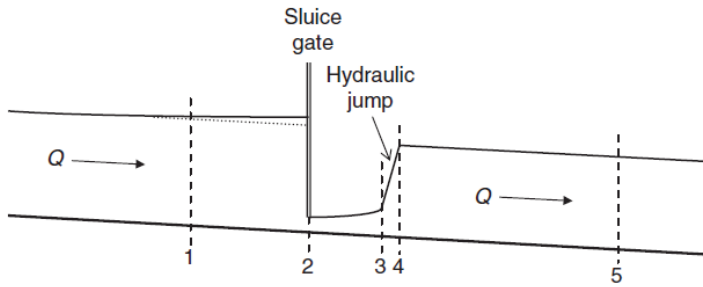


Figure 4. Various type of flow (Akan 2006)

2.3.1.4 Erodibility Threshold (Annandale’s method)

Annandale (1995) used data from numerous unlined spillways as well as published data on incipient motion of non-cohesive earth materials to plot the stream power against the erodibility index for each of the dataset as shown in Figure 5. From Figure 5 the Erodibility threshold, which is the correlation between the erodibility index and the critical stream power (P_c) was developed for lower and higher erodibility values (K_r) as expressed in Equations 10 and 11, respectively (Annandale 2006).

$$P_c = 0.48K_r^{0.44} \text{ for } K_r \leq 0.1 \tag{10}$$

$$P_c = K_r^{0.75} \text{ for } K_r \geq 0.1 \tag{11}$$

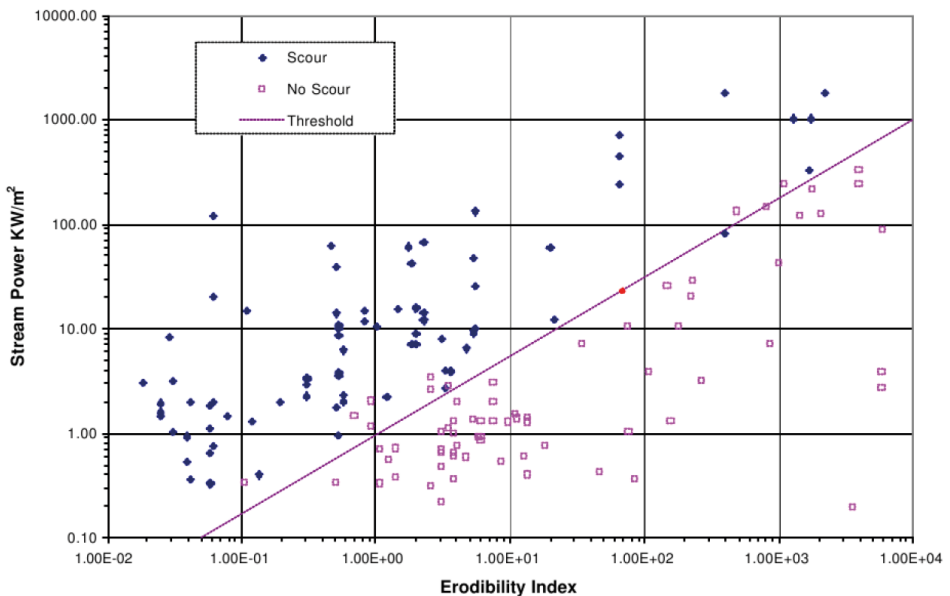


Figure 5. Annandale Erodibility Threshold (Annandale 1995).

2.3.1.5 Pells' Method

The Pells (2016) approach for the assessment of rock mass erosion in unlined spillways follows the same concept as that of Annandale (2006). Erosion risk was determined by comparing the stream power with the erodibility index of the rock mass. The procedure for the determination of the unit stream power dissipation is similar to that of Annandale (2006) however, Pells (2016) opined that the recommendation of Annandale (2006) to assume the effective length of the hydraulic jump to be 1m would overestimate the stream power hence the hydraulic jump length (y_2) was taken as $6y_2$ after Henderson (1966).

2.3.1.6 Erodibility Index (Pells' Method)

Pells (2016) observed that the rock indices used for the erodibility index (Annandale 1995; Annandale 2006) were not specifically developed for such purpose and for the improved representation of the erodibility of fractured rock, Pells (2016) and Pells et al (2017) modified Geological strength Index (GSI) (Hoek et al. 2000). New discontinuity orientation adjustment was introduced to the GSI to account for rock mass vulnerability to erosion. The $eGSI$ can be expressed as (Pells 2016).

$$eGSI = \max \begin{cases} GSI + E_{doa} \\ 0 \end{cases} \quad 12$$

where $eGSI$ is the rock mass index and E_{doa} is the discontinuity orientation adjustment for erodibility. Pells (2016) recommended that the GSI value for the erodibility in Equation 2-12 be obtained from the GSI chart (Marinos and Hoek 2001) and the E_{doa} values be determined from Figure 6 or Figure 7 (Pells 2016).

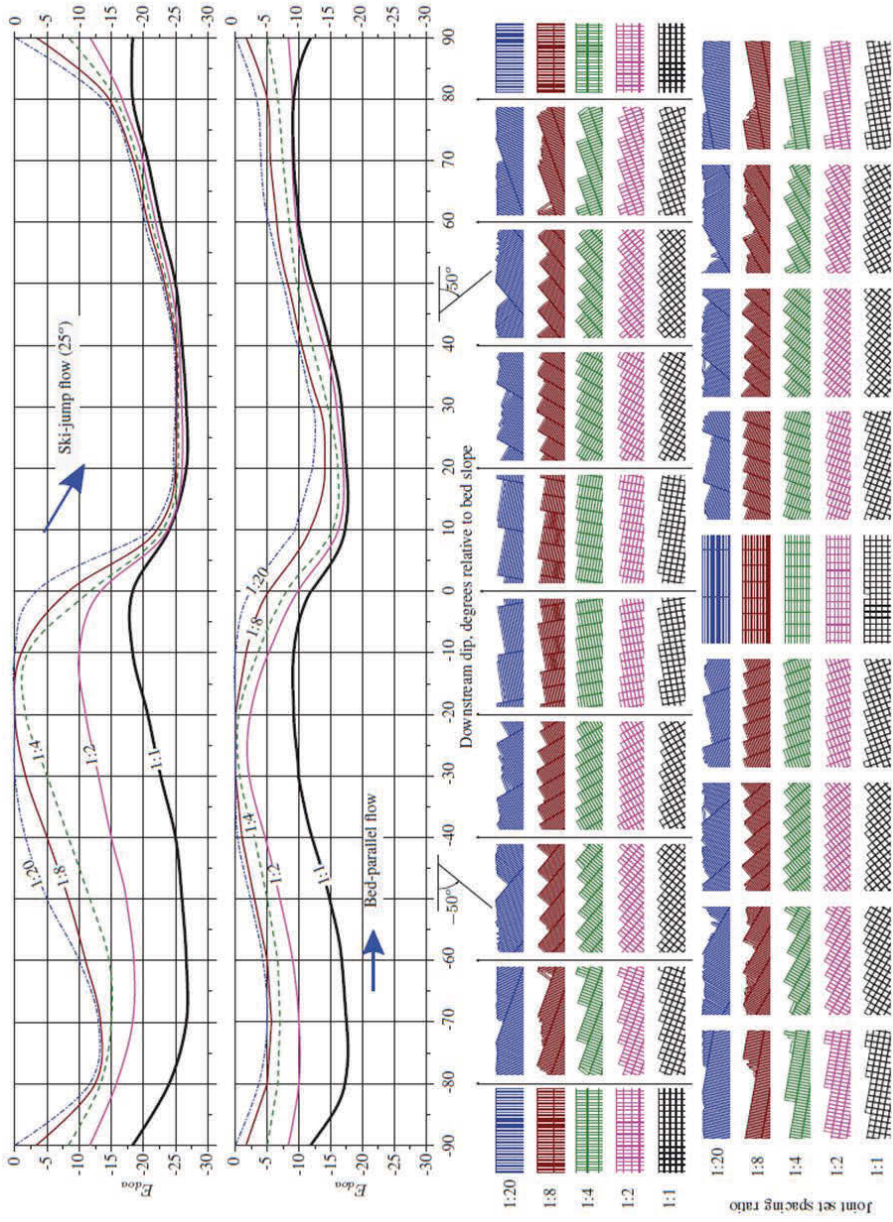


Figure 6. Discontinuity orientation adjustment for erosion (E_{doa}) for horizontal beds and various approach flows (Pells 2016).

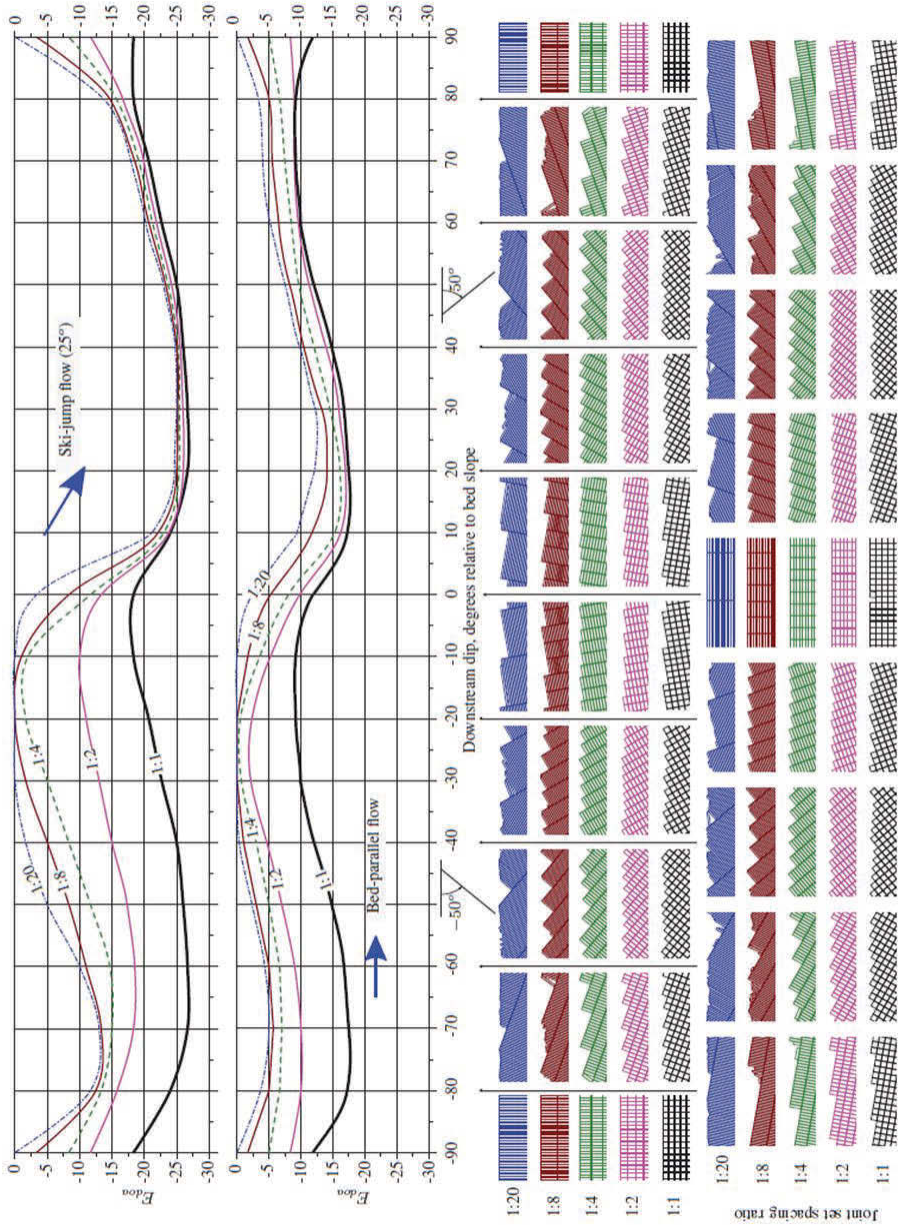


Figure 7. Discontinuity orientation adjustment for erosion (E_{don}) for inclined beds and various approach flows (Pells 2016).

2.3.1.7 Categorisation of Erosion Risk

In contrast to Annandale’s method, Pells method provides the categorisation of erosion risk based on graduation of the risk rather than a threshold. Pells (2016) plotted the unit stream power dissipation versus $eGSI$ index for each of the dataset compiled from numerous case studies and published data as shown in Figure 8. Using the values of $eGSI$ and the unit stream power, the likely category of erosion of rock mass in a spillway can be estimated using Figure 8.

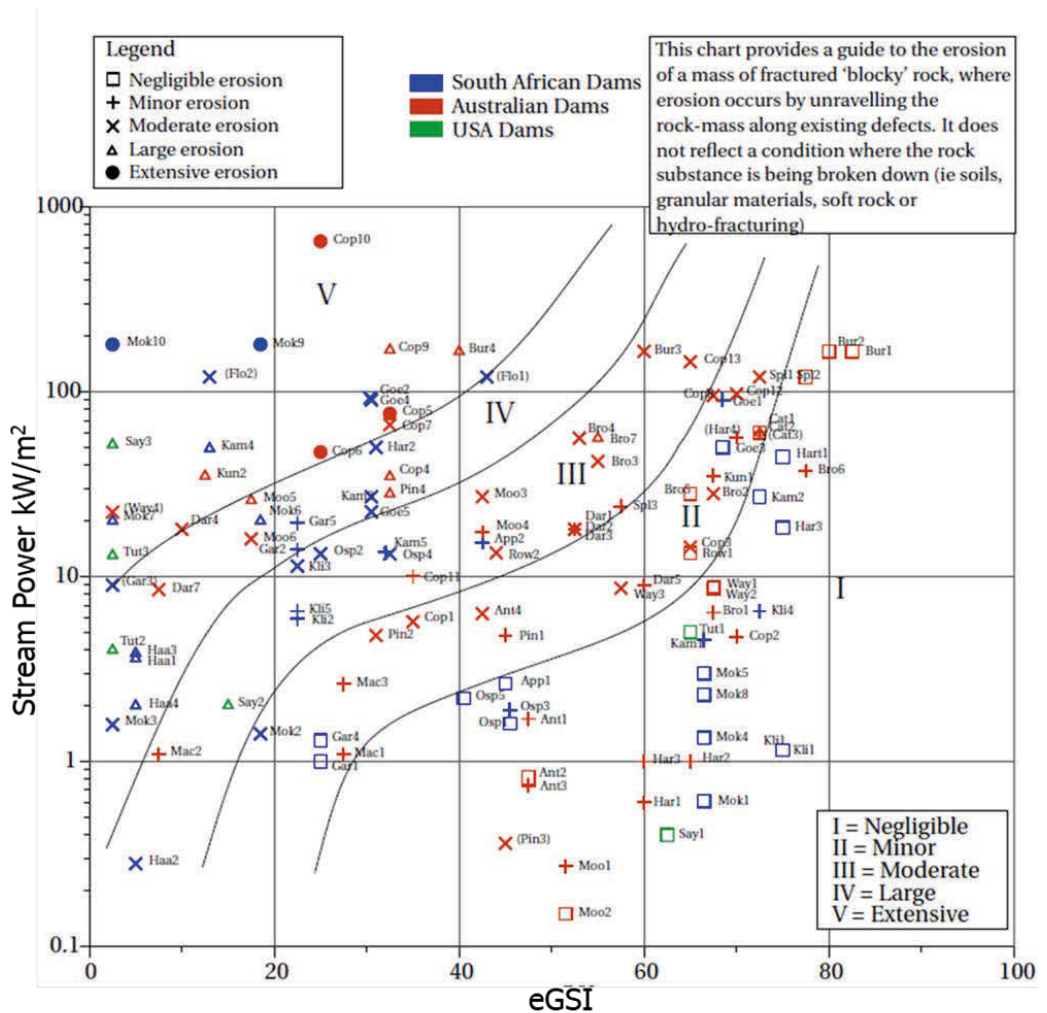


Figure 8. Unit Stream Power Dissipation versus $eGSI$ (Pells 2016).

2.3.2 Numerical Analytical Approach

Numerical modelling of rock erosion along spillway canals have been performed using both the discontinuum and continuum methods. Lorig (2002), Mören (2005), Mören & Sjöberg (2007) used the discontinuum code UDEC to study block erosion of Midskog spillway channel. Dasgupta et al (2011) used ANSYS FLUENT to investigate the erosive of capacity or scour formation in the plunge pool in Kariba Dam in Zimbabwe. At the same time, they used UDEC to model erosion of the spillway rock mass. Goodman & Hatzor (1991) used 3D-DDA to analyse block scour in 3D using block theory for the Kendrick Dam Project in Wyoming, USA. Wibowo (2009) applied key block theory from Goodman & Shi (1985) and 2D-DDA to find removable blocks exposed by an excavation for unlined rock spillways.

However, George (2015) in PhD thesis argues that block erosion is three-dimensional and therefore is best captured by a three-dimensional code, in which George (2015) recommended Itasca's 3DEC as the most suitable. 3DEC allows for the possibility to either construct a fully couple hydro-mechanical model or further still a fully couple hydro-mechanical-dynamic model. These kinds of the models will capture block erosion due various mechanics resulting from water pressure, dynamic pulsating conditions and shear resistance.

3. FIELD INVESTIGATIONS

The block erosion field studies were conducted at the spillways of two of the largest hydropower dams in Sweden, referred to as Dam 1 and Dam 2 in this report.

Field investigations were conducted in two phases:

- Phase 1: initial site visit; to inspect the canals, perform manual data collection where possible, perform qualitative assessments, collect rock samples collection for laboratory testing, assessment of the canals for phase 2 investigation using UAV, and speaking to site engineers to collect relevant information, including publications.
- Phase 2: This phase of the inventory involved using UAV to perform photogrammetry of the canals (Figure 9). An Explorian (XLT) Pitchup drone, equipped with Sony Alpha 50 mm high resolution camera (1.5-2 cm/pixel) and Agisoft Photo Scan Professional software. It was able to fly between 80-120 m to avoid crashing into trees. And it was flown from a safe distance without the need for entry into the canals.

Data collected from Phase 1 and Phase 2 were analysed and reported separately in this report. Phase 1 analyses and assessment involved characterisation of channels which could not be done using the drone data. On the other hand, it involved limited amounts of quantitative data on geological structures. The drone data required the assistance of consultants with professional photogrammetry data analyses software programs and expert skills for data processing, analyses and interpretation. The output from the drone data in principle included complete structural data of the canals, terrain topography and canal geometry. The drone data assisted in the quantitative assessment rock blocks sizes, which is a critical factor in block erosion.



Figure 9. An Explorian (XLT) Pitchup drone, mounted with a Sony Alpha high-resolution camera taking off to perform photogrammetry.

3.1 Dam 1

Dam 1 is one of the largest hydro-power dams located in northern Sweden. Block erosion of its spillway canal is a concern like many other dams experiencing this kind of erosion.

The dam embankment is oriented east-west, and the spillway channel is in the south-east direction, which is the principal water flow direction. The slope of spillway varies between 3 to 5% in gradient over approximately 300 m length.

3.1.1 Bedrock geology

Geological maps from Swedish Geological Survey (<https://www.sgu.se>) shows the bed geology of Dam 1 area to be primarily composed of porphyry textured granite. The blocky rock mass is observed also upstream areas of the dam. Figure 10 and Figure 11 show the block erosion characteristics of Dam 1. These sub-horizontal formations resulted from stress release during isostatic uplift after glaciation. This phenomenon is very common in Scandinavian rock formations, irrespective of rock types, but quite pronounced in crystalline rocks like the granite formation observed in the dam area. This block formation is susceptible to erosion.



Figure 10. Dam 1 bedrock characteristics.



Figure 11. Dam 1 spillway block erosion.

3.1.2 Structural geology

The rock mass at Dam 1 can be generally classed as blocky, with Geological Strength Index (GSI) values of 60 to 80 (Figure 12). There is a zone of crushed rock mass, approximately 30 cm wide, that runs diagonally near the spill gates to west side of the channel (Figure 13). This shear zone acts as a small diversion channel. The rock is quite blocky (GSI of 50 to 60) on the hangingwall side of the shear zone and makes up less than 10% of the spillway channel bed rock.

During the field visit approximately 40 odd structures were measured. The stereoplots of these structures are shown in Figure 14. The most dominant joint set is the shallow dipping set; $14^{\circ}/107^{\circ}$ (dip/dip-direction). With spacing of approximately 20 to 40 cm, it forms slabs that are susceptible to erosion (Figure 15). Two main sub-vertical to vertical joint sets are random and sparsely spaced; $58^{\circ}/110^{\circ}$ and $81^{\circ}/108^{\circ}$.

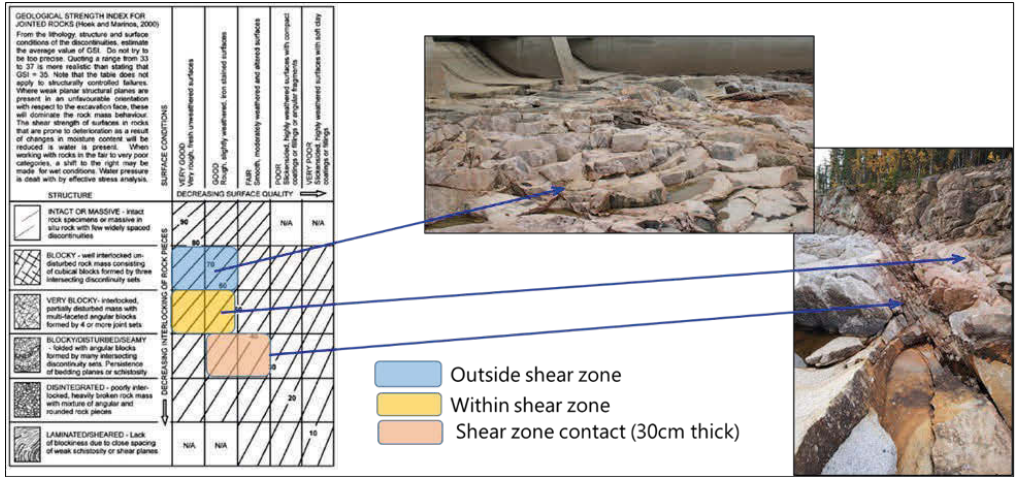


Figure 12. GSI classification of the spillway bedrock at Dam 1.

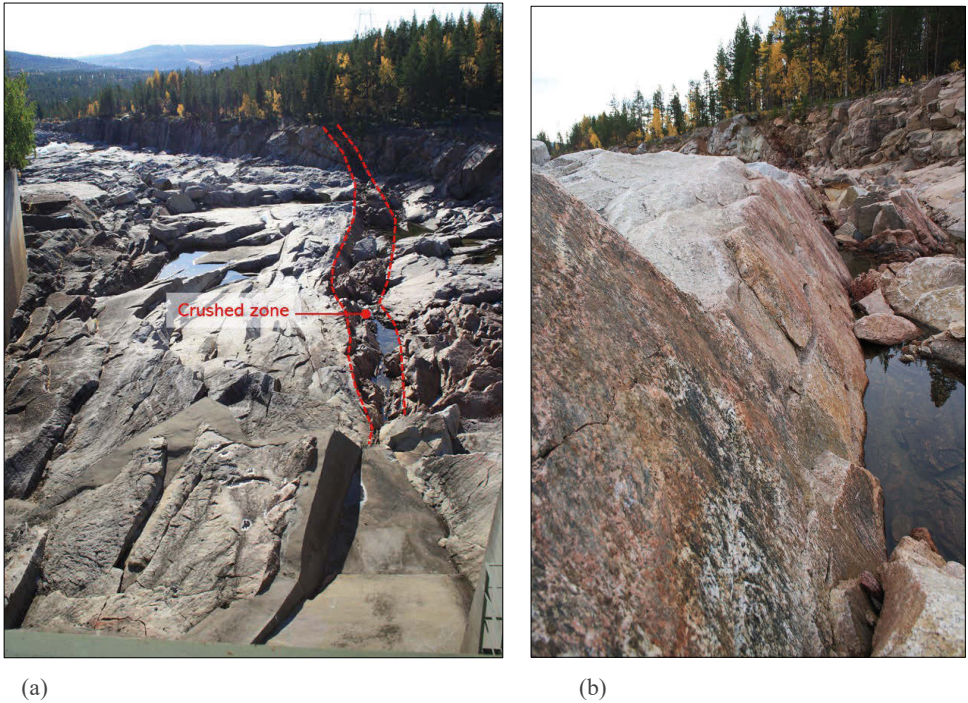
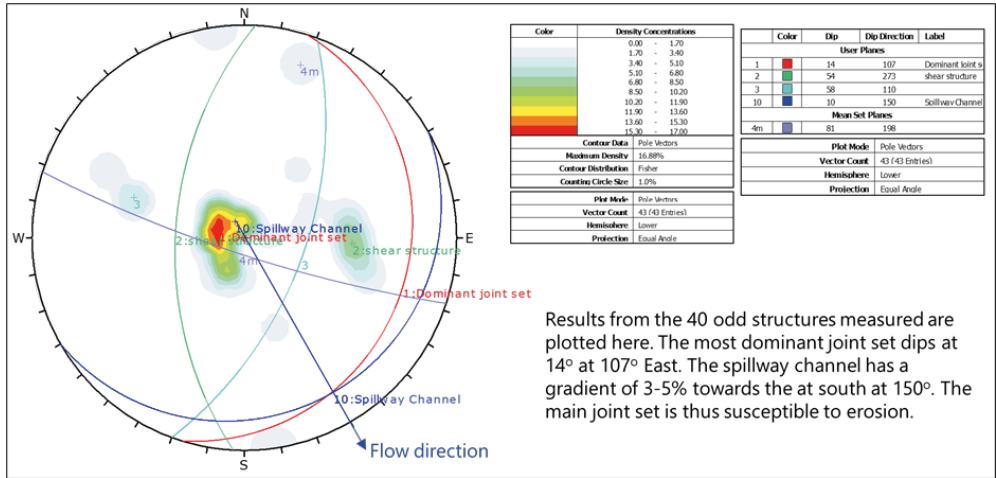


Figure 13. (a) The shear or crushed zone, (b) shear zone showing preferential flow path.



Results from the 40 odd structures measured are plotted here. The most dominant joint set dips at 14° at 107° East. The spillway channel has a gradient of 3-5% towards the at the south at 150°. The main joint set is thus susceptible to erosion.

Figure 14. Stereonet of structures mapped at Dam 1 spillway channel.



Figure 15. The flat lying blocks formed by sub-horizontal structures.

3.1.3 Block erosion mechanisms

Blocks of 1 to 5 m³ are formed where the vertical structures intersect the sub-horizontal structures, see for example Figure 16. However, the dominant mechanism is the fracturing of the flat lying rock slabs under the action of water pressure. This typically happens upstream where the pressure is the highest (Figure 17). Larger blocks that could not be easily ripped-off or fractured undergo a period of fatigue, leading to development of water pressure induced fractures (see Figure 18).

The most common form of block erosion at Dam 1 appears to be related to fracturing or tearing of the intact rock slabs by water pressure and the transportation of these rock blocks downstream. Fatigue also results in formation of blocks of various sizes. However, this fatigue induced rock fracturing takes time.

Scouring above the plunge pool (Figure 19) appears to have resulted from the remediation work to divert flow away from concrete wall towards the east. The flat lying rock slabs are notably peeled off.

The joint surfaces were observed to be largely smooth and undulating (Figure 20). The smoothing of channel bedrock surface is largely due to abrasion caused by the moving blocks during flooding.



Figure 16. Large block formed by the dominant sub-horizontal structures intersected by the two random vertical joint sets, which has been dislodged by water pressure.

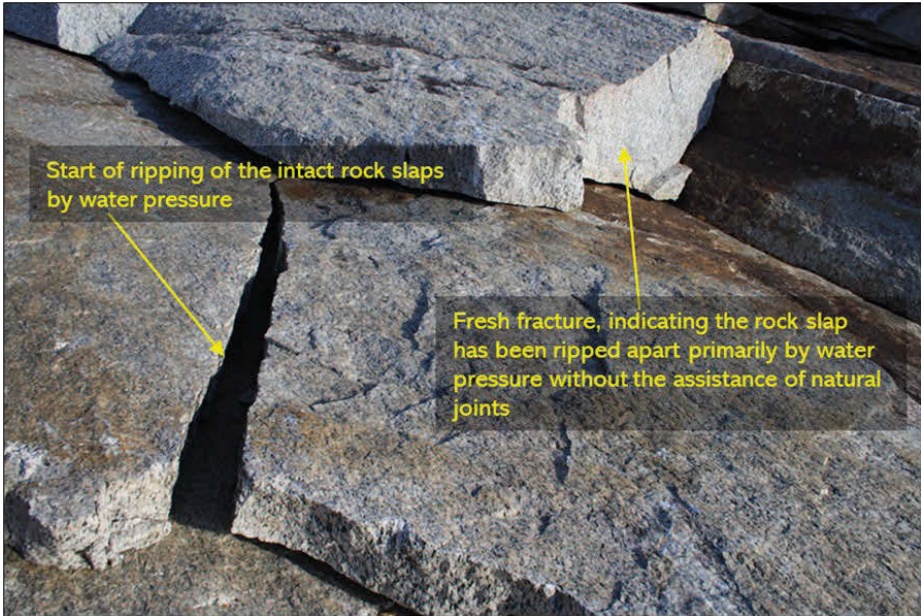


Figure 17. Intact rock slabs being ripped apart by water pressure.



Figure 18. Fatigue fractures induced by water pressure.



Figure 19. Peeling of the rock surface above the plunge pool by water jet. The surface has been engineered for controlled erosion.

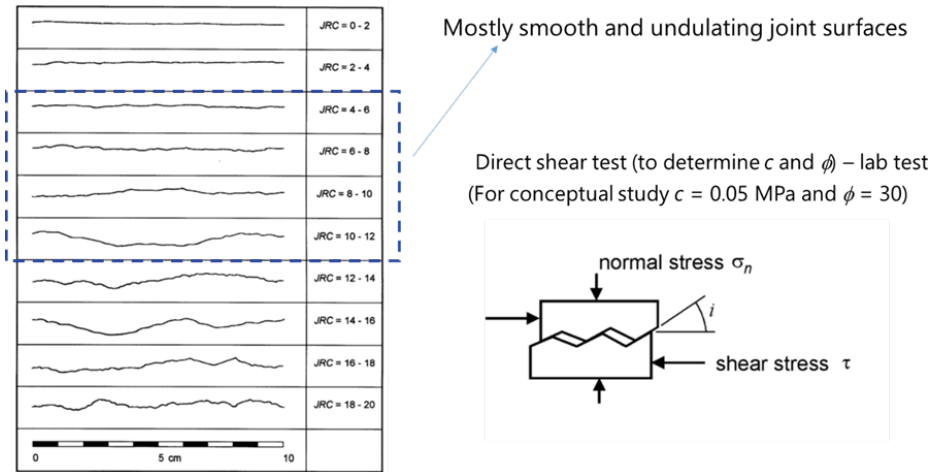


Figure 20. Smooth and undulating joint surfaces.

3.1.4 Fracture aperture

Fracture apertures were observed to be very significant (Figure 21). Large openings in the joints were observed through which water rushes through during flooding. Field estimation of the aperture sizes range between 1 and 50 mm. It was also observed that the same fracture had more open (larger aperture) on upstream side than on down streamside (smaller aperture). With cyclic

flooding the water pressures continuously force the aperture to open (Figure 22), thus allowing increased pressure on the blocks. With time the pore pressure becomes significantly large enough to fracture the blocks.

The water pressure also reduces the abrasiveness of the fracture surfaces with scouring action. The fracture surfaces become smoother with flat or undulating surfaces.

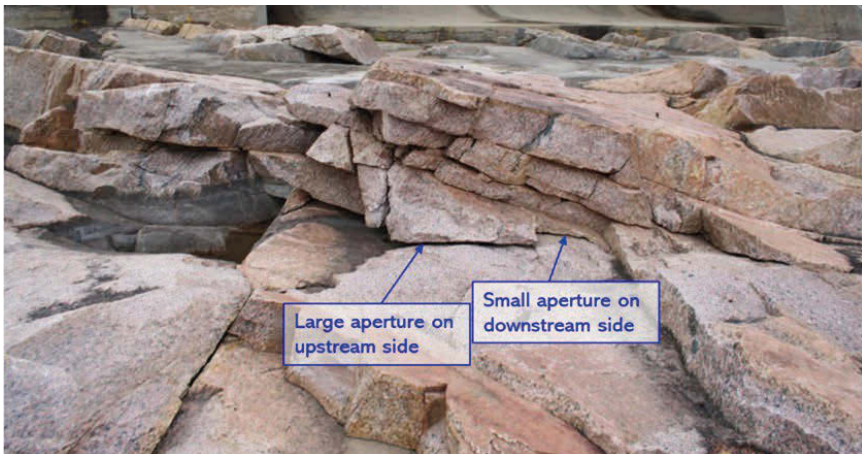


Figure 21. Significantly large open fracture apertures.

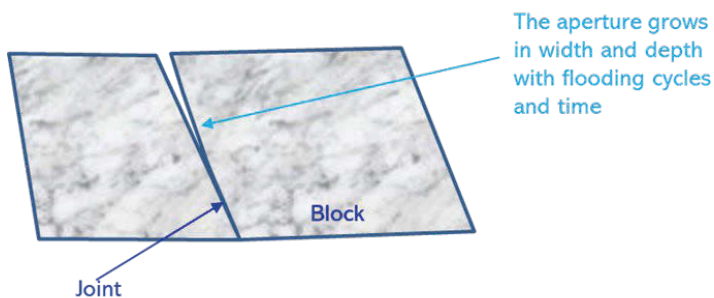


Figure 22. Idealisation of aperture growth with flooding cycles and time.

3.1.5 Spillway channel domains

The spillway channel has been visually dominated by assessing the scale of block erosion, and deposition and distribution of rock blocks (Figure 22). Three main domains were established:

- Domain A: Most of the blocks are eroded and transport downstream. The length of this domain is about 50-75 m. The gradient of the slope of domain is gentle at about 3%.
- Domain B: Large blocks of 1 to 5 m³ are deposited here. The length of this domain is about 150 m. The gradient of the slope of domain is slightly steeper than domain A about 5%.
- Domain C: Blocks of smaller sizes, <1 m³, are deposited here. The length of this domain is about 300 m. The gradient of the slope of this domain becomes gentler again, about 3%.

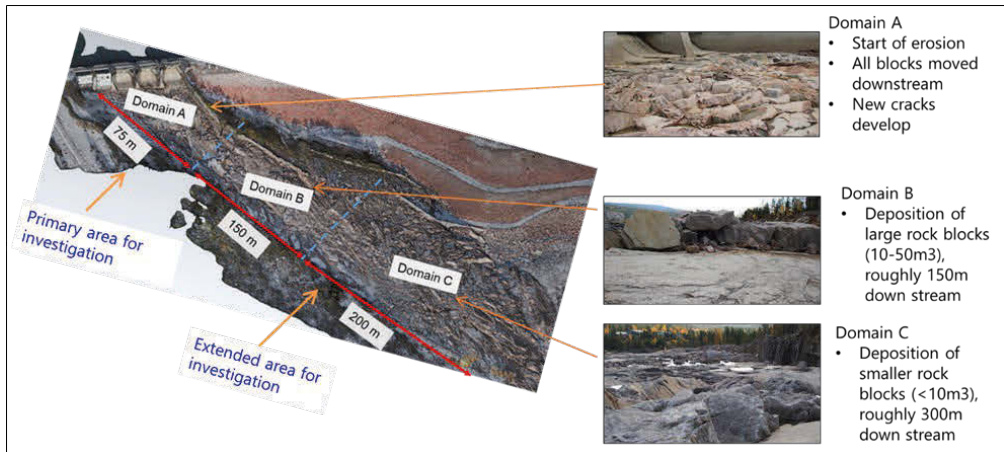


Figure 23. Dam 1 Spillway channel domains for Dam 1.

3.1.6 Drone data mapping and analysis

In phase 2 of the investigation the spillway channel was surveyed using a drone to capture the geological features as well as the channel topography. Several software packages including Agisoft, CloudCompare and GEM4D were used to pre-process the data before analysing it in Sirovision software.

Figure 24 shows the structural mapping and analyses performed using Sirovision for the Dam 1 spillway. Table 5 shows the analysed data of the block forming joints. The shallow dipping joint set (red arrows) is the most dominant, which agrees with phase 1 mapping data. The sub-vertical joint sets (blue and green arrows) are widely spaced structures, while the dark cyan and dark magenta arrows represent random vertical joints. Even though the mapping has been conducted for each domain the structural data do not deviate significantly for each of the domains.

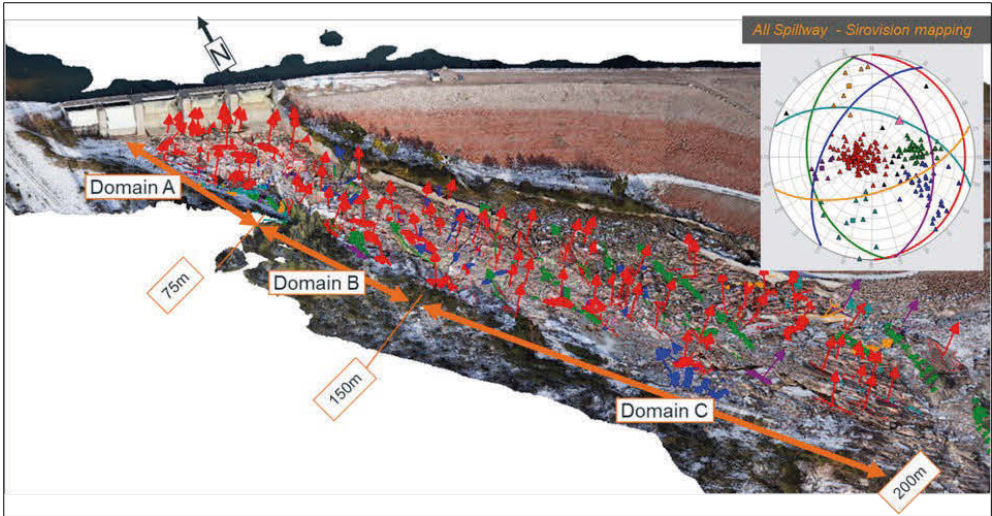


Figure 24. Structural mapping of drone captured data using Sirovision software.

Table 5. Joint set data from drone data and Sirovision analyses

Id	Set Name	Poles	Mean Dip	Mean DDN	StdDev Dip	StdDev DDN	Fisher K	R90	R99
1	Red	38	9.6	80.9	5	40.4	79	13.9	19.7
2	Green	14	44.9	276.1	11.8	8.4	32.3	21.8	31
3	Blue	4	26	322.7	10	9.5	0	0	0
4	DarkMagenta	3	35.5	98.1	4.6	13.2	0	0	0
5	DarkCyan	4	82.8	352.1	29	4.9	0	0	0

3.1.7 Block size analysis

Figure 25 shows the joint spacing data from Sirovision analysis for the key joint sets. To determine the block sizes the program BCF (a block cave mining application software) was used to perform statistical analysis of possible sizes (Figure 26). The average block size in domain A ranges from 0.2 – 0.3 m³, domains B and C range from 1.5 – 3.0 m³. These are blocks formed by the joint sets, and not related to the loose and migrated blocks observed in the channel. The BCF analysed block sizes confirm the visual estimation from phase 1 assessment, where 1.0 – 5.0 m³ block sizes were observed in the spillway channel.



Figure 25. Spacing of the joints at Dam 1.

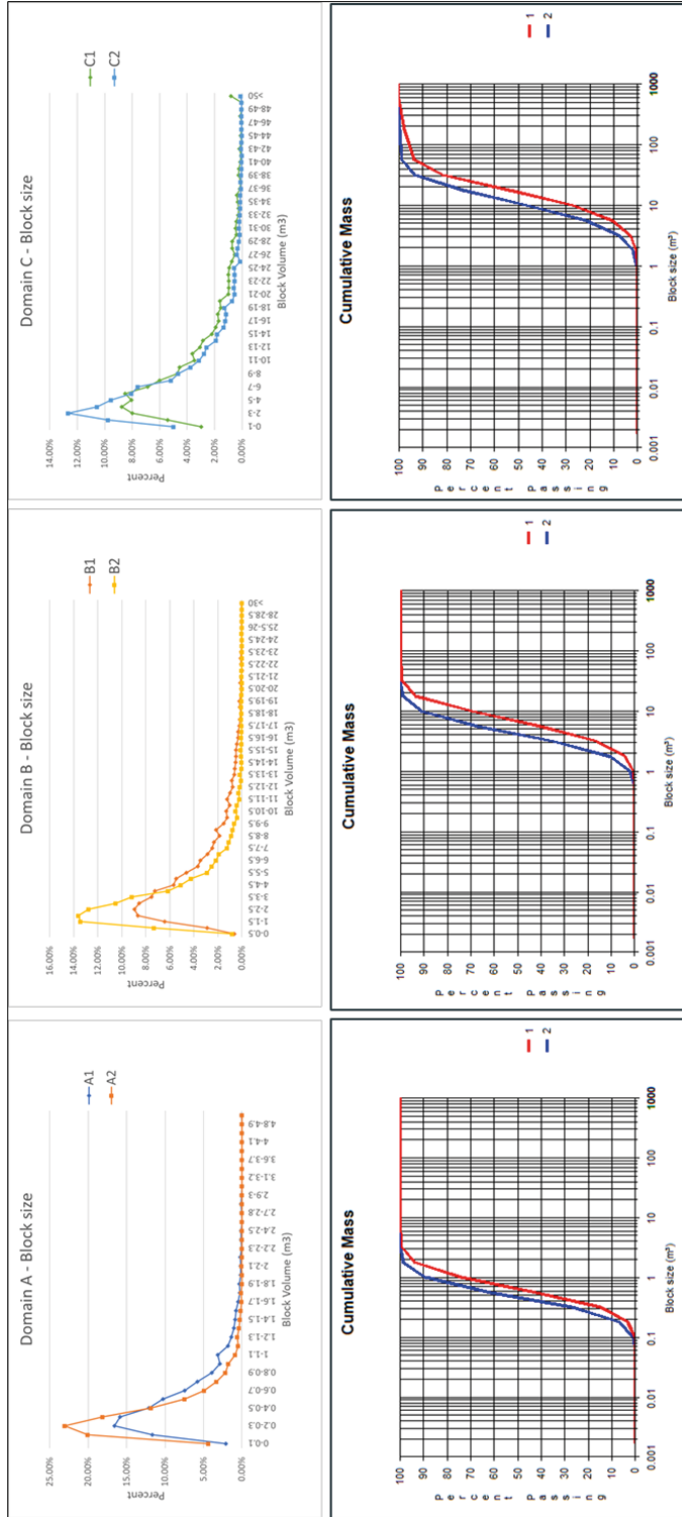


Figure 26. Block sizing of the Dam 1 rock mass.

3.2 Dam 2

Dam 2 is one of largest hydro-power dams in Sweden. The main embankment of Dam 1 strikes north-south (Figure 27). Thus, the spillway channel is in the easterly direction.

During the site visit the spillway area immediately below the concrete apron was drill and blasted for removal to create even surface and better flow conditions.



Figure 27. Dam 2 and its spillway channel.

3.2.1 Bedrock geology

The geological maps from Swedish Geological Survey (<https://www.sgu.se>) shows the bedrock geology of Dam 2 primarily comprising granites and granodiorites. The bedrock in the spillway channel is massive (Figure 28) and sparsely jointed. The sub-vertically dipping structures mainly run across the spillway channel. These structures look like tension and/or compression induced cracks, which are probably related to compression and extension of the bed rock during deglaciation. When separated the blocks are massive (Figure 29), with block sizes of 5 – 50m³ or more.



Figure 28. Massive granitic bedrock at Dam 2 spillway channel.



Figure 29. Widely spaced vertical structures that form massive rock blocks.

3.2.2 Structural geology

The rock mass can be generally classed as massive, with estimated Geological Strength Index (GSI) values of 80 to 100 (Figure 30). There are few and widely spaced structures, spaced in the order of several meters, and are predominantly near vertically dipping. Where they intersect, they form massive rock blocks.

There is a set of shallow dipping joints upstream at the base of the concrete apron (Figure 31). At the time of field visit the massive slaps formed this joint set was prepared for blasting and removal (Figure 31). These structures are not observed downstream.

During the field visit approximately 11 odd structures were measured. The limited number mapped is due to the fact that these joints were few and sparse. The stereoplot of these structures are shown in Figure 32. The most dominant joint set is that one that dips at 62° with dip-direction of 153°. The random ones have orientations of 86°/254°, 81°/286° and 35°/231°.

Rock joints are smooth and undulating (Figure 33), which is largely due scouring and abrasion. The roughness values are in the JRC class of 6 to 14 and undulation class of IV to VI the surfaces are not slickensided as defined by the Q-system of rock mass classification.

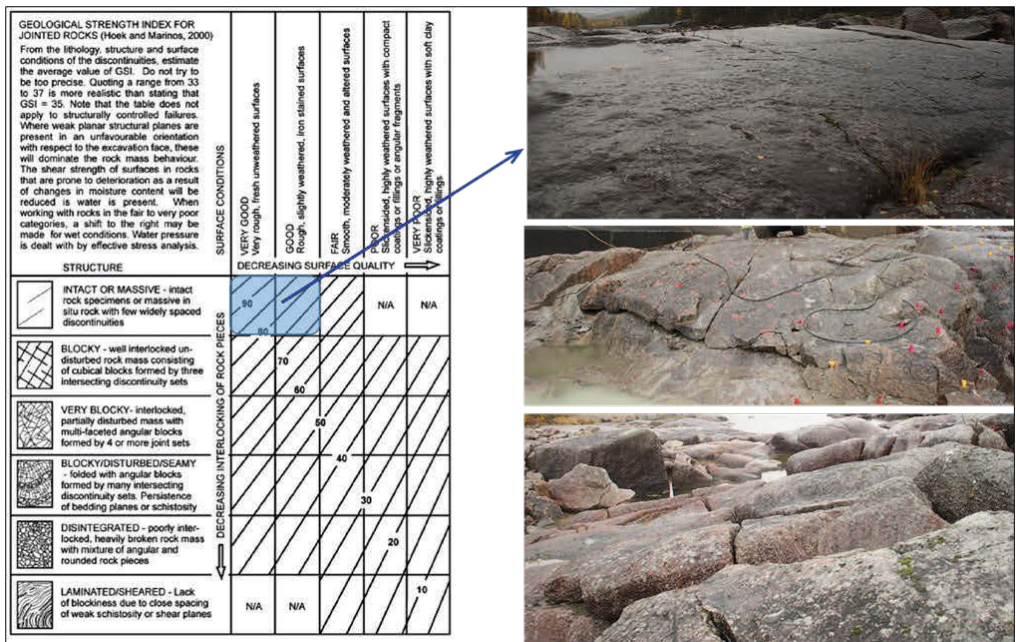


Figure 30. GSI classification of the spillway bedrock at Dam 2.



Figure 31. Shallow dipping joints that form flat lying slabs near the hydraulic jump slope.

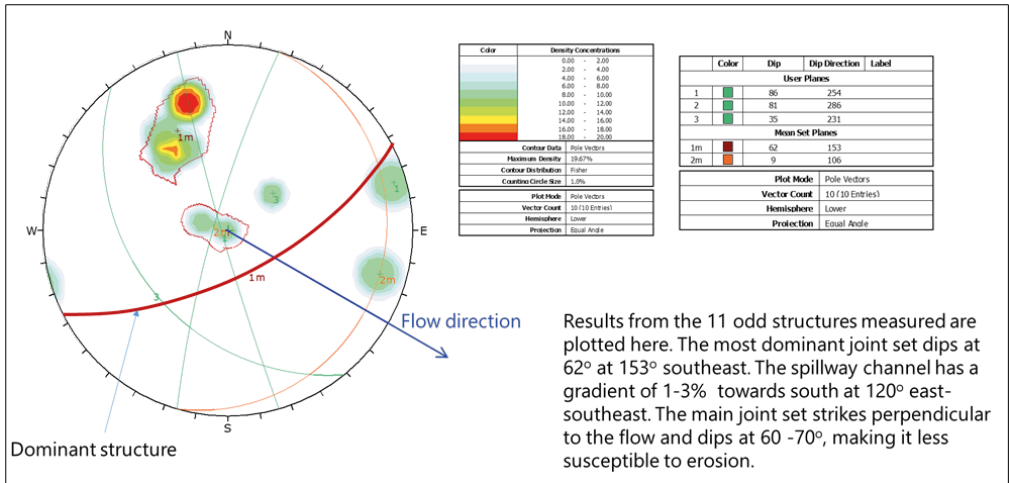


Figure 32. Stereonet of structures mapped at Dam 2 spillway channel.

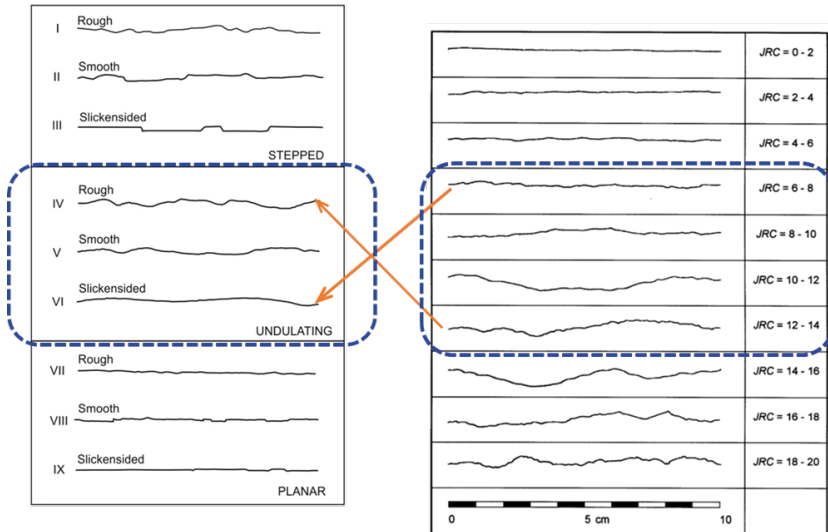


Figure 33. Joints are smooth and undulating, largely resulting from scouring and abrasion.

3.2.3 Block erosion mechanisms

The principal mechanisms for block erosion at Dam 2 appear to be related to fatigue and scouring (Figure 34). Over time the massive blocks appear to show fatigue related cracking. The scouring of the cracks gradually opens the fractures until blocks are separated and dislodged.



Figure 34. Fatigue and scouring are the main mechanism driving the deterioration of rock fractures and eventual dislodgement.

3.2.4 Fracture aperture

At Dam 2 the fracture apertures in the spillway are notably large, 1 to 50 mm, similar characteristics as observed in Dam 1 (Figure 35). The apertures are very wide near the surface, due to the impact of scouring, but gets narrower at depth. The apertures are commonly observed to be filled with sand and gravels, which help in abrasion and scouring of the fractures during flooding. The sand and gravel are mostly eroded materials from upstream.



Figure 35. Large apertures are observed.

3.2.5 Spillway channel domains

The spillway channel at Dam 2 is domained into the 3 sections, based observations of the block erosion and deposition characteristics (Figure 36).

Domain A consist of roughly a 150 m section starting from the dam embankment and going down stream. Domain A consist of massive rock blocks that are still locked to the bedrock. Some of the slabs near the base of the hydraulic jump apron were being manually removed by drilling and blasting at the time of site visit. Block sizes of up to 50 m³ were visually estimated in this domain and noted to be part of bedrock formation (since they are still jointed to bedrock). In the low-lying areas and rock groves, deposition of gavels as well as small and medium size boulders were noted (Figure 37). These gravels and boulders are erosion materials from upstream.

Domain B is a section of bare bedrock. This section is approximately 200 m long. Most of the blocks in this section have been transported downstream. This section also consists of the plunge pool. And scouring of the rock surface is very dominant. The slope of the bedrock is slightly raised towards the downstream side. This could be an important contributing factor for the significant reduction of velocity downstream and thus less erosion. Even vegetations were observed to survive in Domain C (Figure 38), which may also relate to the frequency of the spills.

Domain C is section consisting of materials of various sizes; gravels, boulders (small, medium, large) and massive intact rock blocks (up to 50 m³ or more). Gravels and boulders were part of the eroded rock material that were transported downstream. The massive intact rock blocks are part of bedrock formation.

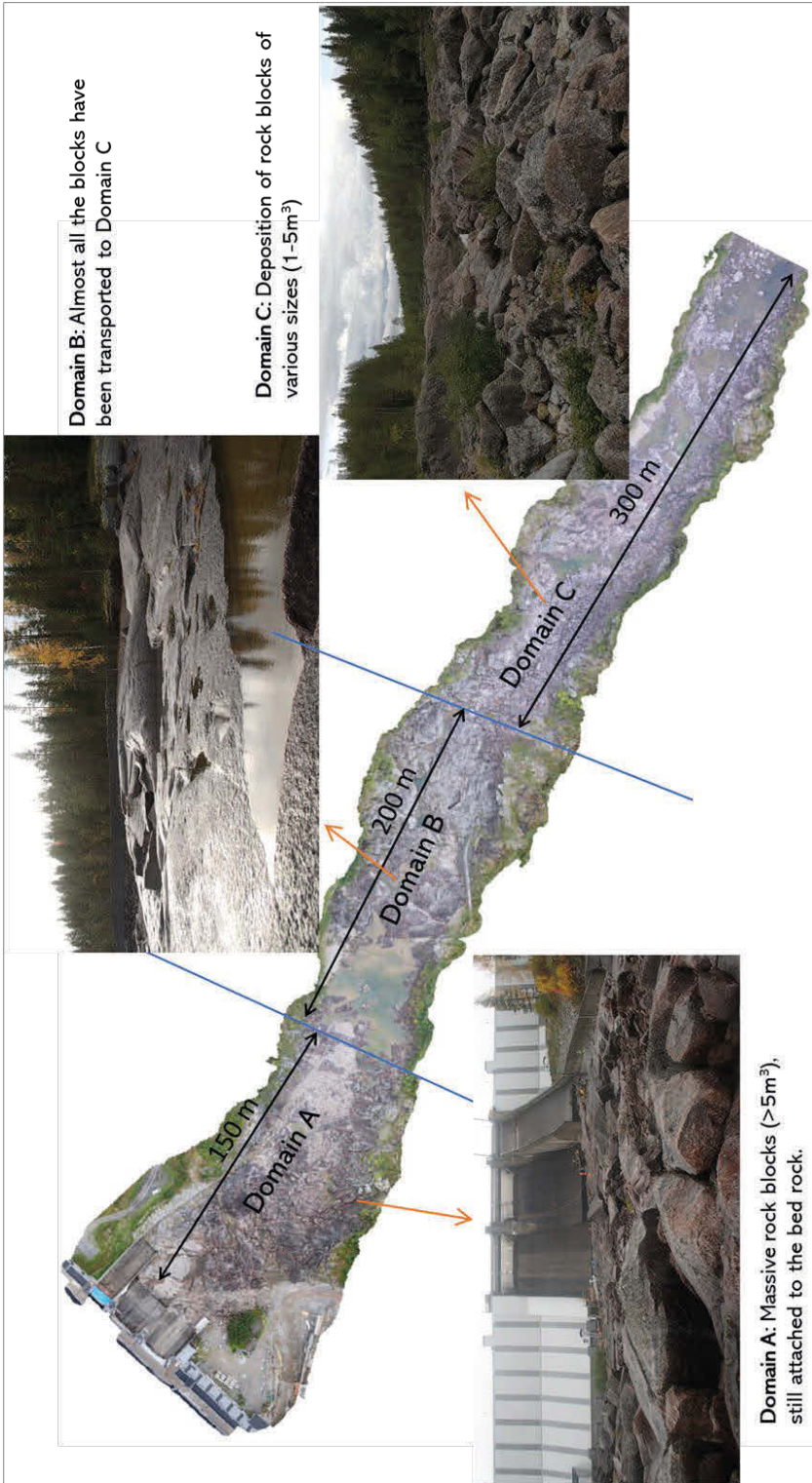


Figure 36. Dam 2 spillway channel domains with representative photos of the domains.



Figure 37. Common sight of gravels, and small and medium sized boulders in low lying areas and groves in the rock in Domain A.

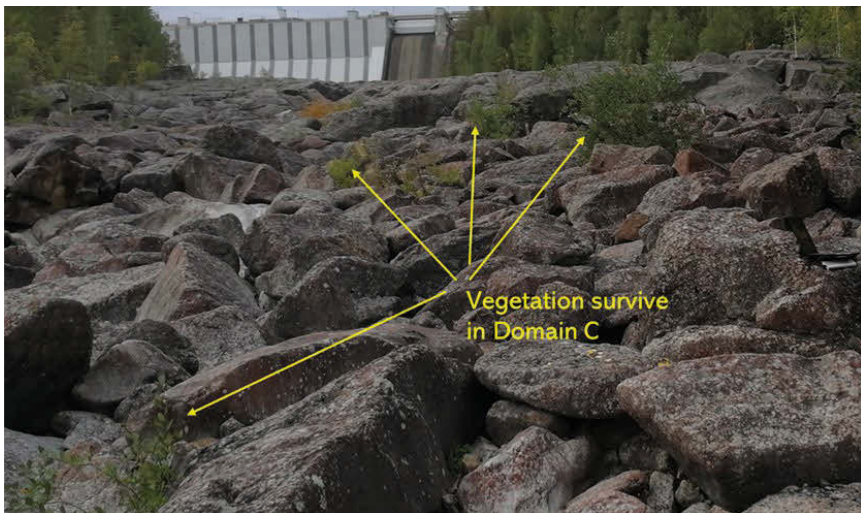


Figure 38. Vegetations survive among rocks, indicating drastic reduction in erosion.

3.2.6 Drone data mapping and analysis

Figure 39 shows the Sirovision structural mapping and analyses of Dam 2 spillway data captured by the drone for Domain A. Inserted in the figure is the table containing the structural data for this domain. There are approximately 5 main block forming joint sets (with IDs 1, 2, 3, 4 and 7). Joint sets with IDs 5, 6 and 8 are random. The inserted stereoplot is for the 5 main joint sets.

However, to get a better averaging of the orientations of the structures they were plotted on equal area and equal area stereonet. This resulted in only 3 dominant joint sets as shown in Figure 40. One joint set dips in the same direction as the flow in the channel, but this joint set is steeply dipping (85°). The most dominant of the 3 joint sets is one that dips at 48° with direction of 263° , which means this set dips upstream. The third structure dips almost vertical (89°) but has a strike that is parallel to the flow direction.

The Sirovision analysed data agrees in principle with the manual mapping that was conducted on site by the LTU team, as well as mapping and analyses conducted by Norconsult AB (2016).

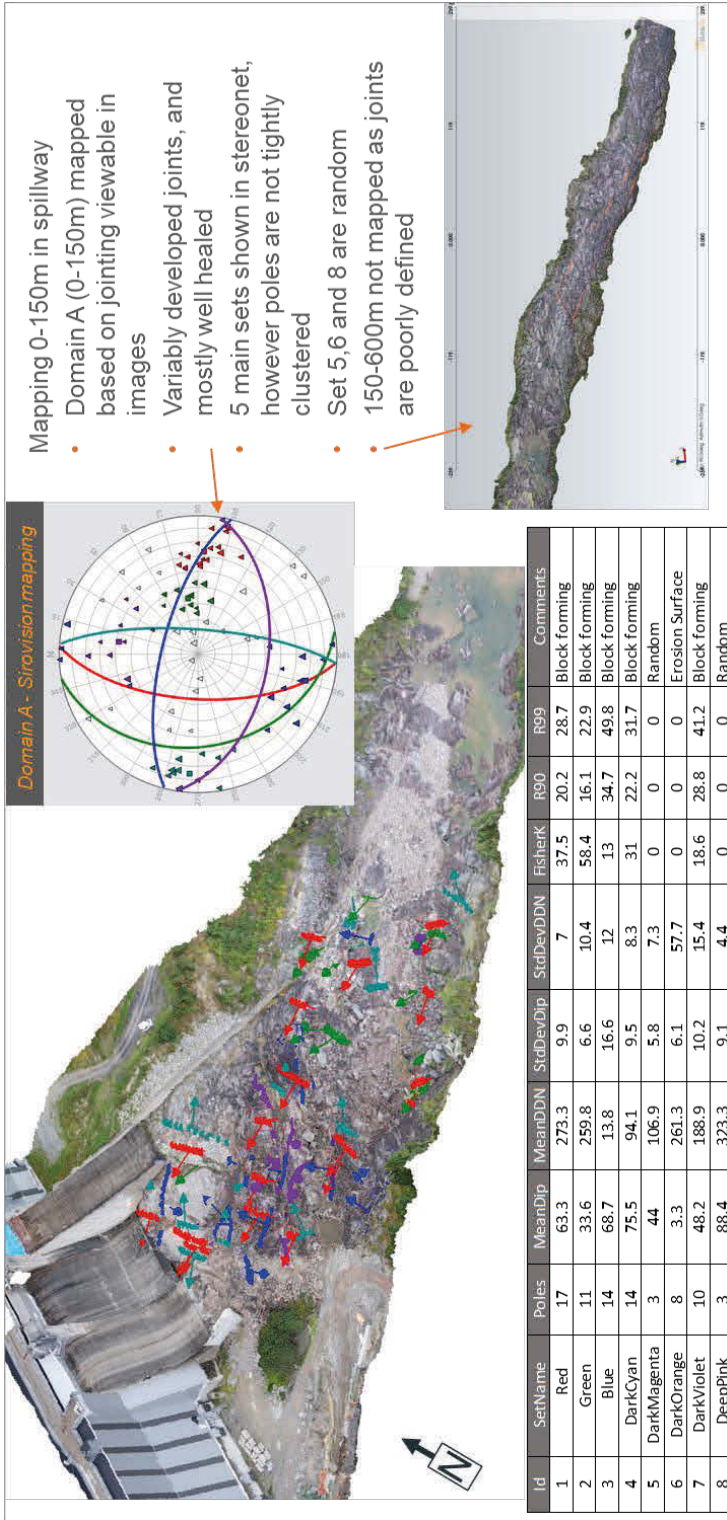


Figure 39. Sirovision mapping of the Dam 2 spillway channel.

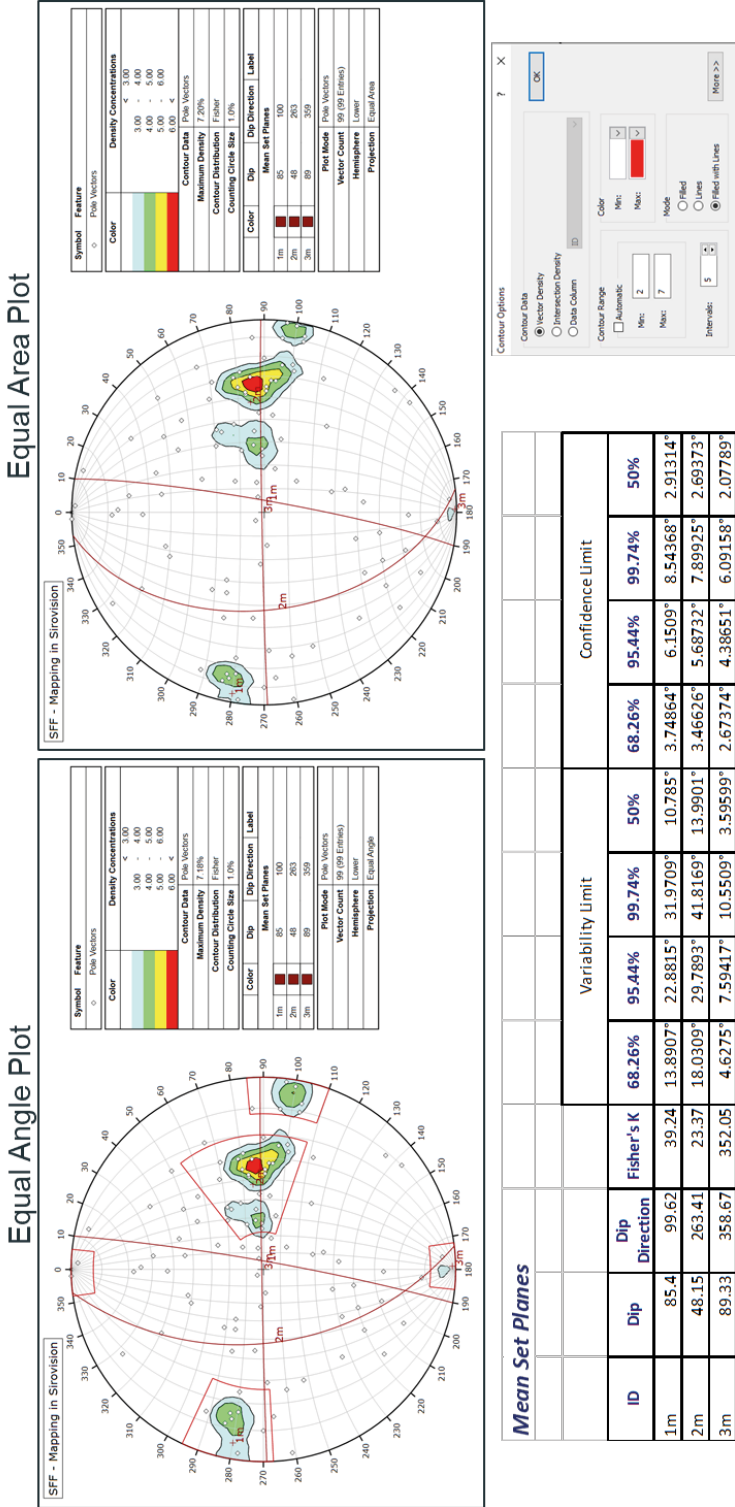


Figure 40. Orientation of structures plotted on Equal Angle and Equal Area stereonets.

3.2.7 Block size analysis

The block forming joints are responsible for the block sizes. These joints need to intersect each other to form the blocks, which means their orientations are essential. Figure 41 shows the data of the spacing and persistence of the main block forming joints. The spacing of the dominant joint sets range between 4 m and 17 m. If the spacing is 4 m then the smallest block that can be formed by the 3 dominant block forming joints (shown in Figure 41) is 35m^3 . This is consistent with the visual observations where blocks of up to 50m^3 were estimated in Domain A, and that most of the blocks are still intact and connected to the bedrock. Domain B consists of massive bedrock with no visible individual blocks. However, in Domain C, gravels and boulders of various sizes (eroded material) and large undetached blocks are seen.

The erosion of small to medium boulders mostly occurs between the large rock block channels and deposited in bays where the water pressure stagnates (Figure 42). Some of them get transported downstream and get deposited in rock groves.

Figure 43 shows the block size analysis for Dam 2. A mining application software BCF (Block Cave Fragmentation) used in block analyses for block caving mining was used to analyse the blocks sizes and distribution. The average block sizes at Dam 2 is about $60 - 80\text{m}^3$. This block range is massive and cannot be easily moved. Hence, the spillway channel at Dam 2 was less vulnerable to block erosion.

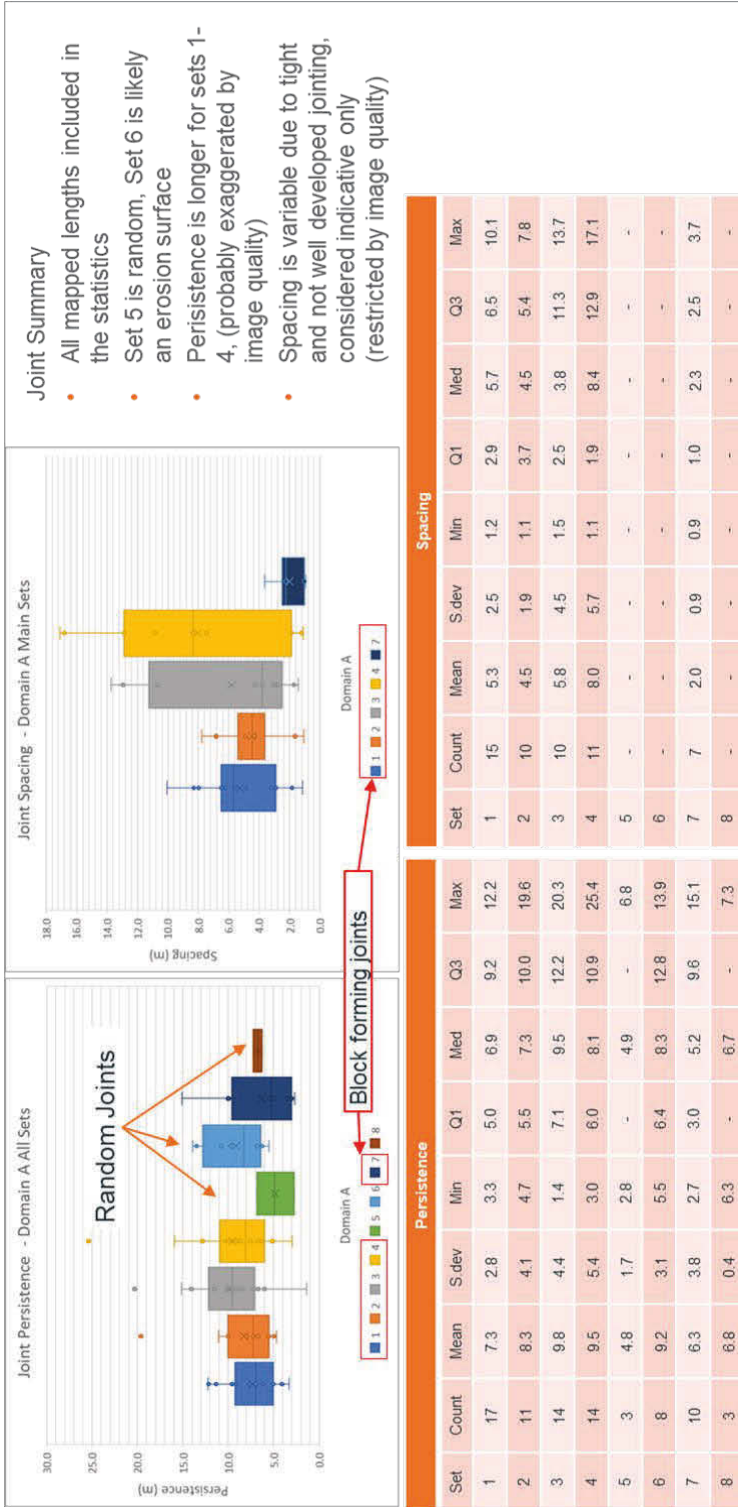


Figure 41. Spacing of block forming joints at Dam 2.

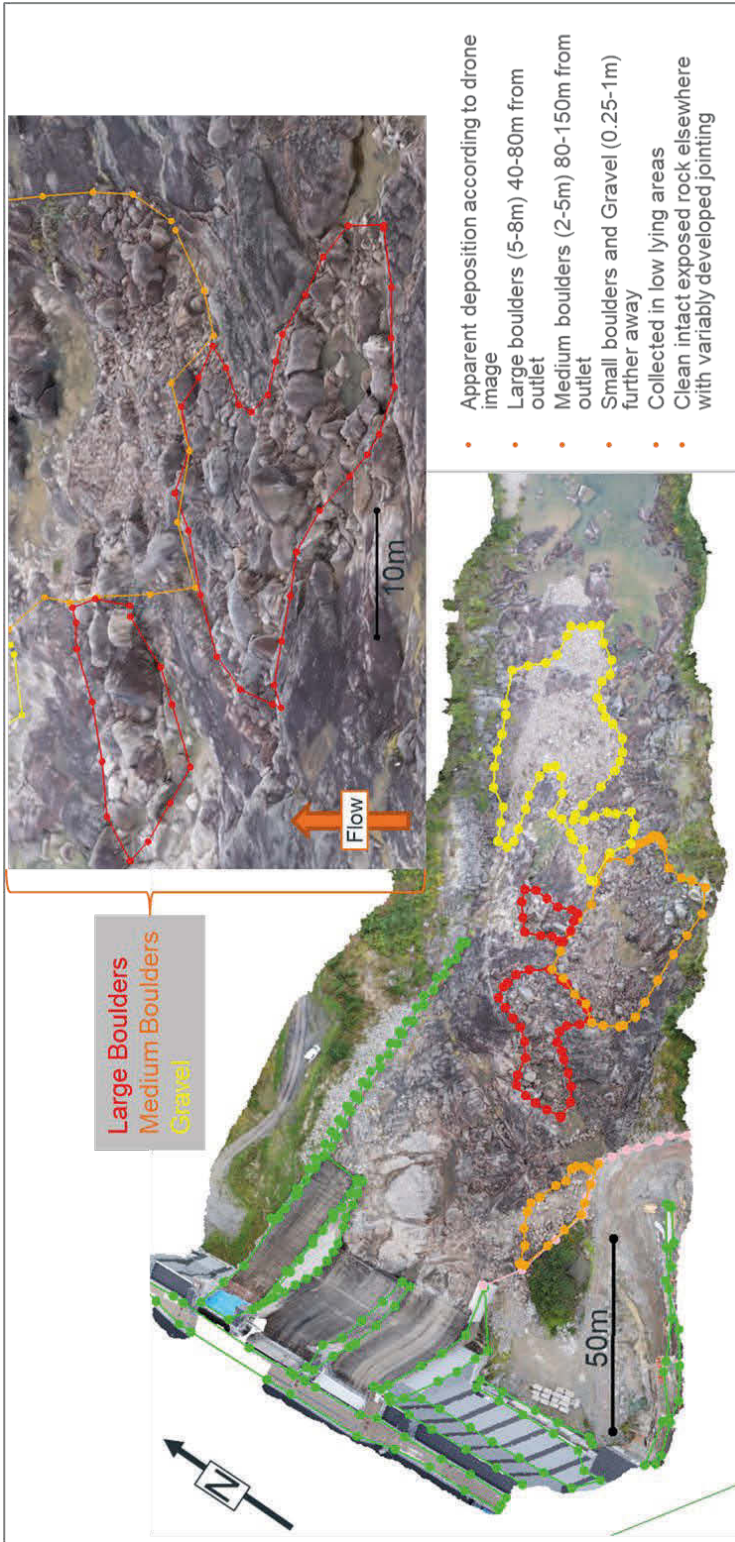


Figure 42. Erosion of small to medium sizes boulders occurs between the channels and large blocks and deposited in bays where the water pressure stagnates.

File Options

Project : SFF BCF
 File: SFFD0MA_0001_1.ram

Rock Type: SFF

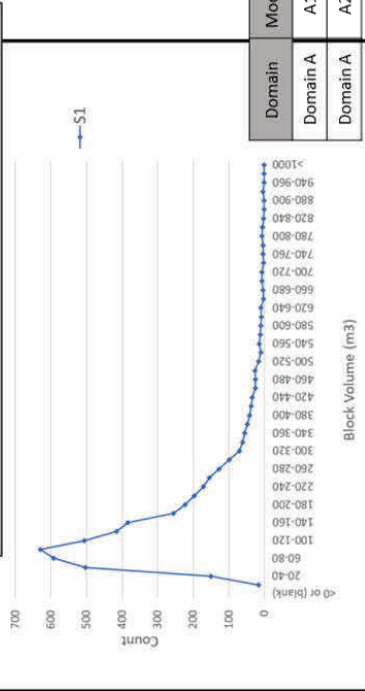
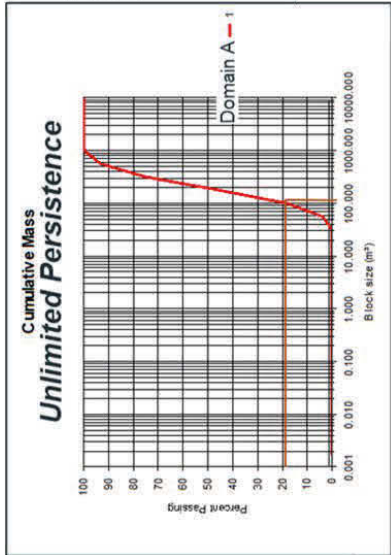
Fracture/veinlet frequency (per m): 0.25
 Fracture/veinlet condition (1-40): 30.00
 Intact block strength (BS (MPa)): 169.0 Calc

Number of sets: 3

Rock mass rating (RMR): 80.00
 Hoek-Brown m-value for rock mass: 25.00
 Intact rock strength (BS (MPa)): 300.0

Joint data

Joint dip		Dip direction		Joint spacing			Joint condition		
Average	Range	Average	Range	Average	Minimum	Maximum	Average	Scaler	
85.00	15.00	99.00	15.00	9.00	3.00	12.50	30.00	5.00	
48.00	15.00	263.0	15.00	5.00	3.50	8.00	30.00	5.00	
85.00	5.00	388.0	5.00	5.00	2.50	13.70	30.00	5.00	



BCF Results Summary

- Results considered indicative for relative comparison to the HAR results only
- Only the 3 main sets are used
- Unlimited persistence at SFF results the block size cumulative mass and volume distribution shown
- With persistence integrated in the analysis the BCF software cannot form blocks
- The average block size is 165m3 from the drone mapping data suggesting a small probability of blocks removable by water flow from the spillway.
- This BCF analysis for SFF is not considered optimal for the erosion potential determination

Domain	Model	Persistence influenced	No. Blocks	Ave. Vol (m³)	S.dev Vol (m³)	Max. Vol (m³)
Domain A	A1	no persistence data used	10000	164.9	129	1154
Domain A	A2	persistence data used	10000	No Blocks Formed		

Figure 43. Block sizes analysis of the Dam 2 spillway canal using BCF software.

3.3 Laboratory tests

Tilt test was conducted to estimate the basic friction angle, while point load tests were conducted to estimate the uniaxial compressive strength (UCS) from the rock samples collected from the two hydropower dam spillways. Table 6 shows the basic friction angles for Dam 1 and Dam 2 from the tilt test conducted.

Table 7 shows the UCS from point load tests on the rock blocks from the respective dam spillways. The Schmidt hammer tests by Norconsult (2016) indicate the UCS of the Dam 2 granite to be about 155 MPa, whereas the point tests conducted by LTU shows UCS of over 200 MPa. The UCS of Dam 2 rock samples ranges between 100 and 300 MPa.

Table 6. Joint basic friction angles determined from tilt test.

Basic friction angle (°)	
Dam 1	Dam 2
36	36
38	26
33	30
40	42
34	35
	46
	35
	29
	23
36.2	33.6

Table 7. Uniaxial Compressive Strength (UCS) estimated from point load test.

Is (bar)	(mm)	σ_c (MPa) Broch	σ_c (MPa) Bieniawski	Description	σ_c (MPa) Average	Standard deviation
Dam 1						
42	56	100.8	100.0	Greyish granite	107.0	8.3
49	48	117.6	109.8			
123	54	295.2	288.4	Brownish granite	307.2	18.7
127	52	328.8	316.5			
Dam 2						
116	68	278.4	300.4	Greyish granite	226.3	49.7
101	46	242.2	222.7			
108	66	259.2	275.9			
97	61	232.8	239.3			
72	39	172.8	149.9			
73	50	175.2	166.1			

4. EMPIRICAL ANALYSES

4.1 Hydraulic Parameters

The flow condition in the spillways is steady and non-uniform hence the hydraulic parameters such as water velocity, Froude number, hydraulic jump properties, unit stream power dissipation etc. are not constant but vary along the spillways. Hydraulic jump often developed when a flow is non-uniform with rapidly flow condition (Chow 1959) and this condition has also been observed at the spillways especially at Dam 2 (Norconsult 2016).

4.1.1 Average water velocity

The average water velocities for the spillways were determined using a 1-D hydrological modelling software HEC-RAS 5.05 (USACE Hydrological Engineering 2016). The HEC-RAS model was used in order to obtain the varying velocities at each domain. The model was established using the spillway aerial view and the discharge capacities from the dams. A key limitation of HEC-RAS is that spatial variation is not considered, which is an important factor of the spillway channel geometry.

4.1.1.1 Dam 1 spillway canal

A channel length of about 450 m from the upstream (toe of the dam) to the downstream was considered (Figure 44) and the channel length was divided into three domains – A, B and C based on their different structural features. Cross-sections were manually drawn perpendicular to the water flow along the channel centreline and the model was solved for steady, non-uniform flow conditions using dynamic wave equations. A manning's coefficient of 0.035 was adopted for the model based on the recommendation of Chow (1959). The discharge capacities of 2000, 2300, 2900 and 3200 m³/s were also considered to study the effect of varying discharge capacity on the spillway erosion. The plot of the mean velocities obtained for all the discharge capacities is presented in Figure 45. The maximum velocity at each domain for each discharge capacity is summarized in Table 1. For all the different discharge capacities as shown in the table domain B has the highest velocity, which is about 10% higher than the maximum velocity at domain A.

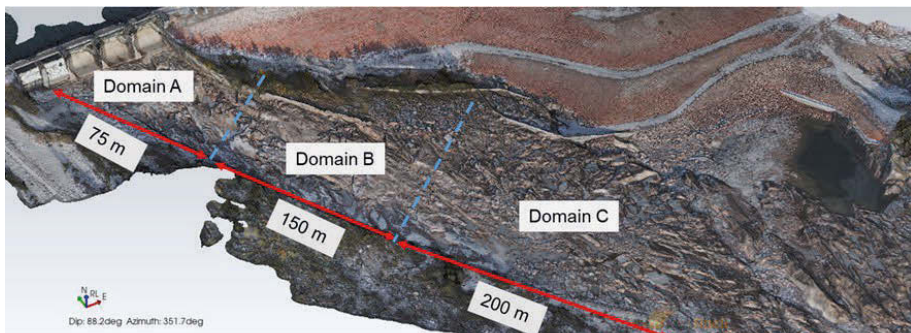


Figure 44. Dam 1 spillway aerial view showing the domains.

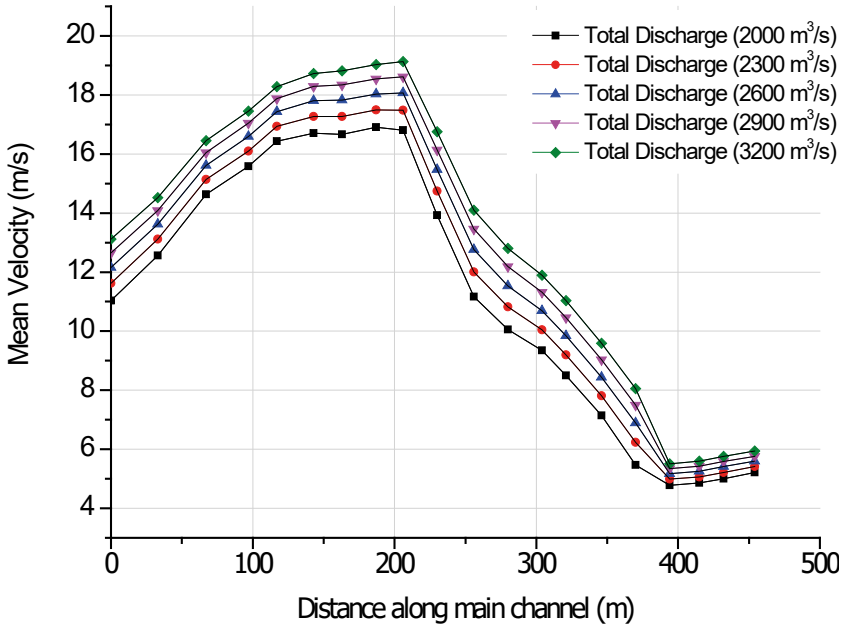


Figure 45. Mean velocities along main channel at Dam 1 spillway for different total discharge capacities.

Table 8. Maximum velocity for different total discharge at each domain for Dam 1 spillway.

Total Discharge (m³/s)	Maximum Velocity (m/s)		
	Domain A	Domain B	Domain C
2000	15.6	16.9	13.9
2300	16.1	17.5	14.7
2600	16.6	18.0	15.5
2900	17.1	18.6	16.1
3200	17.5	19.1	16.8

4.1.1.2 Dam 2 spillway canal

The length of the Dam 2 spillways considered for the HEC-RAS model is about 650 m. The spillway was also divided into three domains – A, B, and C based on the structural features (Figure 46) Cross-sections were also manually drawn perpendicular to the water flow along the channel centreline and the model was solved for steady, non-uniform flow conditions. A Manning's coefficient of 0.035 was adopted for the model based on the recommendation of Chow (1959).

The maximum total discharge capacity of the dam based on the model tests conducted in 2014 is 1163 m³/s at higher reservoir level (HWL) if all the three surface spillways are fully operational simultaneously (Norconsult, 2015). The dam has 3 surface spillways, left, centre and right with

capacity of 265, 452 and 446 m³/s, respectively. The dam also has a bottom outlet, which the capacity is around 450 m³/s. The bottom outlet is yet to be operational, and it will increase the total discharge capacity of the dam when it is operational (Norconsult, 2015). The discharge capacity of 1163 m³/s was used as base value in the HAC-RAS model. The discharge capacities of 1000, 1200, 1400 and 1600 m³/s were also considered to study how the varying discharge capacity affect the extent of the erosion. The plot of the mean velocities obtained for all the discharge capacities is presented Figure 47. The maximum velocities obtained for each domain for the five different total discharges are shown in Table 9.

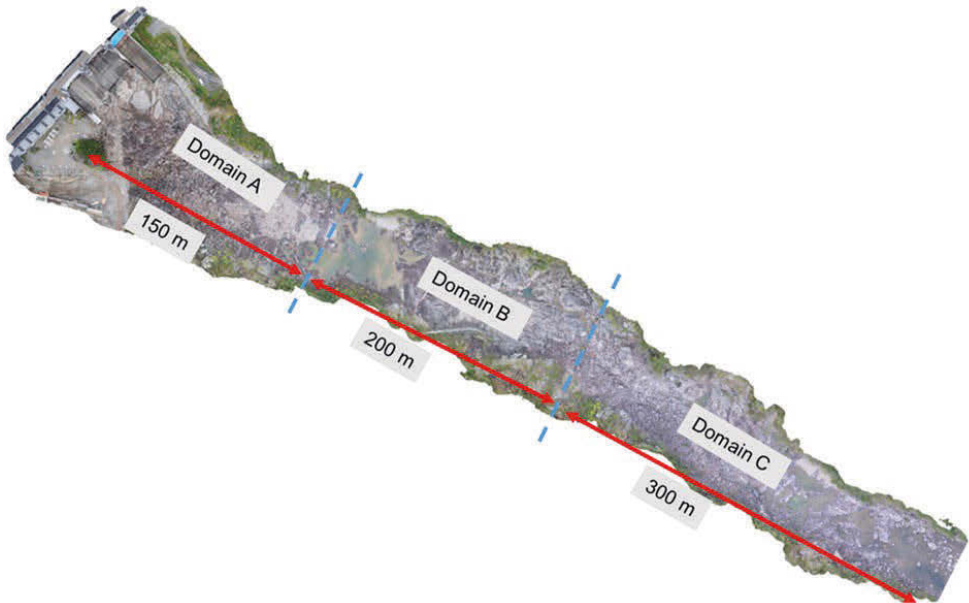


Figure 46. Dam 2 spillway channel aerial view showing the domains.

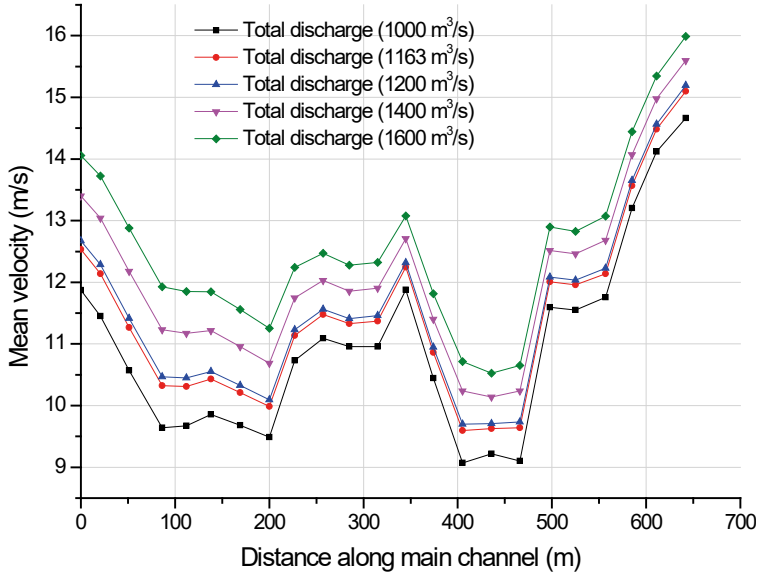


Figure 47. Mean velocities along main channel at Dam 2 spillway for different total discharge capacities.

Table 9. Maximum velocity for different total discharge at each domain for Dam 2 spillway.

Total Discharge (m ³ /s)	Maximum Velocity (m/s)		
	Domain A	Domain B	Domain C
1000	10.1	11.0	14.1
1163	10.7	11.3	14.6
1200	10.8	11.4	14.7
1400	11.5	11.8	15.2
1600	12.1	12.1	15.7

4.1.2 Unit stream power dissipation

The unit stream power dissipation was determined for Dam 1 and Dam 2 spillway channels following the calculation procedure explained in section 2.3.1.3. The unit stream power dissipation for each domain at Dam 1 and Dam 2 spillway channels are presented in Table 10 and Table 11, respectively. Both Annandale and Pells' approaches were considered in the calculation of the stream power dissipation. The significant difference observed between the values of the stream power dissipation obtained from Annandale's approach and Pells' approach is as a result of the fact that Annandale's approach assumes the length of the hydraulic jump to be 1.0 m while the Pells' approach considers the length of the hydraulic jump based on the relationship proposed by Henderson (1966) and Hager (1991) depending on the Froude number.

Table 10. Unit stream power dissipation for different total discharge at each domain for Dam 1 spillway channel.

Total discharge (m ³ /s)	Unit stream Power Dissipation (kW/m ²)					
	Annandale's Approach			Pells' Approach		
	Domain A	Domain B	Domain C	Domain A	Domain B	Domain C
2000	1505	2016	944	29	36	21
2300	1794	2441	1241	33	41	25
2600	2115	2862	1602	36	45	29
2900	2471	3389	1935	39	49	33
3200	2802	3903	2374	41	53	37

Table 11. Unit stream power dissipation for different total discharge at each domain for Dam 2 spillway channel.

Total discharge (m ³ /s)	Unit stream Power Dissipation (kW/m ²)					
	Annandale's Approach			Pells' Approach		
	Domain A	Domain B	Domain C	Domain A	Domain B	Domain C
1000	199	298	782	8	11	21
1163	265	344	954	10	11	23
1200	280	360	994	10	12	24
1400	378	422	1206	12	13	27
1600	494	490	1431	14	14	29

4.2 Rock mass erodibility

Erodibility index, which is a geomechanical index that quantifying the resistance of the rock mass to erosion was estimated for the rock mass underlying the spillways at Dam 1 and Dam 2. The index (Kr), as explained in section 2.3.1.2, is expressed in the form of $Kr = MsKbKdJs$ where Ms is the material strength of the rock material, Kb is the block number, Kd is the joint shear strength number and Js is the number for the relative ground structure. In addition to the erodibility index, the Geological strength index (GSI) was estimated for the rock mass underlying the spillways at the two dams based on the description of the rock mass as observed during the field visit to the spillways. From the GSI the values, rock mass index ($eGSI$) (Pells 2016) was estimated. The $eGSI$ is expressed as $GSI + Edoa$ where $Edoa$ is the orientation adjustment factor to represent the effect of rock block shape and orientation relative to the direction of the flow (Pells 2016). Annandale's method uses the erodibility index for the determination of erosion threshold while Pells' approach utilizes the rock mass index for the categorization of the erosion risk.

4.2.1 Erodibility and rock mass indices for the spillway

The uniaxial compressive strength (UCS) of the rock samples from Dam 1 based on the point loads test conducted at LTU ranges between 100 and 300 MPa and the reported UCS of the Dam 2 granite ranges between 140 and 155 MPa (Hellström 2012). By using the equation proposed by

Wyllie (1999) the M_s for the Dam 1 and Dam 2 should range between 98 and 294 and 137 and 152, respectively. For the assessment of the erosion the worst case was assumed hence the smaller values of M_s was considered. It is also assumed that the M_s for the domains is relatively the same.

The RQD for the rock mass underlying the spillways at the dams was estimated using the equation proposed by Hudson and Priest (1979), which is expressed as $RQD=100e^{(-0.1\lambda)} (0.1\lambda+1)$ where λ is the joint frequency. The joint spacings for the Dam 1 and Dam 2 have been presented in Figure 25 and Figure 41, respectively. There are three main joint sets at Dam 1 spillway and three sets plus random at Dam 2 spillway. Table 1 was used determine the J_n and together with the RQD the corresponding K_b was determined for the spillways.

The field mapping at the two dams showed that the joints at the spillways are mostly smooth and undulating with slightly altered joint walls (see Figure 20 and Figure 33). Therefore, K_d for the spillways at the two dams is $2/2 = 1$ according to Table 2 and Table 3.

The most susceptible joint sets to erosion in Dam 1 and Dam 2 spillway channels are $14^\circ/107^\circ$ and $65^\circ/180^\circ$ (dip and dip direction) respectively. The effective dip, which is the difference between the apparent dip and the spillway slope, was determined for the joint sets. The values of the effective dip were used together with joint spacing ratio to determine J_s for Dam 1 and Dam 2 spillways using Table 4.

The rock mass at Dam 1 spillway was observed to be blocky with GSI values of 60 to 80 especially at the domain A of the spillway and there is shear zone within this domain which is very block with GSI value of 50. Domains B and C was observed to be massive and the GSI value ranges between 80 and 90. Meanwhile, the rock mass at Dam 2 spillway can be classified to be massive with GSI values ranging from 80 to 100, the GSI value is almost the same for all the domains. The rock mass ($eGSI$) was determined by modifying the GSI values to account for discontinuity orientation adjustment ($Edoa$) (Pells 2016). The $Edoa$ was determined for both spillways using Figure 7. It is important to note that the minimum of the range of GSI is chosen for the assessment.

The summary of the erodibility (K_r) and rock mass ($eGSI$) indices for the Dam 1 and Dam 2 spillways rock masses are presented in Table 12 and Table 13, respectively.

Table 12. Erodibility and rock mass indices for Dam 1 spillway.

Domain	M_s	K_b	K_d	J_s	K_r	$eGSI$
A	98	35	1	0.98	3400	40
B	98	36.5	1	0.98	3500	60
C	98	36.4	1	0.98	3500	60

Table 13. Erodibility and rock mass indices for Dam 2 spillway.

Domain	M_s	K_b	K_d	J_s	K_r	$eGSI$
A	137	29.9	1	0.42	1720	65
B	137	29.9	1	0.42	1720	65
C	137	29.9	1	0.42	1720	65

4.2.2 Erodibility Threshold

The potential erosion of the rock in the spillways at Dam 1 and Dam 2 was determined by comparing the calculated unit stream power dissipation to the erodibility index of the rock mass at the spillways as shown in Figure 48 and Figure 49 for Dam 1 and Dam 2, respectively. The figures show that erosion of rock is expected to occur at the Dam 1 and Dam 2 spillways at the total discharge capacities of 2600 m³/s and 1163 m³/s, respectively. The erosion is expected to occur at the three domain areas of the spillways. These erosion potentials at the spillways matched the observation during the field visits to the spillways. To determine the effect of the varying discharge capacities on the erosion potentials the stream power dissipations provided by the discharge capacities were also compared with the erodibility index of the rock mass. The results show that the rock erosion is expected on all the domains of Dam 1 and Dam 2 spillways at all the discharge capacities considered.

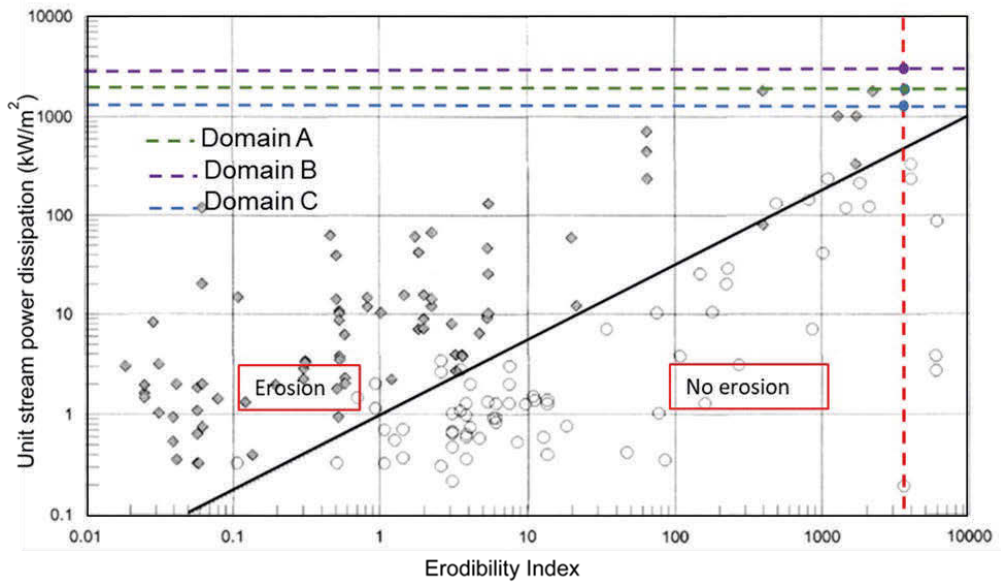


Figure 48. Erodibility threshold for rock at the spillway of Dam 1 at its average discharge capacity.

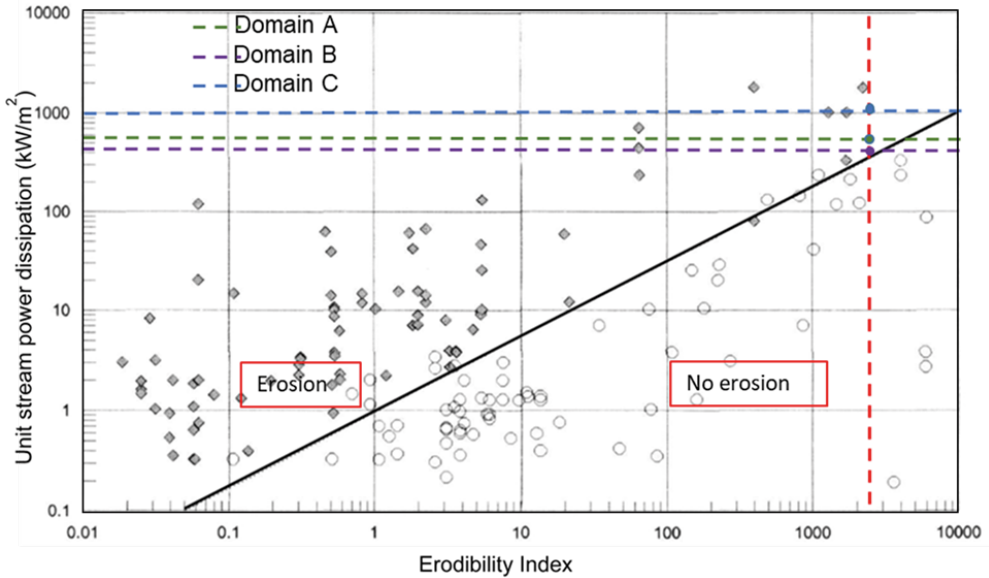


Figure 49. Erodibility threshold for rock at the spillway of Dam 2 at its average discharge capacity.

4.2.3 Categorization of Erosion Risk

The Annandale's approach of erosion threshold only indicates the potential of rock erosion without any information about the severity of the erosion. To determine the category of the risk of the rock erosion at the Dam 1 and Dam 2 spillways the calculated unit stream power dissipations for the spillways were compared with the corresponding rock mass index ($eGSI$) as shown in Figure 50 and Figure 51. Figure 50 shows that at the discharge capacity of $2600 \text{ m}^3/\text{s}$ the erosion expected at Dam 1 spillway at the three domains is moderate. According to Pell's (2016) an erosion is categorized as moderate when erosion depth ranges between 1.0 and 2.0 m. There is no significant effect of the varying discharge capacities on the categorization of the erosion at Dam 1 as the risk of the erosion is moderate for all the three domains for the different discharge capacities considered except in domain C for discharge capacity of less than $2600 \text{ m}^3/\text{s}$ that the erosion risk is minor.

The category of the erosion risk expected at Dam 2 spillway for all the domains as shown in Figure 51 is minor with erosion depth of 0.3 to 1 m based on the Pell's (2016) categorization of erosion. Like the observation at Dam 1 the varying discharge capacities did not change the risk of the rock erosion at Dam 2 spillway – the risk remains minor for all the domains for the different discharge capacities considered.

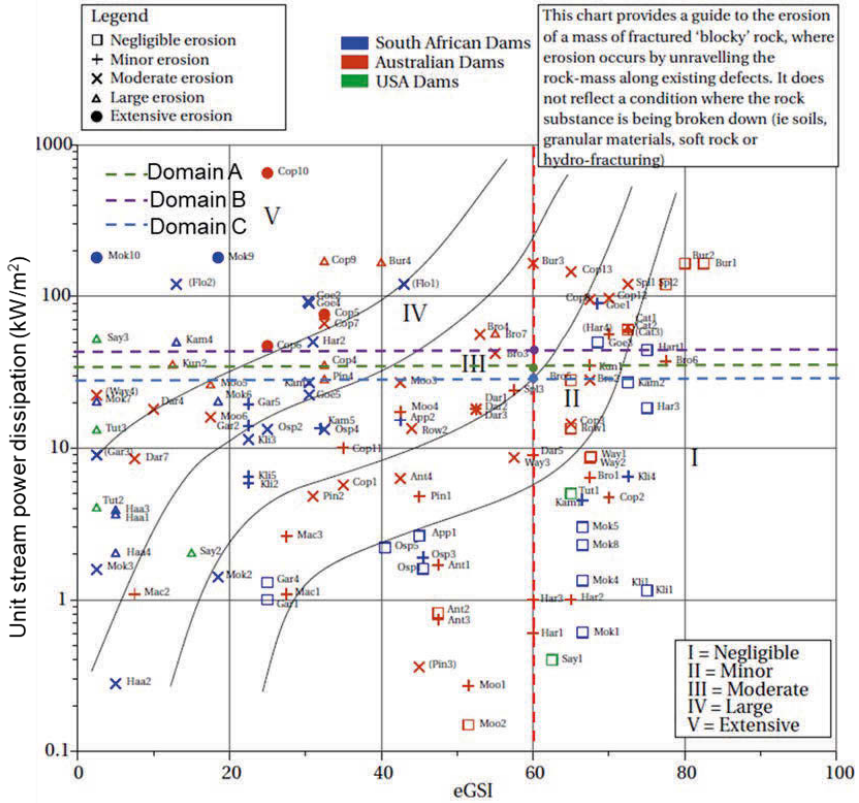


Figure 50. Erosion risk category for rock at the spillway of Dam 1 at its average discharge capacity.

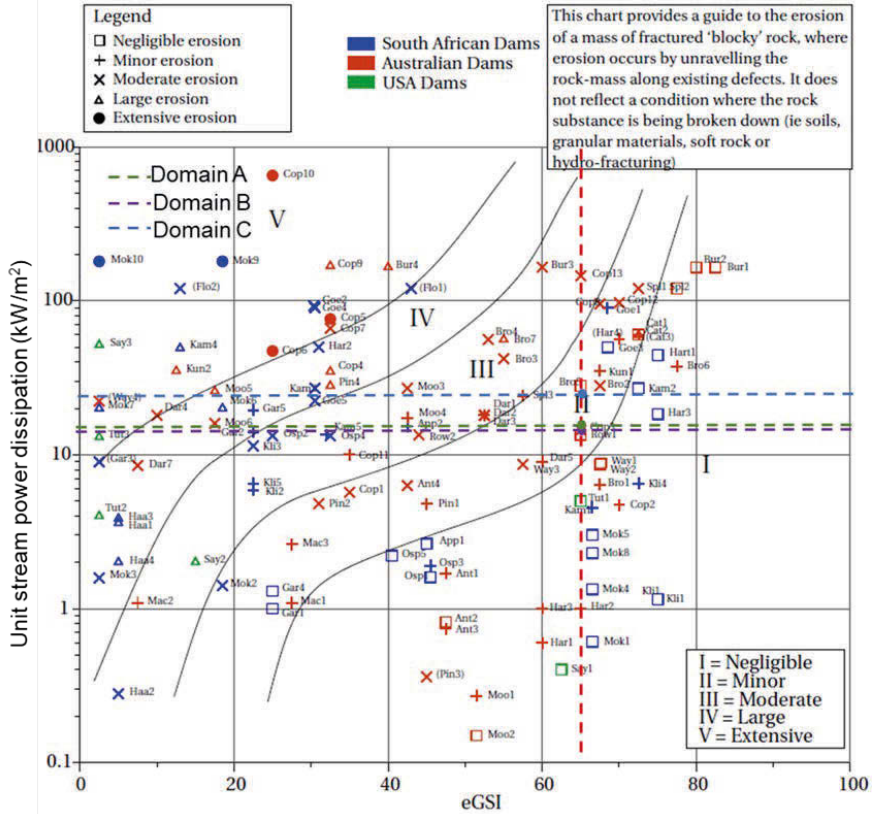


Figure 51. Erosion risk category for rock at the spillway of Dam 2 at its average discharge capacity.

5. NUMERICAL ANALYSES

5.1 Modelling approach

Two important hydraulic actions work in tandem to initiate and drive rock block erosion in an open channel, and they are:

- (i) the pore pressure and fluid flow within the jointed rock mass, and
- (ii) the moving water column.

The pore-pressure and flow in the jointed rock mass contribute towards the dislodging of rock blocks within the rock mass, while the moving water column creates shear stress on the floor of the open channel. Thus, on the upper surface exposed to the moving water the rock block will experience shear stress, while under and around it will experience the effect of pore pressures. Some rock blocks especially those located within the zone where the water velocity is zero, will experience stagnation or static pressure from the under blocks and dynamic pressure on the top surface (e.g., George 2015). In open channels the stagnation pressure occurs in the region near the channel floor where the flow velocity is equal to zero. This is to be differentiated from pore pressure which builds up within the fractured rock mass and is a function of hydraulic head.

Since 3DEC is a static numerical code, the water column mesh is connected to the spillway channel bedrock mesh. This is presented and discussed in the model setup section later. On the boundary of the water column a shear velocity is applied instead of shear stress. This is because it is easier to apply velocity boundary with the dip and dip direction so as to make the velocity boundary conform to the channel geometry and flow direction. The shear velocities were calculated using empirical relations (or law of the wall relations) using the average velocities and water column height determined from HEC-RAS simulations (section 4.1.1).

For the rock mass the pore pressure are applied on the boundaries to allow flow to occur from high pressure region to low pressure region. In these models, flow is allowed to occur only through the fractures or joints and not through the rock matrix.

Two approaches were used in the modelling. Dam 1, modelled by Itasca Sweden, involves modelling only with pore pressure and flow in the joints. Their models do not consider the shear stresses created by the moving water column. Dam 2, modelled by LTU, considers both the pore pressure and flow in joints, as well as the shear stress created by the moving water column. The differences in the results are presented in the discussion section of this chapter.

The processes and limitations of modelling of a hydro-mechanically coupled dynamic problem in 3DEC are discussed throughout sections 5.6 to 5.11.

5.2 Rock mass inputs

Inputs for the numerical modelling are summarized in this section. They have been either measured or derived from field investigations, laboratory testing, literature and empirical analyses, i.e., Chapters 3 and 4. Table 14 shows the rock mass parameters for Dam 1 and Table 15 for Dam 2. The hydraulic parameters applicable to spillway canals are shown in Table 16.

Table 14. Dam 1 rock mass parameters.

Basic rock parameters	Description and/or values
Rock type	Granite
UCS	200 MPa (average from PLT)
Deformation modulus	-
Poisson's ratio	0.25
Basic friction angle	36° (from tilt test)
GSI	65 (average, fair to good rock)
Rock mass modulus	2.7 GPa
Joint aperture	1-50 mm
JRC	6-12
Joint cohesion	0.05 MPa
Joint normal stiffness (Kn)	10 GPa*
Joint shear stiffness (Ks)	10 GPa*

*From Möreen (2005).

Table 15. Dam 1 rock mass parameters.

Basic rock parameters	Description and/or values
Rock type	Granite and granodiorite
UCS	200 MPa (average from PLT)
Deformation modulus	-
Poisson's ratio	0.25
Basic friction angle	34° (from tilt test)
GSI	80 (good to very good rock)
Rock mass modulus	2.7 GPa
Joint aperture	1-50 mm
JRC	6-14
Joint cohesion	0.05 MPa
Joint normal stiffness (Kn)	10 GPa
Joint shear stiffness (Ks)	10 GPa

Table 16. Hydraulic parameters.

Hydraulic parameters	Description and/or values
Water density	1000 kg/m ³
Water bulk modulus	2.0 GPa
Viscosity	8e-4 Pa/s

5.3 In-situ stresses

The in-situ stresses for the mechanical coupling are those stresses that are commonly used for rock mechanical modelling in Sweden. In this case the stress regime reported by Stephansson (1993), based on hydrofracturing measurements are used:

$$\sigma_v = \rho g z \quad 12$$

$$\sigma_H = 2.8 + 0.04z \quad 13$$

$$\sigma_h = 2.2 + 0.024z \quad 14$$

Where σ_v is the vertical stress, ρ is the rock density, g is gravity and z is the depth. σ_H is the major horizontal stress, and σ_h is the minor horizontal stress.

5.4 Water pressure

It is assumed that the flow velocity is uniform along the channel. Therefore, the total hydraulic pressure can be calculated as:

$$\text{Total water pressure} = \rho g h + \frac{v^2}{2} \rho \quad 15$$

Where ρ = water density, g = gravity, h = water column height and v = average flow velocity, $(v^2/2)*\rho$ is the kinetic pressure component.

At the top of the water column the water pressure is equal to the kinetic pressure due to the flow velocity and is therefore not equal to zero (see Figure 52). The kinetic pressure is added to the potential pressure to give the total water pressure, which is distributed in the model as shown in Figure 52. The pore pressure that is developed in the jointed bedrock is due to this total water pressure, which is represented by equation 15.

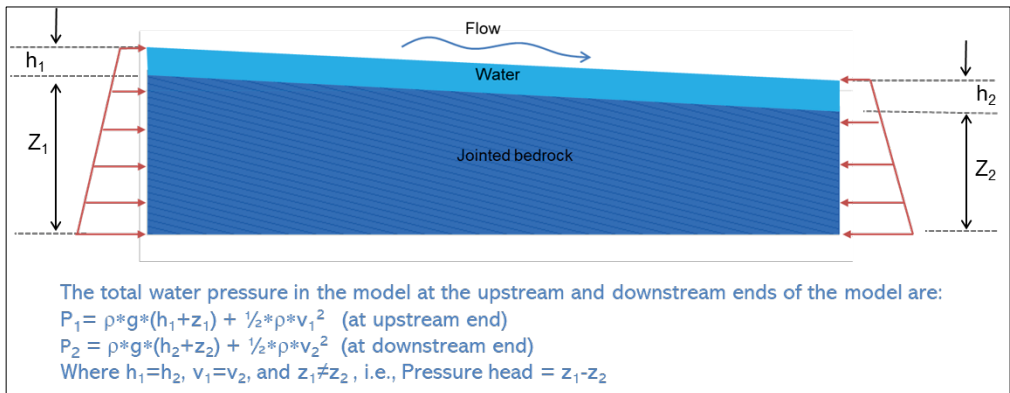


Figure 52. Pressure boundary conditions.

5.5 Shear velocity

At base of the channel a rock block would experience both the hydraulic pressure as well as the shear stress applied by the moving water. This is illustrated in Figure 53, where the block is hydraulically jacked by a combination of pore pressure and stagnation pressure, as well as turbulent uplifting induced by pressure fluctuations (e.g., George 2015). The stagnation pressure occurs in the region where the velocity goes to zero. According to the law of the walls this region is correlated to the surface roughness wall. In the case of the open channel this protruding height of blocks in the channel (see Figure 54). In the case of the open channel. For Dam 1 this roughness or protruding height (Z_0 in equation inserted in Figure 55) was measured over a 100 m length and found to average around 20 cm (see Figure 55). The same protruding height was assumed for Dam 2.

The shear velocity which is responsible for the development of shear or drag force acting on the canal floor in the direction of flow can be calculated by re-arranging the equation shown in Figure 54. The von-Karmen's constant, K , is about 0.41. In the 3DEC model, the shear velocity corresponding to average velocity and water column height were applied to the water column to create the drag force. The average velocity (V) profiles and corresponding was column heights (Z) along the two canals were determined using the software HEC-RAS and the actual canal profiles.

Because the channel has a slope, the dip and dip direction were also defined for the shear velocity, which corresponds to that of the channel slope. An example of the script in 3DEC model where the shear velocity is applied on the water column is given by this script example: `boundary velocity 5 dip 5 ddirection 180 range group "water_column"`. This line means that a shear velocity of 5 m/s is applied with a dip of 5° and dip direction of 180° , which corresponds to the dip and direction of the channel slope.

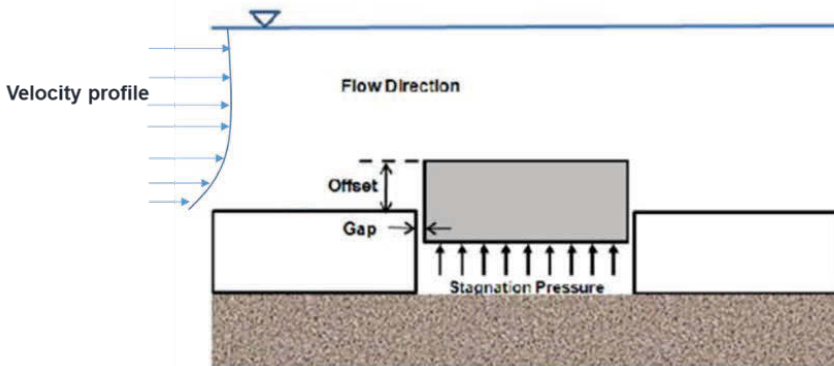


Figure 53. Lifting of rock block by resulting from stagnation pressure (modified after George 2012).

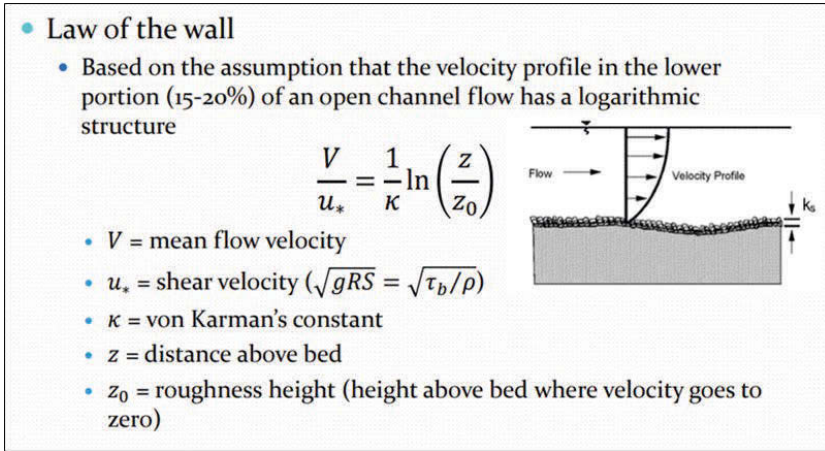


Figure 54. Law of the walls (Julien, 2008).

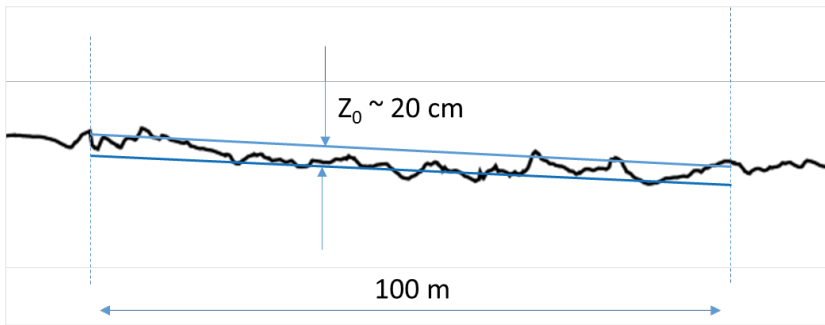


Figure 55. The roughness or protruding height (Z_0) at Dam 1 channel.

5.6 Modelling approach

The first attempt in the numerical analyses involved both continuum and discontinuum methods. For the continuum method, LS-Dyna was attempted to allow water to dynamically accelerate against a protruding block of rock. It was aimed at investigating fatigue development on the block with cyclic dynamic loads. However, this approach was abandoned after a reference group meeting that deemed it unnecessary given the time limitations. Nevertheless, the approach still presents itself as a useful technique to investigate fatigue and scouring processes. As referenced to in the literature chapter, a similar approach was used by Dasgupta et al (2011) where they used ANSYS FLUENT to investigate scour formation in Karina Dam in Zimbabwe, while at the same time they used UDEC to investigate block erosion in the rock mass, with inputs obtained from ANSYS FLUENT analysis.

George (2015) argued in his PhD thesis that rock erosions in an unlined spillway is truly a 3D problem and used 3D DDA method to study scouring and rock erosion of unlined spillways. The LTU team also agree with George's view and therefore felt that Itasca's 3DEC software was best suited for the block erosion study herein.

For details about coupled hydro-mechanical modelling procedures the reader is referred to Itasca's 3DEC manual (Itasca 2022). A link to the manual website is shown in the reference list.

5.7 Assumptions

The flow in an open spillway channel is complicated to numerically model. The most important assumption for the models herein is that the flow along the channel is uniform, in which case the flow velocity is constant for the entire length of the channel being modelled. Non-uniform flows, including hydraulic jumps, are not considered in the models (see Figure 56).

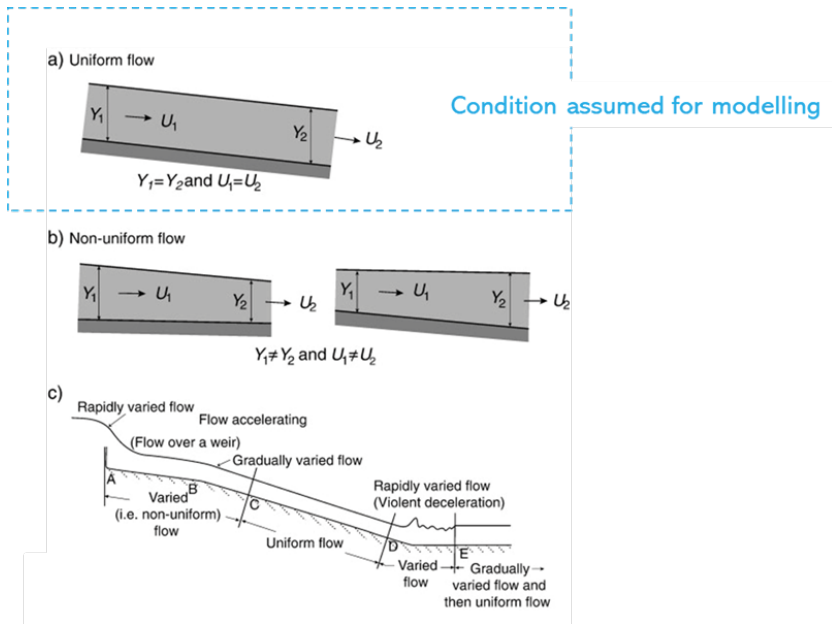


Figure 56. Flow conditions and assumptions in open spillway channel (from Lindblom's lecture notes, 2020).

5.8 3DEC Modelling

Itasca's (Itasca 2019) three-dimensional distinct element code, 3DEC, was considered suitable and thus used in numerical modelling for the block erosion study. To study the displacements in jointed rock mass along the spillway the models were fully coupled hydro-mechanically so that the impact

of fluid flow and mechanical response on the rock blocks are captured. For this study the models were configured to only allow flow to occur through the rock joints and not through the rock matrix. In a fully coupled model the responses due to both action of fluid flow and corresponding mechanical response lead to the total displacements observed. The model coupling procedures are described as part of modelling process in the proceeding sections.

5.9 Single block models

Single block models were setup to specifically study various parameters that influence the block response. This can be considered as a parameter study. The parameters varied were block size, water column height, water velocity and gradient of the channel slope. The fracture apertures and the dip and direction of the block were kept to observations made at Dam 1.

5.9.1 Model setup

Figure 57 shows a sample geometry of the single block model in 3DEC. The block is created by the 3 distinct joint sets observed at Dam 1. To achieve a desire block size the spacing of joints are varied in 3DEC and querying the block (in 3DEC) to determine the exact geometrical parameters and the block size. In Figure 57 for instance, the block formed by the joints is a prism with trace lengths of 0.8 m x 1.5 m x 1.5 m and apex height of 0.4 m. This resulted in block size of $\sim 0.5 \text{ m}^3$, which is a good representation of the blocks observed at Dam 1.

The properties of the joints are shown in the Table 17. The apertures are estimated from field observations, which ranged between 1 mm and 50 mm. The apertures of the joints dipping in the direction of the flow were observed to be larger, which in this case would be Joint 1. Friction is estimated from tilt test from the blocks collected from the spillway. The cohesion, K_n and K_s , are taken from previous studies (e.g., Mören 2005).

Measurements points were located at the nodal points around the block to observe for example the pore pressure, normal stress, velocity and displacements. Figure 58 shows an example of the placement of the measurement points around the base of the prism at the nodal points.

The geometry of the single block 3DEC model is shown in Figure 59. The model is 10 m x 10 m x 10 m (x, y, z) and is divided into upper and lower blocks. The lower block is unfractured, so the joints do not continue down to this block. The upper block is fractured by the joints, so flow can occur through the joints in the block. The flow is only allowed to occur through the joints and not the matrix. This option was configured in 3DEC.

The model block is mechanically fixed on the walls and the base. To initiate flow, pressure gradients were initiated with a head loss (h_1-h_2 , see Figure 52) on the right and left of the model, see Figure 60. As described earlier the shear velocity applied on the water column has a dip and dip direction, which correspond the slope dip and slope direction.

Note that, the water column mesh is connected to the canal rock mass as shown in Figure 60. The shear velocity applied on the water column at the boundary is translated into shear stress acting on the floor of the canal. This shear stress induces the drag force acting parallel to the flow direction.

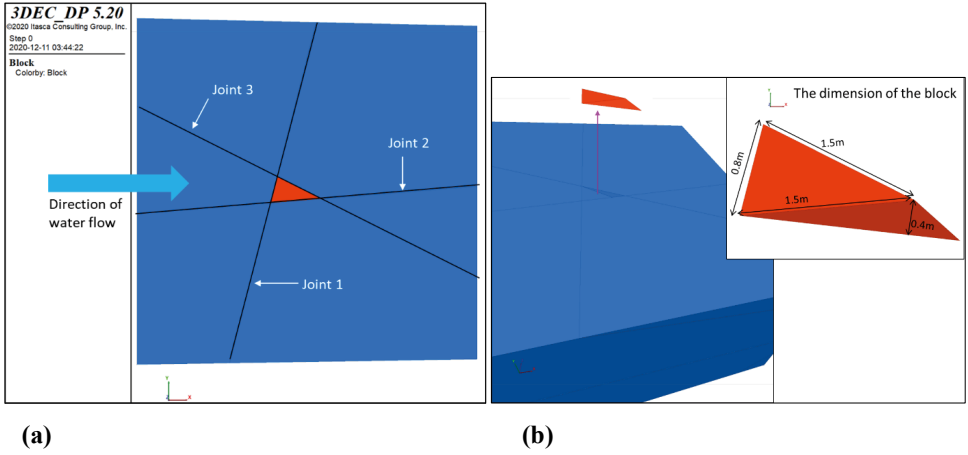


Figure 57. (a) Single block formed by the distinct joint groups at Dam 1, (b) the geometry of the block.

Table 17. Properties of the single block forming joints.

	Joint orientation		Aperture			Joint mechanical parameters			
	Dip (°)	Dip-Dir (°)	Ave. (m)	Min (m)	Max (m)	Friction (°)	Cohesion (MPa)	Kn* (Pa/m)	Ks** (Pa/m)
Joint 1	14	81	5e-3	5e-4	5e-2	36	0.05	10e9	10e9
Joint 2	58	110	1e-4	1e-5	1e-3	36	0.05	10e9	10e9
Joint 3	30	170	1e-3	1e-4	1e-2	36	0.05	10e9	10e9

*Kn = Joint normal stiffness

**Ks = Joint shear stiffness

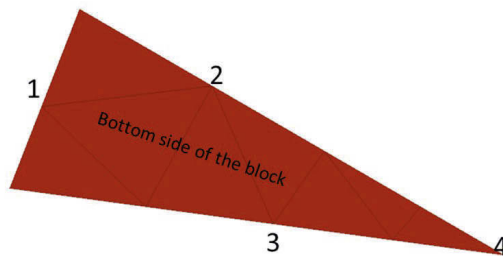


Figure 58. Measurement points on base of the block at the nodal points

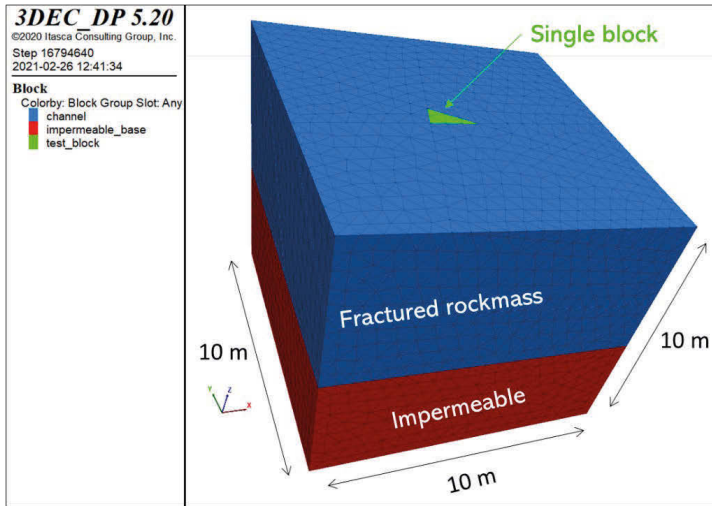


Figure 59. Single block 3DEC model.

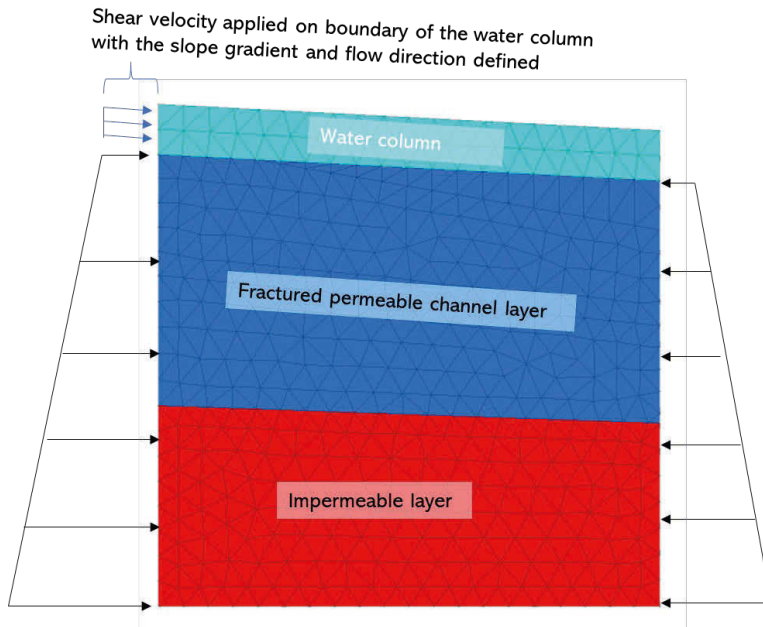


Figure 60. Boundary conditions for the simulation, with pressure gradient on the model block and shear velocity on water column.

5.9.2 Cases simulated.

Four cases shown in Table 18 were simulated. In Case A the flow velocity is varied while the water column height (1.0 m) and the block size (0.5 m³) are kept constant. In Case B the flow velocity (15 m/s) and block size (0.5 m³) are kept constant while the water-column height is varied. In Case C the water column height (1 m) and flow velocity (15 m/s) are kept constant while the block size varies. And in Case D all the channel slope is varied between 5 and 15 degrees.

The flow velocities used here are those derived for Dam 1 using the HEC-RAS software and channel profile captured by the drone. For Dam 1 the average flow velocities were found varies between 10 and 20 m/s from HEC-RAS analysis.

Table 18. Cases simulated.

	Flow velocity (m/s)	Water column height (m)	Block size (m ³)	Channel slope gradient (degrees)
Case A	10, 15, 20	1	0.5	3
Case B	15	1,2,3,4,5	0.5	3
Case C	15	1	0.5, 1.0, 3.0, 5.0	3
Case D	15	1		5, 10, 15

5.9.3 Simulation procedure

A coupled hydro-mechanical model has two parts; (i) mechanical component and (ii) fluid component (see Itasca 2020). After the geometry has been constructed, material and fluid parameters assigned, and boundary conditions set, the next step is to achieve the initial conditions. The first step in this initialisation process is to initialise the mechanical component while the fluid flow component is turned off, to allow the in-situ stresses to equilibrate in the model. The second step is to initialise the hydraulic component with the fluid flow component turned on and the mechanical component turned off. This will allow fluid to flow through the fractures and build pore pressure without mechanically affecting fractures. Once the initialisation has been achieved, the next step is to turn both components on to active a fully coupled hydro-mechanical model, which is in principle a static model. If the dynamic component is configured than it is turned on after dynamic parameters are defined and that will result in fully coupled hydro-mechanical-dynamic model.

However, in order to perform the simulation in real fluid flow time the model was configured as a hydro-dynamic-mechanical simulation, in which case the model was capable of simulating a fully coupled hydro-dynamic-mechanical simulation, even though in the current models the interest is concerned with the response due to the hydro-mechanical coupled simulation. Each component can be turned off or on to freeze one component and activate the other. The basic 3DEC command lines that do this are shown in Figure 61. The dynamic component is turned off throughout the

simulations. Because of this setup a single block model simulation took an average of approximately 4 hours of computation time to achieve a fluid flow time of 15 minutes or 900 seconds.

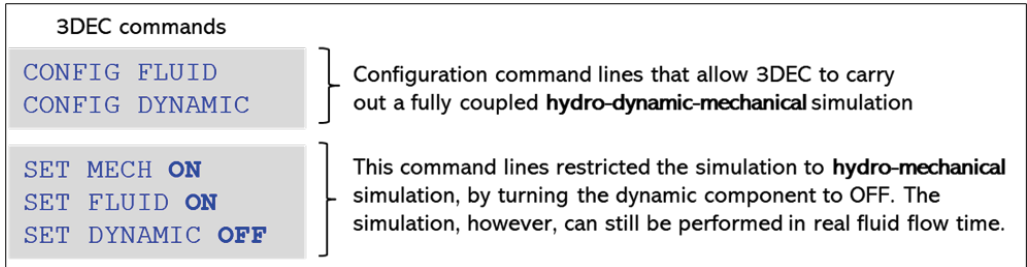


Figure 61. 3DEC commands for a coupled hydro-dynamic-mechanical model.

5.9.4 Results

5.9.4.1 Flow velocity variation (Case A)

Figure 62 shows the displacements experienced by a 0.5 m³ block with average flow velocities of 10, 15 and 20 m/s. The water column height was kept constant at 1.0 m.

In 1200 seconds (or 20 minutes) the displacements experienced by the rock block were:

- >100 m for average velocity of 20 m/s
- >50 m for average velocity of 15 m/s
- >50 m for average velocity of 10 m/s

With these magnitudes of displacements, which are notably large, it can be assumed that the 0.5 m³ block could have been easily removed and transported downstream with the applied average flow velocities and water pressures. The greater the flow velocity the greater the displacement and greater the erosion potential. Figure 63 shows that displacement appears to increase exponentially when the average flow velocity increases from 15 m/s to 20 m/s.

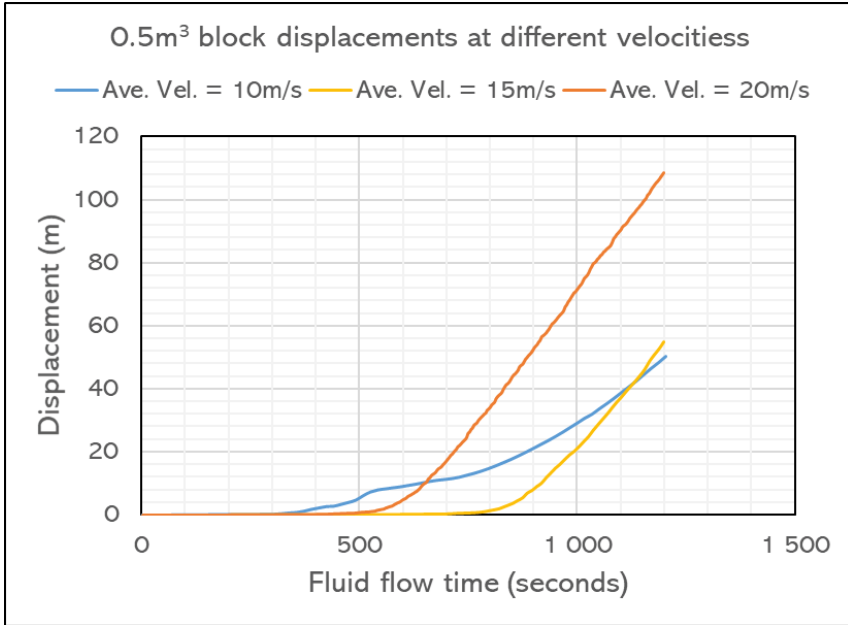


Figure 62. Displacement of a 0.5m³ block after 20 minutes (1200 seconds) of water flow at different velocities.

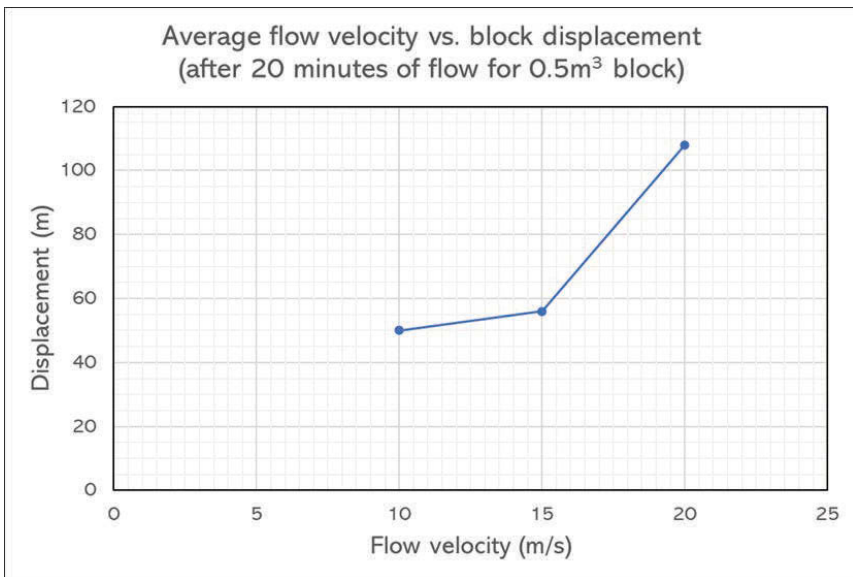


Figure 63. Relationship between displacement of a 0.5 m³ block and flow velocity.

5.9.4.2 Water column height variation (Case B)

Figure 64 shows the displacements experienced by the 0.5 m³ block during 1200 seconds of flow than those resulting from 1.0 m and 2.0 m water columns. This observation can be correlated to the fact the shear velocity is greater with shallow water columns. However, water column heights greater than 3.0 m result in greater displacements. This is largely due to increase in pore pressures.

Figure 65 shows the relationship between the displacement of the 0.5 m³ and the water column height. The optimum water column height appears to occur between 1.0 and 2.0 m.

Figure 66 shows another character of block displacement for the different water column heights simulated. The displacements tend to be higher from the direction of flow. In the figure the flow is entering from the left. The joints with the largest apertures, joints #1 and #3 (see Table 17 and Figure 59) seem to influence the displacement magnitudes. Maximum displacements are observed on the planes of joints #1 and #3.

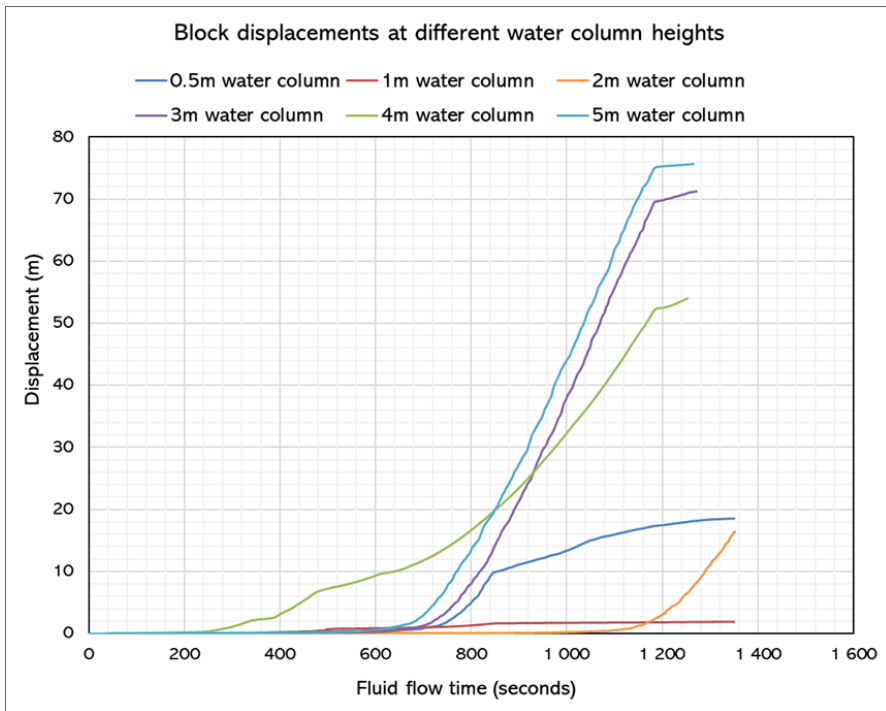


Figure 64. Block displacement for different water columns during ~20 minutes of flow.

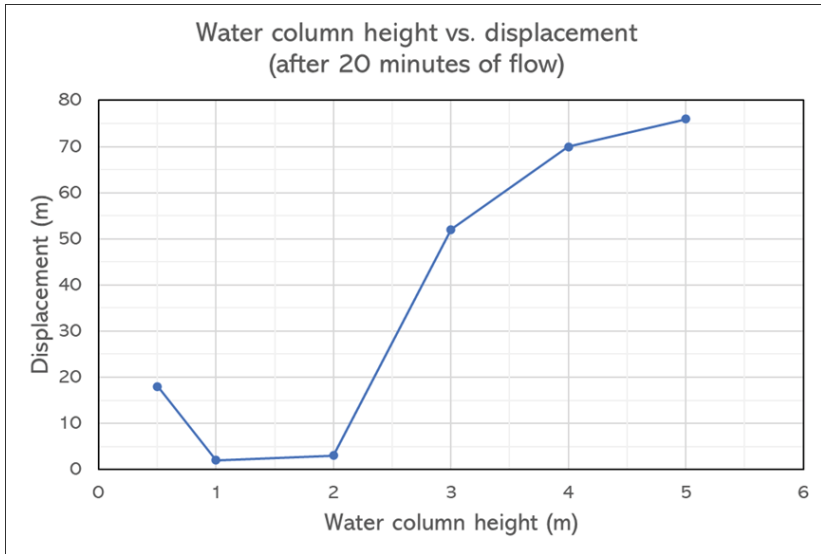


Figure 65. Relationship between displacement of a 0.5 m³ block and water column height.

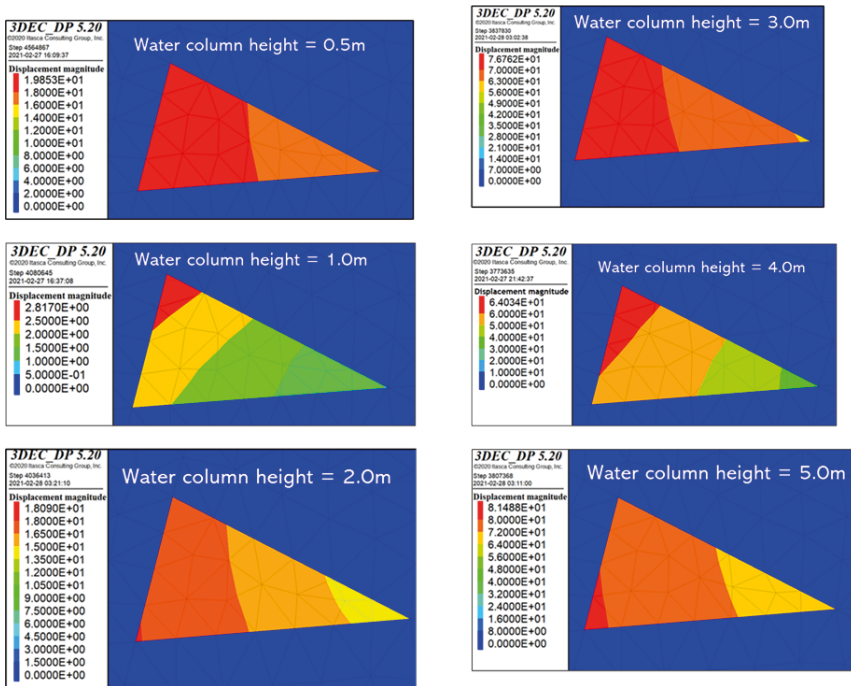


Figure 66. Block displacement characteristics for different water column heights.

5.9.4.3 Block size variation (Case C)

In case C the block sizes were varied, while other parameters were kept constant. Figure 67 shows the results of the displacements after a flow time of 600 seconds or 10 minutes. It shows that the smaller block the larger the displacement, for example, the 0.5 m^3 block experienced over 19 m of displacement in 10 minutes of flow, while the 5 m^3 block experienced $\sim 20 \text{ cm}$ of displacement in the same time period. Figure 68 shows an exponential decrease in displacement as the block size increases. This was clearly the case at Dam 1 where the smaller blocks have migrated further downstream, while larger blocks (3 to 5 m^3) moved very short distances.

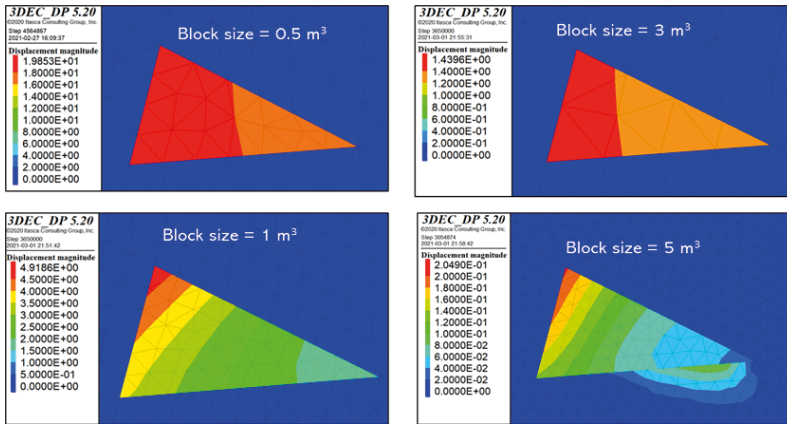


Figure 67. Displacement of different block sizes for 600 seconds (or 10 minutes) of flow.

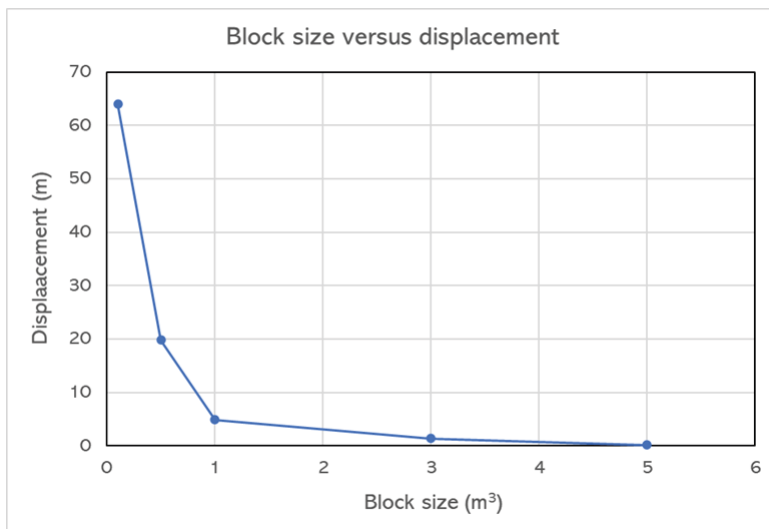


Figure 68. Relationship between block size and displacement.

5.9.4.4 Channel slope variation (Case D)

In case C, three channel slope gradients or angles (5° , 10° and 15°) were applied to the model. These slopes realistically represent the slopes along the various sections of the spillway. Even though the average slope of Dam 1 and Dam 2 spillway channels were between 3° and 5° , there were sections where the slopes were steeper. These steeper sections were noted to show significant erosion.

Figure 69 shows the displacements experienced by the 0.5 m^3 block during flow time of up to 1200 seconds. The plot for 20° degree slope was reduced to 600 seconds since the displacement reached over 100 m under 900 seconds (or 15 minutes) so it became difficult to plot results for the 10° and 5° slopes on the same graph. The block experiences an exponential increase in displacement magnitudes within 10 to 20 minutes of flow. When the slope gradient was higher the displacements become very critical.

Figure 70 shows the relationship between block displacements and slope gradient. The displacements experienced by the block starts to take an exponential form when the slope gradient increases from 10° to 15° . It implies that channel slope gradient greater than 10° will be critical for block erosion, both for initiation and transportation. Both, Dam 1 and Dam 2 have overall channel slope gradients that vary between 3° and 5° . However, there are slope local variations long some sections of the channel. Dam 1 for example, has increased slope gradient in Domain B (see section 4.1.1.1), while at Dam 2 the slope gradient in Domain B gently dips upstream which reduces the flow velocity significantly (see section 4.1.1.2. However, back flow seemed to occur at Dam 2 in Domain B where the slope dips upstream.

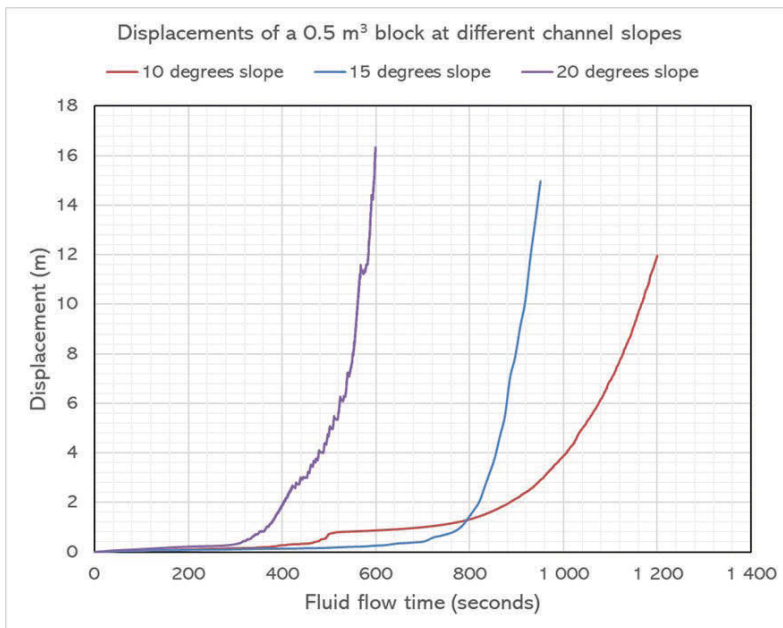


Figure 69. Displacements experienced by 0.5 m^3 block for different slope gradients.

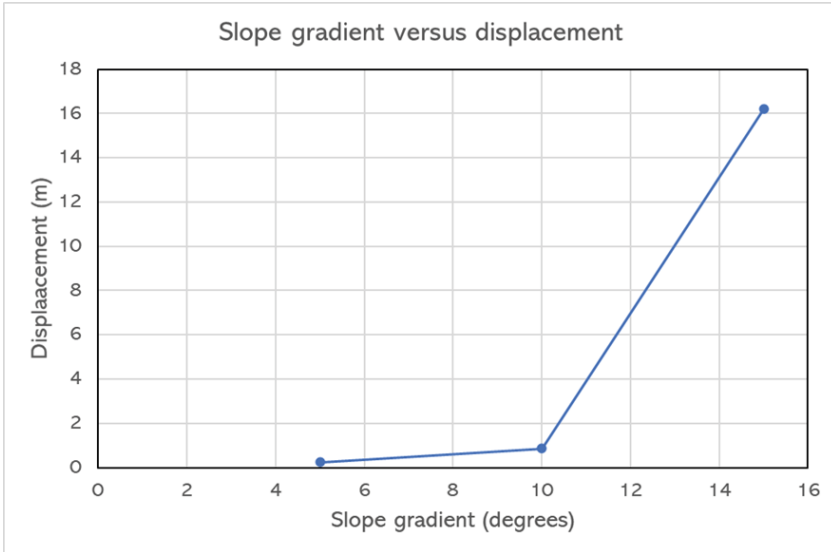


Figure 70. Displacements experienced by the 0.5 m³ with slope gradients of 5°, 10°, 15°.

5.9.5 Results – joint parameter impact

Since the actual joint sets observed at Dam 1 were used in single block models, the block erosion mechanisms observed in the models apparently reflect the actual observations at Dam 1 spillway channel. Figure 72a shows the block experiencing distinct zones of displacement magnitudes, which potentially indicate the block fracture lines. This kind of fracturing coincides with fracturing observed at Dam 1. The block forming joints (at Dam 1) typically intersect to form prisms that are best illustrated by the two-dimensional shapes in Figure 72b. Even though the upper prism in Figure 72b can slip, it will nevertheless need to overcome the shear resistance against steeper plane which dips upstream. In this case the block may fracture as at thinner end, as precisely indicated by Figure 72a. The lower prism in Figure 72b will neither slip nor be plucked. This block will need to be fractured before it can be removed. This is one of the typical cases observed at Dam 1 and it seems to be captured by the results single block model as shown in Figure 72a.

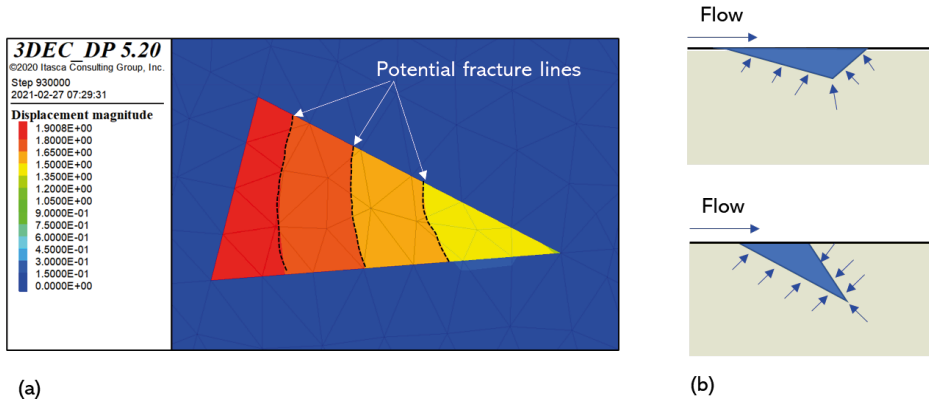


Figure 71. (a) potential fractures consistent with block fracturing at Dam 1, (b) typical rock prism geometries when joints intersect – typical observation at Dam 1.

5.9.6 Summary of observations

The summary of the block erosion mechanisms observed in the single model are conceptualised as illustrated in Figure 72. Even though the main rock blocks at Dam 1 spillway channel are shallow dipping tabular granite slabs, they nevertheless form prisms when intersected by other shallow dipping joints. Two kinds of prisms typically observed were illustrated earlier in Figure 71.

At Dam 2 the cubic blocks are formed by the sparsely distanced near vertical joints. These cubic blocks are apparently connected to the parent rock, or they could be intersected by a horizontal joint at significant depth. To remove the blocks at Dam 2 it will require significant water pressures. The observation is illustrated by the last case in Figure 72.

In the numerical models here, the blocks cannot translate or move due to the simulation technique that requires the block to be attached at the nodes. Results can however be interpreted against field observations and thus the description in Figure 72.

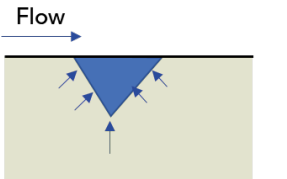
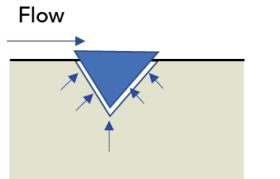
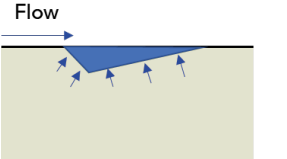
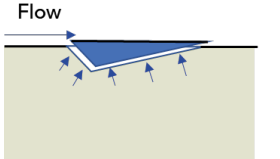
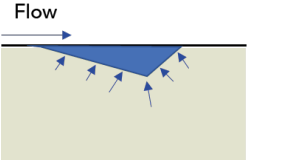
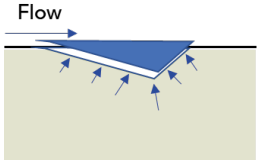
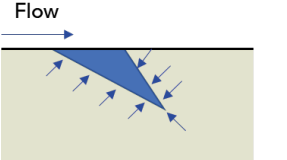
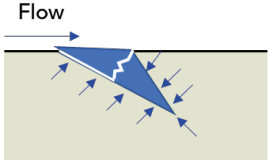
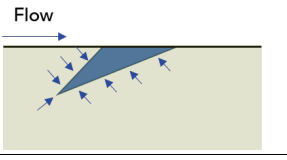
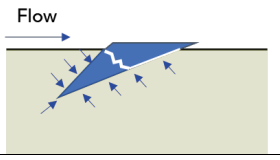
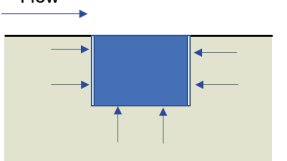
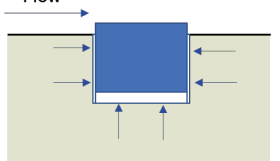
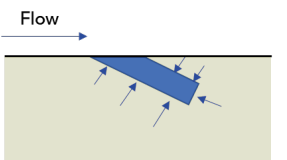
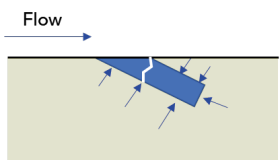
Typical block formations in two dimensions	Erosion process	Erosion mechanisms and descriptions
		<p>The block can be plucked out of the groove by combination of flow, pore pressure and stagnation pressure</p>
		<p>The block can easily slip along shallow plane dipping upstream, by the combined action of flow, pore pressure and stagnation pressure.</p>
		<p>The block can slip along steeper plane dipping upstream. However, shear resistance will increase as the block compresses against the steeper plane, which may create potential block fracture along the thinnest section – a pattern observed at Dam 1.</p>
		<p>The block cannot neither slip nor be plucked out. It will instead be fractured before it is removed. This geometrical block formation is typical at Dam 1, that result in the blocks being fractured prior to removal.</p>
		<p>The block cannot neither slip nor be plucked out. The block will need to be fractured; however, it will also likely result from upstream mining caused by water turbulence.</p>
		<p>The block plucked out of the groove but required increased pore pressure and stagnation pressure to raise the block. This is the case typical for Dam 2, where large cubic blocks are formed by near vertical fractures. However, the blocks apparently are still connected to the parent rock.</p>
		<p>Flat slabs, like observed at Dam 1, are fractured by lift force created by the water pressure. Displacements are great from the direction of flow. The drag force created by the shear velocity plays an important role.</p>

Figure 72. Conceptualised cases of block erosion at Dam 1 and Dam 2.

5.10 Dam 1 spillway model

5.10.1 Model setup

Figure 73 shows the drone scanned image of Dam 1 spillway channel and the section modelled in 3DEC. The completed 3DEC model is shown in Figure 74. To reduce the computation time, only the block comprising the spillway was fractured with rock joints and made permeable for flow to occur in the joints. This block also has a finite depth of approximately 10 m below the channel floor. The rest of the block is impermeable. Water is only allowed to flow through the fractures and not through the matrix.

The impermeable walls and the base of the model form rigid boundaries. That is the entire green block in Figure 74 is rigid and no deformation will occur in that block. Since flow will only occur in fractures, hydro-mechanical response will thus only occur within the fractures in channel.

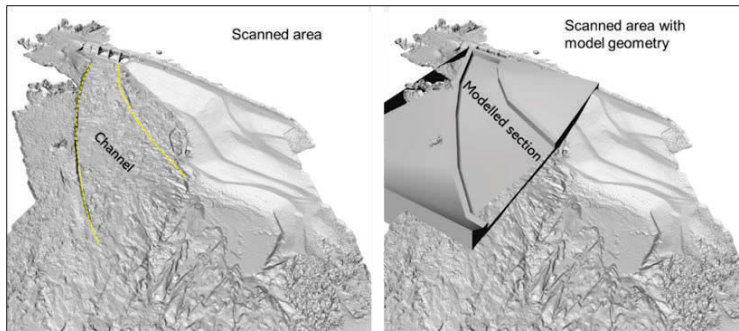


Figure 73. Scanned area of Dam 1 (left image) and section modelled in 3DEC (right image).

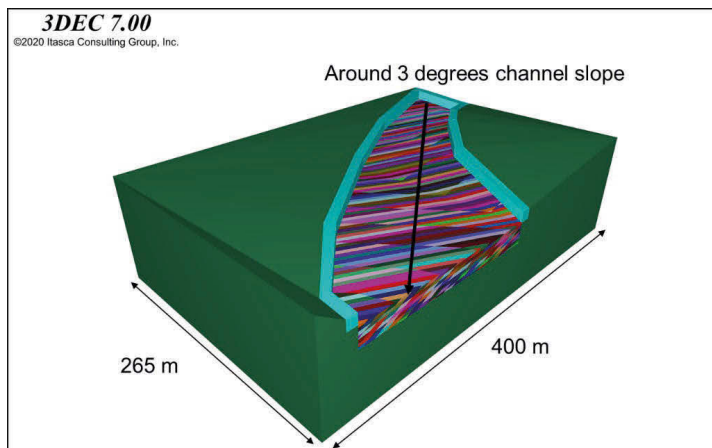


Figure 74. 3DEC model of the scanned Dam 1 channel.

5.10.2 Model parameters

Only dominant block forming joint sets are used in the modelling. Table 19 shows these joints and their properties. The aperture values are based on field observations and assessments. The average velocity applied in the model is that which was determined for Dam 1 spillway channel in the empirical analyses, section 4.1.1.1. The velocity varied between 12m/s and 20m/s between domains A to C. However, for these models the average water velocity of 15m/s is used.

Table 19. Properties of the single block forming joints.

	Joint orientation		Aperture			Joint mechanical parameters			
	Dip (°)	Dip-Dir (°)	Ave. (m)	Min (m)	Max (m)	Friction (°)	Cohesion (MPa)	K_n^* (Pa/m)	K_s^{**} (Pa/m)
Joint 1	14	107	5e-3	5e-4	5e-2	30	0.05	10e9	10e9
Joint 2	58	110	1e-4	1e-5	1e-3	30	0.05	10e9	10e9

* K_n = Joint normal stiffness

** K_s = Joint shear stiffness

5.10.3 Cases modelled

Cases modelled for Dam 1 are shown in Table 20. The average water velocity is kept constant at 15 m/s while the water column height is varied from 1 to 5 m. Case A is a shallowing dipping dominant joint set, representing the granite slabs at Dam 1. Case B is moderately dipping joint and Case C represents all the joint sets combined. Figure 75 shows the cases conceptually.

One case, Case D, was attempted with a dynamic modelling option. For this, the pressure-time values reported by Mören and Sjöberg (2007) were taken and adjusted before inputting into the 3DEC model.

Table 20. Cases modelled.

Cases	Flow velocity (m/s)	Water column height (m)	Joint dip/dip-direction	Comment
Case A	15	1, 2, 3, 4, 5	14°/107°	Shallow dipping joints - granite slabs
Case B	15	1, 2, 3, 4, 5	58°/110°	Moderately dipping joints
Case C	15	1, 2, 3, 4, 5	14°/107°, 58°/110°	Three main joint sets at Dam 1
Case D	15	3	14°/107°, 58°/110°	Dynamic model applied to cases A, B and C

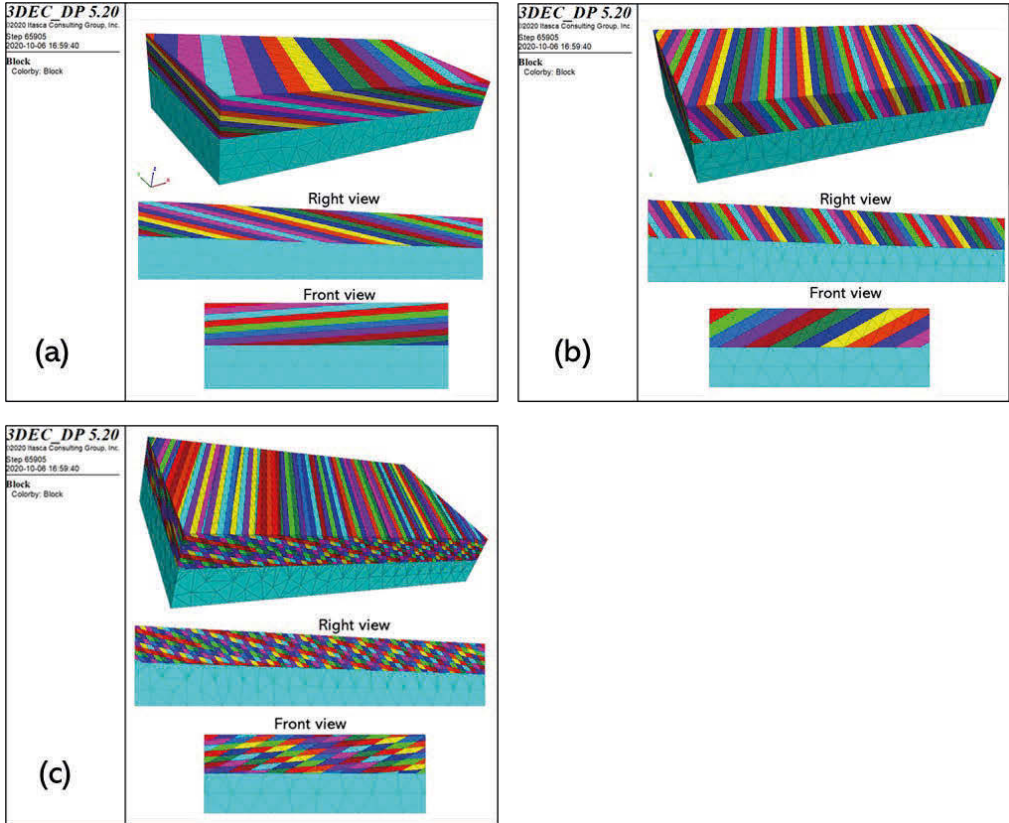


Figure 75. Cases modelled (a) Case A, (b) Case B and (c) Case C.

5.10.4 Modelling procedure

As presented in the single block model section, the first step in a hydro-mechanically coupled model is to initialize the mechanical component while the hydraulic component is frozen. This allows the model to reach mechanical stability. The next step is to initialize the hydraulic component while the mechanical component is frozen. This allows the pore pressure to build up in the fractures, without inducing displacements in the fractures. Figure 76 shows the pore pressures for the cases of the different water column heights (1 to 5 m). The pore pressures are higher at the upstream end of the channel and lower downstream. This allows for flow to occur from upstream to downstream.

After the pore pressure has built up, the next step is to activate both the mechanical and hydraulic components to begin the simulation. All displacements were reset to zero at this stage before the cycling begins.

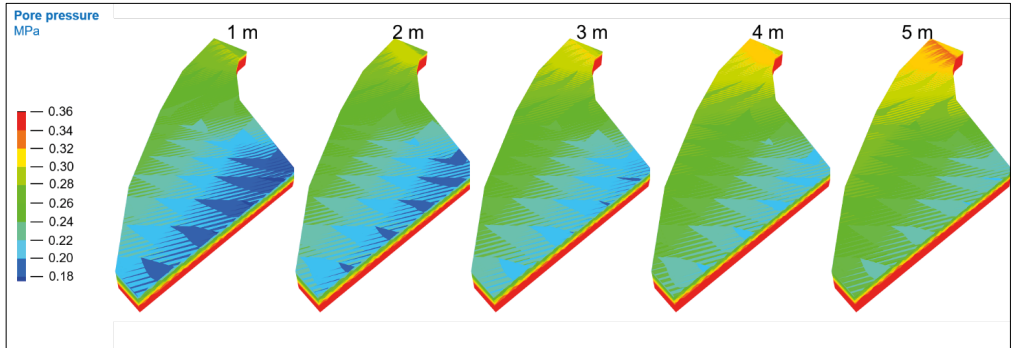


Figure 76. Pore pressure resulting from water column heights of 1 to 5 m.

5.10.5 Limitation of the analysis

It must be stated here that model does not simulate block removal and translation. That is, these models do not simulate block erosion in a practical sense, in that the blocks cannot be plucked or removed and transported downstream. This is because the model is hydro-mechanically coupled and therefore are attached at nodal grids. This necessitates the hydro-mechanical computations that occur at the nodes.

Since the block cannot detach and move, only the displacements experienced by the rock mass which initiate along the fractures can be assessed. The simulated displacement magnitudes indicate erosion potential. Higher displacement magnitudes indicate the potential for a block to dislodge and migrate in the direction of flow. In the 3DEC model, slip along in the joint planes, both normal and shear, are all indicators of block removal.

5.10.6 Results

5.10.6.1 Static model

Figure 77 shows the results for case A, which was specially modelled to see how the rock mass with a shallow dipping joint set (corresponding to the granite slabs) respond to high pressure flow. It can be seen that displacements of up to 10 m are achieved within 400 seconds (that is roughly within 5 to 10 minutes) of time. It means that the rock mass consisting shallow dipping joints are critically prone to block erosion. This confirms the observation at Dam 1 where the tabular granite rock slabs were visibly fractured by water pressure before being transported downstream.

Figure 78 shows the results for case B, which was specially modelled to see how the rock mass with a steeply dipping joint set respond to high pressure flow. The displacements in the rock mass with steeply dipping joints show very clear contrast to the rock mass with shallow dipping joints. Within the same amount of time (400 seconds) the rock mass with steeply dipping joints only experiences a maximum in displacement of 1.0 m. That means, rock masses consisting of steeply joints are less prone to block erosion.

Figure 79 shows the results for Case C, where the rock mass consists of both shallow dipping and steeply joints, i.e., all main joint sets observed at Dam 1 are included. The displacements were captured for 15, 100 and 400 seconds of flow time.

The results show that, displacements of more than 10 m are achieved in 15 seconds, particularly on the upstream. This also makes practical sense, in that extremely high pressures tend to induce shock and thus a significant mechanical response of the rock mass. This is illustrated by the fact that, within 15 seconds (Figure 79) some areas of the spillway channel are already experiencing displacements of up to 10 m. After 100 seconds (~1.5 minutes) of flow significant areas of the channel experience more than 10 m of displacements. After 400 seconds (~6.5 minutes) the displacements do not significantly change as were 100 seconds earlier. It is clear that, the displacements in the rock mass within Dam 1 spillway canal start to experience critical levels of displacement immediately in the first 1 to 2 minutes of flow. This is also consistent with the fact that hydropower dam spillway canals receive sudden shock flows in less than a minute.

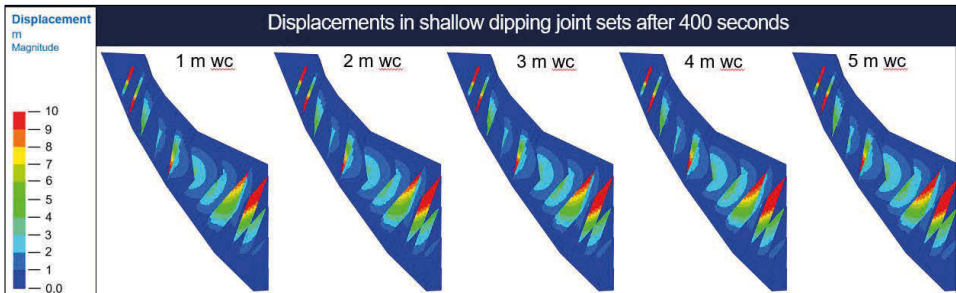


Figure 77. Displacements after 400 seconds of equivalent fluid flow time with shallow dipping joints.

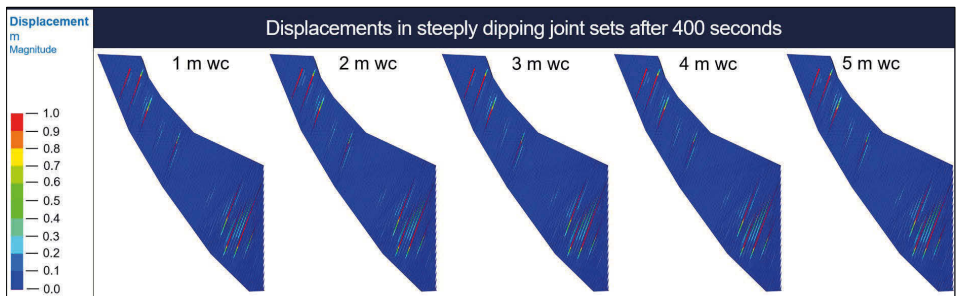


Figure 78. Displacements after 400 seconds of equivalent fluid flow time with steeply dipping joints.

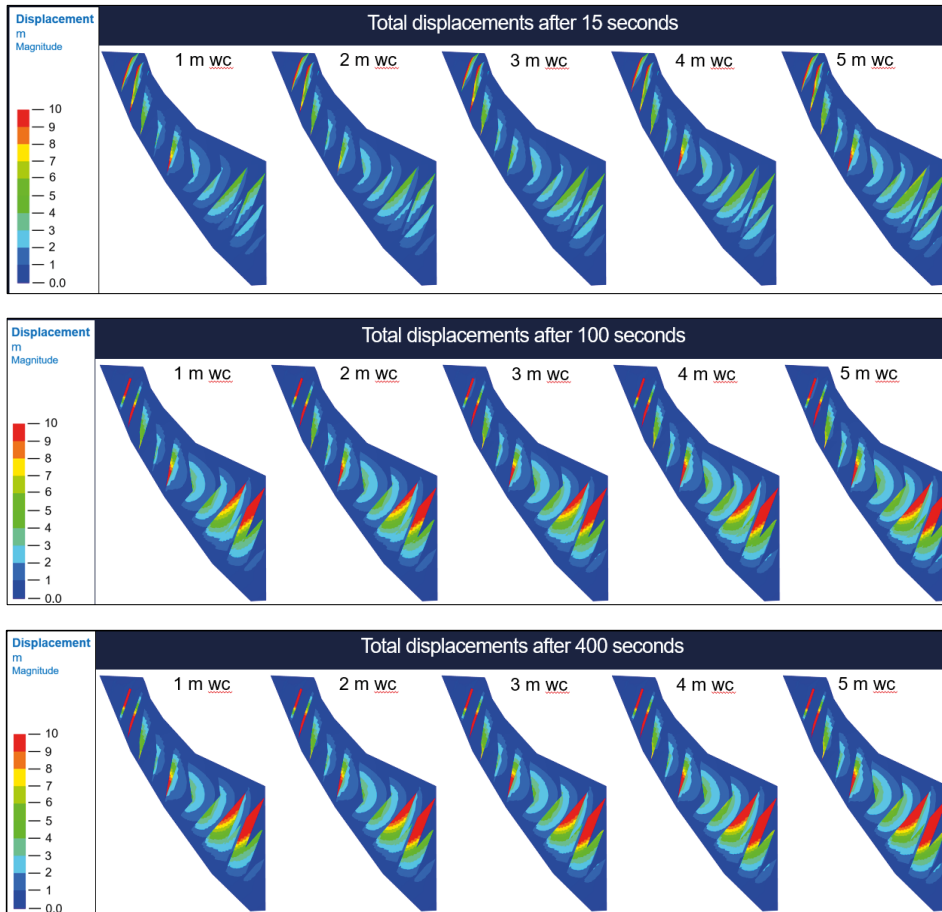


Figure 79. Displacements after 15, 100 and 400 seconds of equivalent fluid flow time.

5.10.7 Dynamic model

In an open spillway channel, the rock mass typically experiences a pulsating water pressure. The rock mass response to this pulsating water pressure can only be realistically modelled by a fully coupled hydro-mechanical-dynamic model. This technique of modelling is very complex and generally ignored in preference of static methods. However, an attempt has been made to create a fully coupled hydro-mechanic-dynamic model to simulate one case for Dam 1. Three sections along the spillway channel were subjected to dynamic pressure. These sections are shown in Figure 80.

In 3DEC the dynamic component is defined in different ways; by a pressure-time history, velocity-time history, frequency-time history, a sinusoidal wave function, etc. In this specific case the pressure-time data reported by Mören & Sjöberg (2007) for Ligga hydropower dam spillway was

adapted. The data is corrected before it was applied in the model. Figure 81 shows a sample of dynamic pressure variation during a 400 seconds period when Case D was simulated. Figure 82, Figure 83 and Figure 84 show the displacements for the spillway canal rock mass with shallow dipping joints (Figure 82), steeply dipping joints Figure 83) and with all the joints (Figure 84).

In order to see the difference in the results of the dynamic and static models, the displacements from both dynamic and static models are placed side by side in Figure 82, Figure 83 and Figure 84. Clearly the static and the dynamic models do not show any significant difference in displacement magnitudes. It can be argued that the static model is sufficient in this case to assess rock mass displacements along the spillway channel. This may be due to fact that the water itself is a remarkable damper of dynamic pressure. Therefore, much of the energy may have dissipated at the soft boundary between liquid and solid interface.

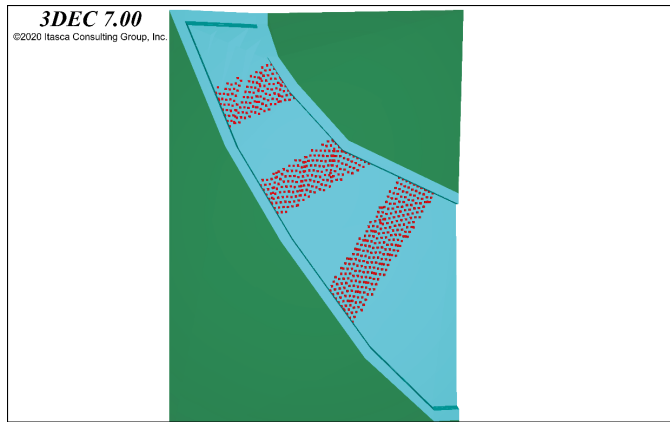


Figure 80. Sections where the dynamic pressure is applied are shown in dots.

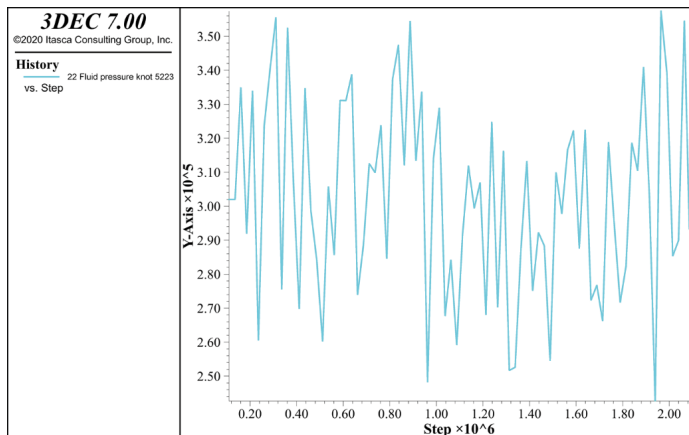


Figure 81. Pressure variation (Pa) during the 400 seconds period.

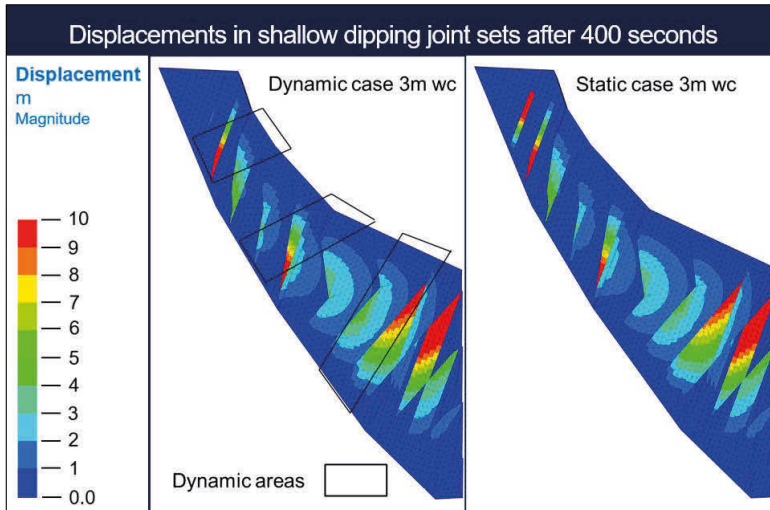


Figure 82. Displacements from dynamic and static conditions during 400 seconds of equivalent fluid flow time for the case of shallow dipping joints.

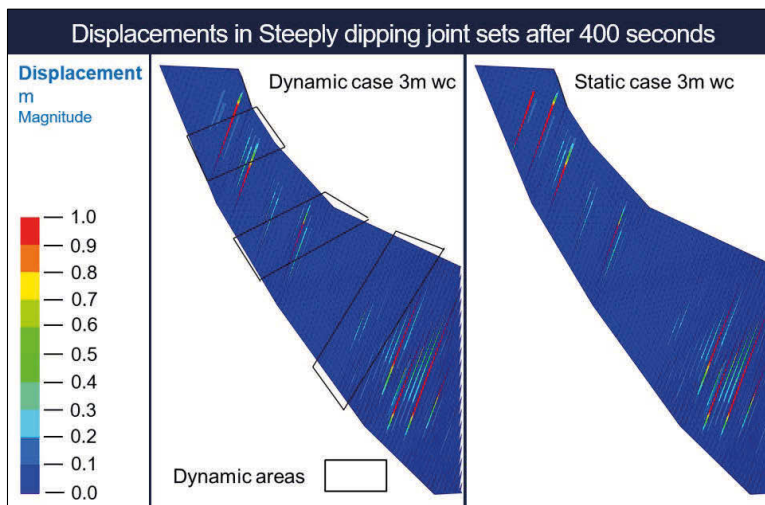


Figure 83. Displacements from dynamic and static conditions during 400 seconds of equivalent fluid flow time for the case of steeply dipping joints.

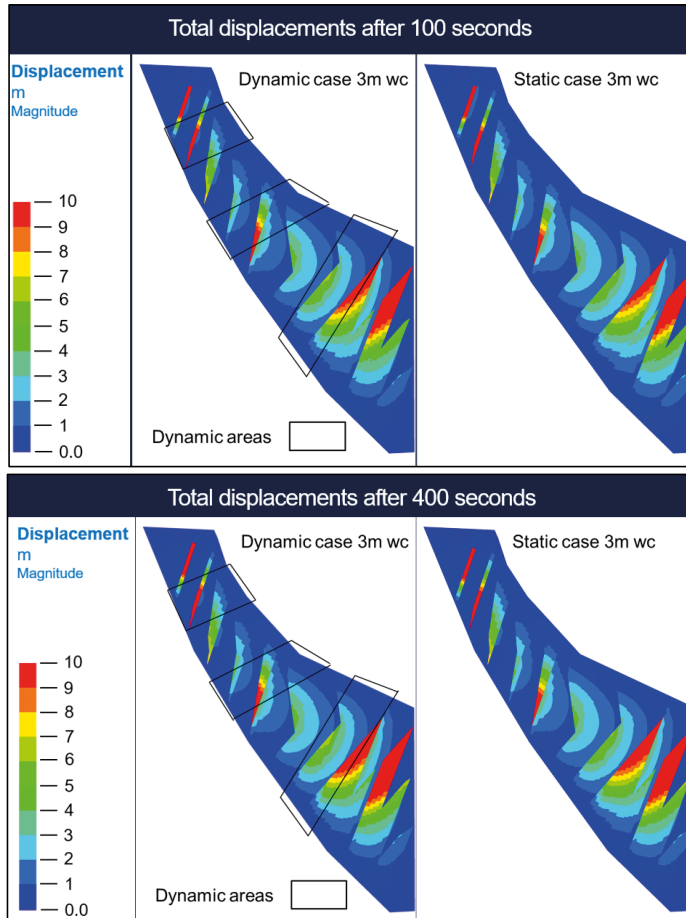


Figure 84. Displacements from dynamic and static conditions during 100 and 400 seconds of equivalent fluid flow time.

5.11 Dam 2 spillway model

5.11.1 Model setup

The model geometry for the Dam 2 3DEC model began by importing the mesh of the spillway channel into 3DEC. The 3DEC mesh was created to follow the channel topography (Figure 85). The final 3DEC model for the Dam 2 spillway channel is shown in Figure 86. The model is 500 m long in the long-axis of the channel and 400 m wide. The length of model in principle covers the entire length of the channel. The channel has 3 notable bends, which obviously affect flow in real environment.

To make computations faster only the spillway channel is made permeable (coloured blocks in Figure 86) to allow flow to occur along the fractures in the rock. The rest of the block is made impermeable (large blue block in Figure 86). The blocks are grided/zoned/meshed since flow calculations are performed on the grid point nodes.

A dynamic model is not considered for Dam 2 since the Dam 1 dynamic models didn't not show any significant difference in displacements between the static and dynamic models. Hence, only static model simulations are performed for Dam 2.

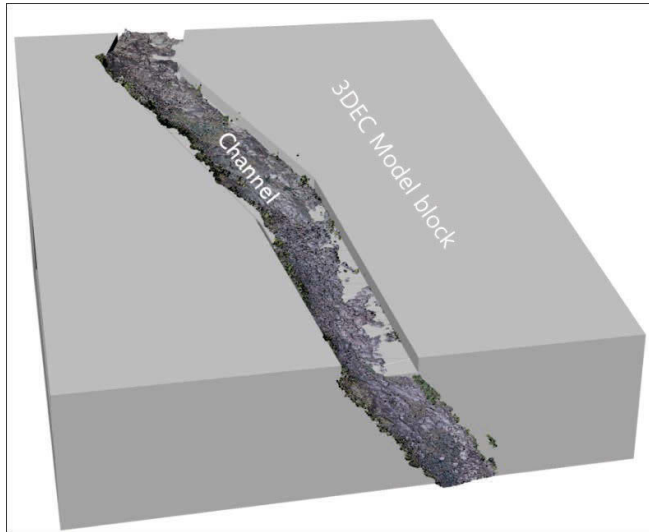


Figure 85. Drone scanned spillway channel with block created for 3DEC model.

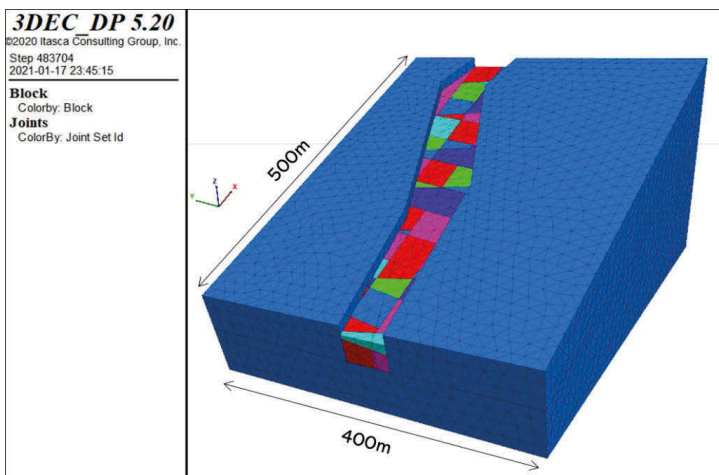


Figure 86. 3DEC model geometry with analysed joint sets for Dam 2 spillway.

5.11.2 Model parameters

For the 3DEC models only the 3 dominant block forming joints are considered, which are shown again here in Table 21. Random joints are spatially distributed and therefore ignored for the purpose of modelling. The joint apertures at Dam 2 are also large, that is, they have similarity to the aperture widths observed at Dam 1. The aperture widths ranged between less than 1 mm to as high as 50 mm. However, the widths of the apertures vary with depth, becoming narrower deeper in the rock.

The average water velocities of the Dam 2 spillway channel have been analysed using the HEC-RAS software and drone scanned profile of the channel. This was presented in section 4.1.1.2. In summary the average velocities of the three domains are shown in Figure 87 below, which range between 11, 12 and 15 m/s for the respective domain classes that were established during the site investigation. For numerical modelling the average velocity of 12 m/s (observed in Domain B) is applied to entire length of channel in the model. The shear velocity calculation procedures were described in section 5.5

Table 21. Properties of block forming joints at Dam 2.

	Joint orientation		Aperture			Joint mechanical parameters			
	Dip (°)	Dip-Dir (°)	Ave. (m)	Min (m)	Max (m)	Friction (°)	Cohesion (MPa)	Kn* (Pa/m)	Ks** (Pa/m)
Joint 1	85	100	5e-3	5e-4	5e-2	33	0.05	10e9	10e9
Joint 2	48	263	1e-3	1e-4	1e-2	33	0.05	10e9	10e9
Joint 3	89	359	5e-3	5e-4	5e-2	33	0.05	10e9	10e9

*Kn = Joint normal stiffness

**Ks = Joint shear stiffness

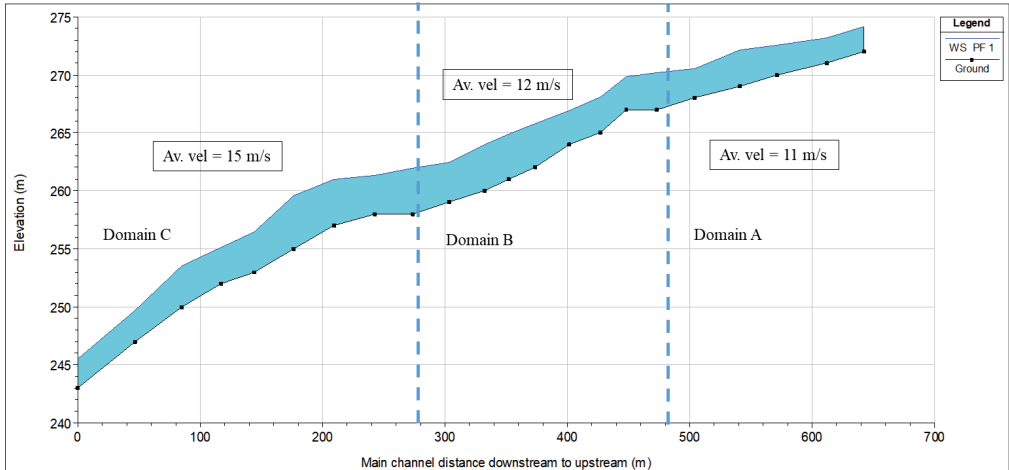


Figure 87. Average velocities and water elevations along spillway canal of Dam 2 based on HEC-RAS analysis.

5.11.3 Simulation procedure

The simulation procedures are the same as that described in the single block modelling procedures in section 5.9.3. The model is fully coupled to conduct a hydro-mechanically coupled simulation. However, in order to perform the simulation in real fluid flow time the model was configured as a hydro-dynamic-mechanical simulation, in which case the model was capable of simulating a fully coupled hydro-dynamic-mechanical simulation. The dynamic component was turned off the current simulations. The Approximately 6 hours of computation time was required to achieve a fluid flow time of 10 minutes or 600 seconds. The corresponding mechanical responses are the assessed.

5.11.4 Results of the modelled cases

Water column (wc) heights of 1 to 5 m were simulated to assess the displacements experienced by the rock mass in the spillway channel. The displacements were recorded after 120 seconds (2 minutes) and after 600 seconds (10 minutes). Results from the simulations are shown Table 22 and Table 23. More than 4 m of the displacements are experienced within 2 minutes for water column height of 1 m and more than 9 m for water column height of 5 m. After 10 minutes of flow the displacements do not appear to change significantly from the 2 minutes of flow time (see Figure 88**Error! Reference source not found.**). This indicates much of the displacements in the rock mass occur within the first of couple minutes. This behaviour is also consistent with what was observed in Dam 1 simulations.

It is difficult to see from the results, i.e., from Table 22 and Table 23, which section of the channel experiences significant displacement. However, it is clear that a structure that is parallel to the flow channel seem to intersect cross cutting structures in areas where the channel makes the bends. Incidentally a photograph taken at the one of the bends in the middle of the channel coincides with an area the numerical model shows significant erosion and precisely at a location where this sub-parallel structure cuts the cross-cutting structures (Figure 89). This behaviour could explain the scouring that was predominant at Dam 2.

Table 22. Numerical observations of rock mass displacements at Dam 2 spillway channel for 1 to 3 m water column height.

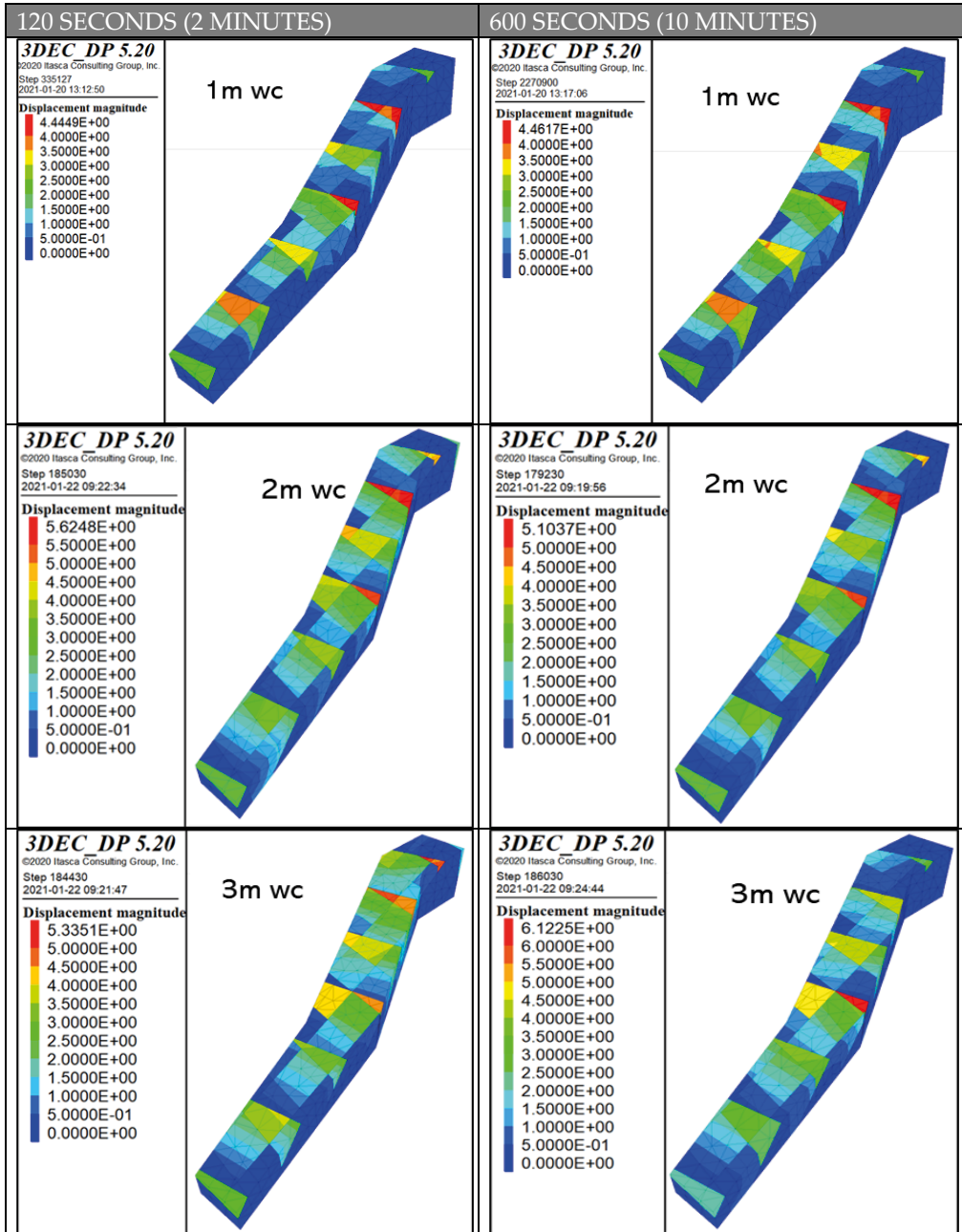
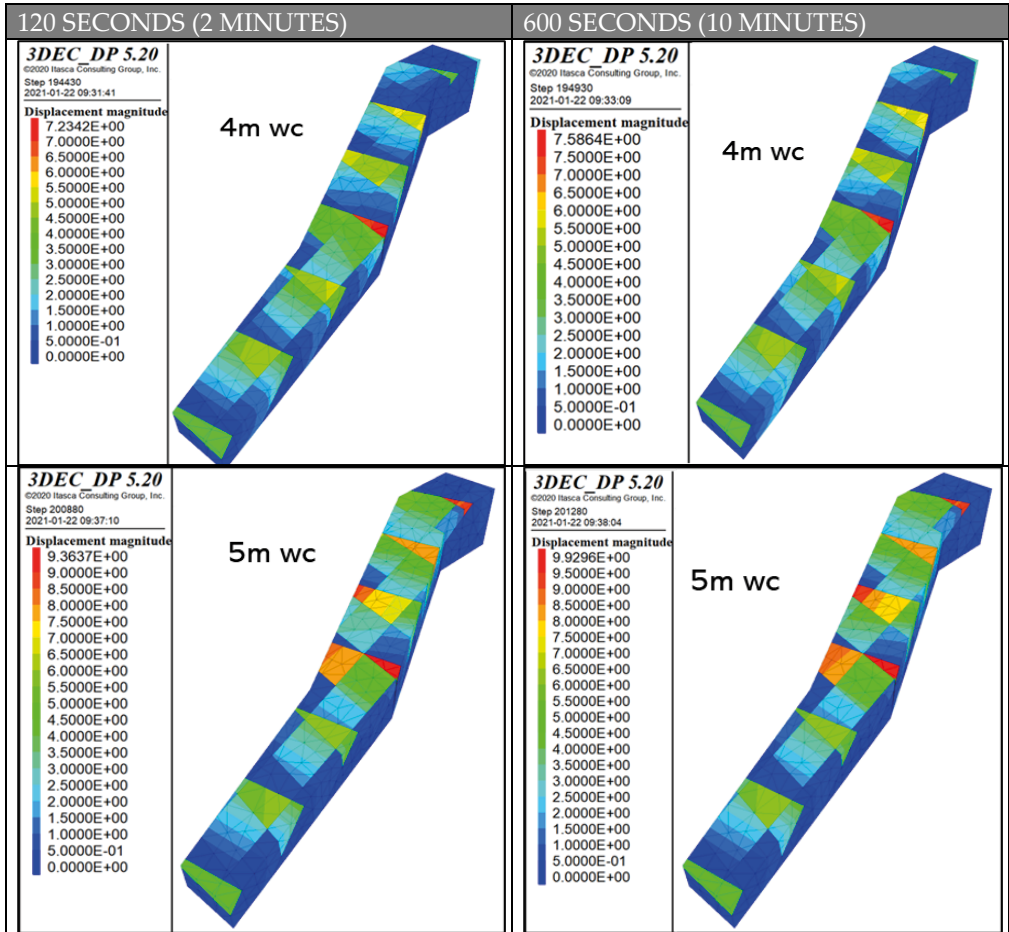


Table 23. Numerical observations of rock mass displacements at Dam 2 spillway channel for 4 to 5 m water column height.



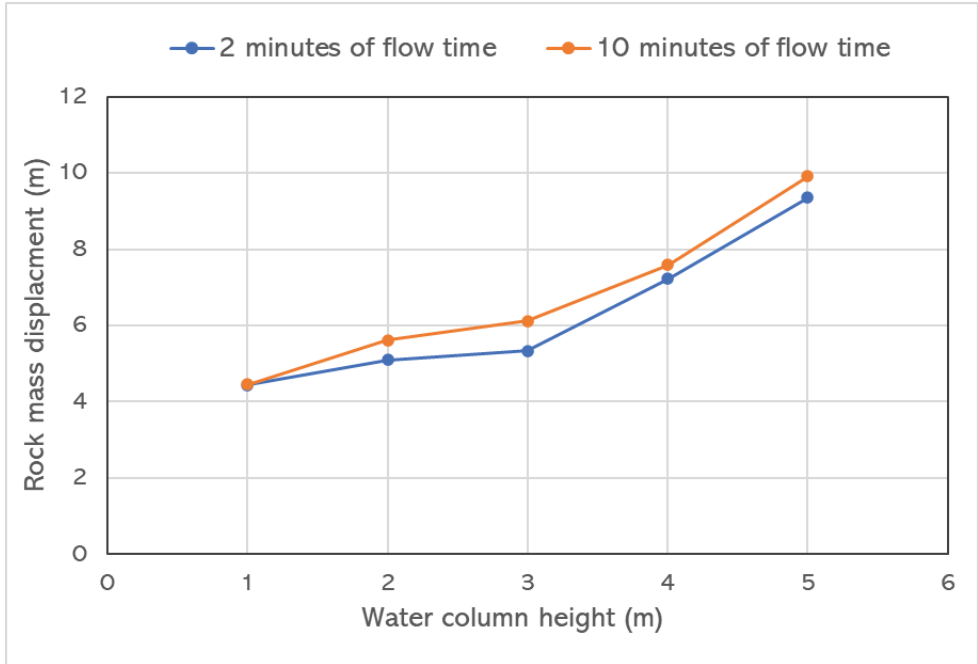


Figure 88. Curves indicating simulated displacements for 2 minutes and 10 minutes of flow.

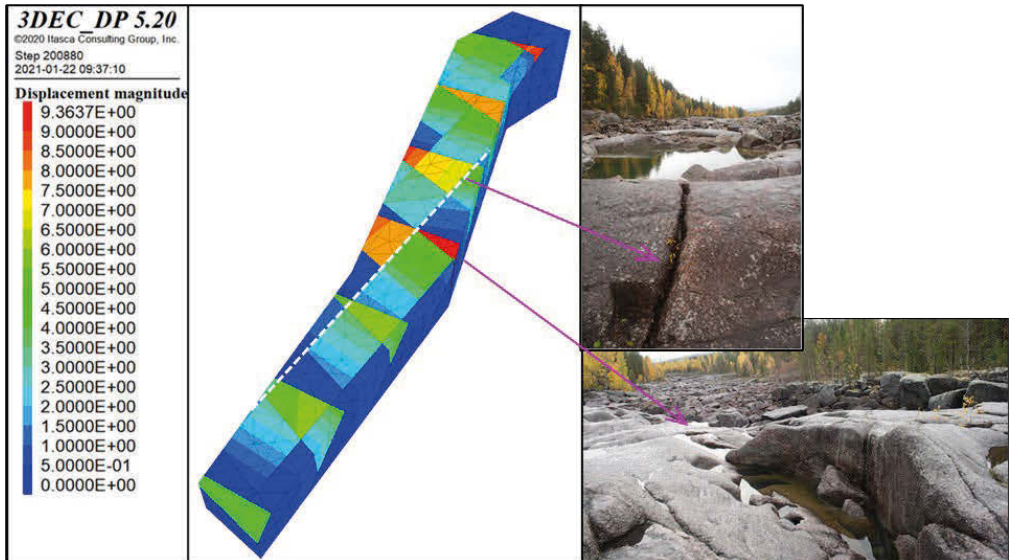


Figure 89. A set of fractures sub-parallel to the channel axis appear to affect erosion.

6. Discussions and conclusions

6.1 Literature

Literature study shows significant amount of literature concerning flow in open channels exist, mostly from a fluid mechanics point of view. Implications of fluid dynamics on rock erosion in open channels, especially with relevance to hydro-power dam spillways, were only recently studied in much detail by for example, Kirsten (1982), Annandale (1995) and Pells (2016), who also successively developed empirical criteria to assess rock mass erosion applicable to spillway canals. Annandale's erodibility criterion was built on the foundation of Kirsten, and Pells' was built on the foundation of both Annandale and Kirsten. Annandale's (1995) erodibility index criteria was widely adapted for rock mass erosion potential in spillway channels. However, the most recent rock mass erodibility criterion by Pells (2016) is the most improved and promising. Unlike the Annandale's criterion which only defines two classes, 'scouring or no scouring', Pells' criterion offers five classes of erosion potential, which are: Negligible, Minor, Moderate, Large and Extensive. This method seems to define erosion in terms of risk potential. Pells' classifications seem to resemble many observations, including the two spillway canals investigated in this study and therefore represents the most updated version for future spillway erosion assessment.

In regard to numerical modelling, rock mass erosion in a spillway canal is a complexly coupled problem that requires high level of knowledge in fluid mechanics and rock mechanics. The dynamic action of water due to shock loads adds to the next level of complexity. Many different numerical techniques, 2D and 3D, continuum and discontinuum methods have been used. The choices of modelling were based on the objectives of the models and the parameters to be investigated. However, George (2015) argues that the interaction between fluid and rock mass in spillway channel is a three-dimensional phenomenon which can be best studied using 3D modelling approach. Itasca's 3DEC has the capability to perform a fully coupled "hydro-mechanical-dynamic" simulation, which George (2015) also suggested, to study block erosion potential.

6.2 Field investigations

6.2.1 Spillway channel rock mass classifications

Field inventory of the spillway channels of the two hydropower dams with distinct rock mass characteristics represent very good spectrum of cases relevant to Sweden. Dam 1 spillway channel consists of a blocky rock mass, which according to GSI classification falls under FAIR to GOOD ROCK category. Dam 2 spillway channel, on the other hand, consists of a massive rock mass with few and sparsely distributed fractures. According to the GSI classification the Dam 2 rock mass falls under the GOOD to VERY GOOD category. The intact rock strength, though, for both rock masses averaged around 200 MPa.

Joint parameters are also similar, JRC of 6-14, were observed for both spillway canals. Because of abrasion the fractures are smooth and undulating. The fracture apertures are also similar for both spillway canal rock masses. Both have apertures ranging between 1-50 mm. They are widely open on the surface but regressively narrow into the rock. Furthermore, they are increasingly open when facing the flow direction. The amount of water that enters the fractures depends heavily on

the aperture sizes and their characteristics. The current study reveals that, a full-scale study is necessary to properly map the apertures in the spillway channels, and this is presented as recommendation for further studies in Chapter 7.

In this study statistical analysis of the joints have been conducted to establish the block sizes for both spillways. The sizes of the blocks are particularly important as the degree of erosion is dependent on it. Dam 1 for example, has a block size distribution between 0.1 and 5 m³ and averaging between 0.5 and 3 m³. As the single block 3DEC model shows in section 5.9, this block sizes are vulnerable for erosion with the given discharge conditions at Dam 1. At Dam 2 the sizes are massive, averaging between 60-80 m³. These blocks are not vulnerable for block erosion, but rock abrasion was the main phenomenon observed.

6.2.2 Spillway channel domains

Domaining of the spillway canals were mainly done by visual observations, that is, by looking at erosion characteristics and distribution of the eroded rock blocks. This resulted in at least 3 domains. Domain 1 normally show significant erosion, Domain 2 shows deposition of large rock blocks (1-3 m³), and Domain 3 shows the deposition of smaller blocks (<1 m³). Domain 1 typically comprise the first 100-150 m length of the channel, Domain 2 from 150-300 m and Domain 3 from 300 m and beyond downstream. The deposition of the rock blocks corresponds to stream power in those areas.

6.2.3 Drone data analyses

The drone captured a significant amount of data along approximately 700 m length of spillway channel, in both cases. Due to the complexity of analysing this data inhouse, it was therefore outsourced to external consultants with capabilities and appropriate software programs to analyse the data. This resulted in accurate profiling of the spillway channels, which were utilized in numerical and empirical modelling and analysis. The flow velocities along the channels were calculated using the HEC-RAS software and profiles generated from the drone captured point data for accurate X, Y, Z coordinates. The 3DEC model of Dam 1 and Dam 2 utilized the drone data generated topographic mesh to create the shape of the spillway canals.

Rock mass analysis for joint parameters (dip and direction of joints) and the block size analyses required detailed analyses of the drone captured data. Mapping of joint orientations, statistical analysis of the joints, and stereographic projections were conducted using the software program SIROVISION. Other software programs utilized in pre-processing the data include, Agisoft, CloudCompare and GEM4D.

6.3 Empirical Analyses

Block erosion of the unlined rock spillway canals of the two hydropower dams was studied using empirical methods – Annandale and Pells. The methods are based on the correlation between the erosive power of the water flow and the resistance of the rock mass. The erosive power, which is the rate of energy dissipation against the bedrock is a function of the flow velocity. HEC-RAS software was used to determine the velocity of the water flow at the spillways using the discharge capacities and map of the spillways captured by the drone. It needs to be mentioned that the

condition of flow in the spillways is non-uniform hence simple analytical calculation of the flow velocity with the assumption of uniform flow could be misleading.

Annandale's approach gives a binary assessment of either there is erosion potential or not. It is difficult with this approach to know the extent of the erosion if it does occur. Nevertheless, the approach shows that there is a potential for erosion at the spillways of the two hydropower dams. These results are similar to the observations at the spillways during the site visits and some earlier reported studies (e.g., Norconsult 2015; Mören and Sjöberg 2007). Determination of the erodibility index, which represent the resistance of the rock material to the erosive power of the flow requires many parameters and suitability of some of them such as material strength number (M_s) is questionable (Pells 2016). Though the results from the method agree to some extent with the site observation the method may not be suitable for spillways in a jointed rock mass that the erosion is govern by the unravelling of blocks along the joints.

Pells' approach, on the other hand, categorizes the risk of the erosion into negligible, minor, moderate, large and extensive. The results from the Pells' approach show that the risk of the erosion at Dam 2 spillway is majorly minor and large at Dam 1. This probably gives more representation of the general conditions at the spillways especially at Dam 2. The approach is easier to use compared with Annandale's method. The $eGSI$, which represent the rock mass resistance to the erosive power, describes the conditions of the jointed rock mass with a single number thereby making it easier to determine and the method is suitable for jointed rock mass. However, it needs to be mentioned that the determination of the GSI is subjective hence it may not absolutely represent the conditions of the rock mass that underlay the spillway.

The empirical methods, both Annandale and Pells, should be used for a preliminary assessment of spillways block erosion. The methods do not take into consideration time factors in erosion process and the process takes place over a period time. They do not specifically indicate the location and the extent of the erosion that would occur.

6.4 Numerical modelling

6.4.1 Approaches in modelling of Dam 1 and Dam 2

It has to be clarified noted that Dam 1 and Dam 2 were modelled using rather two different approaches. Dam 1 was modelled only with pore pressures and flow in the fractures (which will be referred to as Approach 1), while Dam 2 was modelled with pore pressures and flow in the fractures, and moreover with shear velocity applied to the water column (which will be referred to as Approach 2). The displacements observed are not very significantly different despite the fact that two different approaches were used. For example, the displacements in Dam 1 reached about 10 m in 400 seconds of flow time for a 3 m water column height model, while displacements in Dam 2 reached about 6 m in 600 seconds of flow time for the same water column height (i.e., 3 m). The smaller displacements observed in Dam 2 could largely be related to the fact that the rock mass in Dam 2 spillway is of a much better quality than that of Dam 1.

However, it is important to note that, the block erosion potential continuously increases with water column height in Approach 1. This is logical as it corresponds to increasing pore pressure. On the other hand, Approach 2 shows that lower water column height can also result in increased erosion

potential. This is because the shear velocity increases when water column height decreases. That means, this is an optimum water column depth where block erosion becomes minimal. The single block model, with water depth variation, shows the optimum water column height to range between 1 and 2 m. Below 1 m depth the erosion potential increases, mainly because of the increased shear stress. Above 2 m water depth the erosion potential is again higher and is mainly due to increased pore pressure.

6.4.2 Remarks concerning 3DEC modelling results.

The single block models showed that the water velocity and water-column height synchronise in affecting block erosion. It is the shear velocity, which corresponds to water column height, that is responsible for the shear force acting on the rock block at the bottom of the spillway channel. The lower the water-column the higher the shear velocity and greater the erosion potential. The water column height contributes to the pore-pressure. The higher the water column the greater the pore pressure in the fractures. However, the pressure alone is not sufficient to pluck large blocks ($>1\text{m}^3$). It is a combination of pore pressure, shear force and stagnation pressure (lift pressure resulting from zero velocity below the critical velocity).

The 3DEC models show that much of the block erosion occurs under 10 minutes upon the release of water from the dam. This is observed from the high block displacement magnitudes in 60 seconds. The disadvantage of the hydro-mechanically coupled model is that a block cannot dislodge and translate or move. In a hydro-mechanically coupled model the blocks are connected by mesh at nodal points for computation. This prevents the block to separate and translate as in rigid bodies. The assessment is only done by monitoring the displacements.

A fully coupled hydro-mechanical-dynamic model has not been fully attempted in this analysis, except for one case for Dam 1 models. This will require extensive model calibration for damping conditions due to dynamic loads.

6.4.3 Remarks on numerical methods

Even though numerical modelling in this study was conducted primarily using 3DEC (a discontinuum method of numerical modelling) an attempt was also made using LS-DYNA (continuum method) to take advantage of its dynamic fluid simulation capabilities. Although the approach was discontinued earlier in the modelling work, it may still be necessary to review this approach in the future to analyse rock fatigue and scouring potential. Another fluid simulation software ANSYS-FLUENT, with similar capabilities as LS-DYNA, has been used by Dasgupta et al (2011) to investigate scour formation at Karina Dam in Zimbabwe, while at the same time they used UDEC to investigate block erosion in the rock mass. It must be noted that, while 3DEC (used in this study) is a static numerical modelling code, LS-DYNA and ANSYS-FLUENT are dynamic codes. This means that the codes will handle the simulations in completely different ways.

7. Recommendations

7.1 Further study

- Numerically modelling of block erosion should involve both continuum and discontinuum methods. Software such LS-DYNA (a continuum code) with dynamic fluid simulation capabilities can be used to investigate the mechanical response of a rock block in an open channel that is subject to a cycle of dynamic water loads.
- 3DEC has the capability to perform a fully couple ‘hydro-mechanic-dynamic’ simulation. The study herein did not fully utilize the depth of this capability. It is recommended to pursue this possibility in the future. However, it would require data from pressure-time measurements during actual floods and extensive model calibration for the damping factors. Since water is also a damping medium not all the energy will be transferred to the bedrock and therefore the damping factor must be properly established.
- Block size is a function of block forming joints. With displacements exceeding 10 m within 1 to 10 minutes, as shown in the 3DEC simulations, block sizes of up to 1 m³ can be easily dislodged and transported downstream. These smaller blocks can be thought of as key blocks. If they are released the potential for larger blocks to be fractured and released increases. Remedial measures should look at ways to keep these ‘key blocks’ intact, including buttressing the critical mass with concrete slaps, particularly in areas where the velocity and water pressure are the highest.
- Discharge tunnels were not investigated in this study, even though the original proposal encompassed them as part of the project. The rock mass data collected from this study can be directly applied to investigate the erosion potential of the discharge tunnels. As per the law of the wall, the shear force will contribute significantly to dislodging a rock block if it is favourably oriented in the direction of flow. Pulsating pressure must be applied if it can be done.

7.2 Remedial measures

The remedial measures downstream will also depend on way the dams discharge their water. Dam 1 discharges water from the base of the dam, while Dam 2 discharges water over concrete aprons from the top. Both methods use different techniques to reduce energy in the water, nevertheless, is still very high during the flow and is enough to cause erosion of the rock mass in the channel. Remedial measures have been observed at the dam sites. Understanding the erosion mechanisms are important in order utilize that the most appropriate remedial measures to counter block erosion based on erosion mechanisms at work. Listed here are some of the potential remedial measures.

- Numerical modelling shows that the rock mass experiences an immense shock pressure, leading the rock mass to experience displacements in the order of tens of meters within 1 or 2 minutes of flow. Methods to prevent that these shock pressures and dissipate energy include, hydraulic jumps, stilling basins, plunge pools and water breakers. These are observed in many of the spillways.

- The slabby rock blocks near the spillway gates at Dam 1 are particularly susceptible for erosion. Cementing the initial section of the spillway may prevent direct shock pressure on the rock slabs. Or anchoring the slabs by bolting will give additional strength of the slabs. Furthermore, the manner in which water is discharged and amount of discharge may reduce erosion of the shallow dipping granite slabs.
- Anchoring of the rock blocks have been observed at Dam 1 to pin the blocky rock mass together. However, if the water pressure is too high the blocks would be fractured, as in the case of rock slabs observed at Dam 1. Fortunately, in Sweden, majority of the spillway channels comprise very hard rock, and therefore the fracturing process takes time and occurs in the form of fatigue.
- Levelling out the channel floor to allow an even flow will reduce the shear velocity and stagnation pressure, and thus provide stability to the rock mass. Levelling of spillway channels have been observed both at Dam 1 and Dam 2. At Dam 1 the widening of the channel seems to provide an even channel floor and thus reduce flow velocity.
- Water-column height has significant impact on rock mass displacement. The 3DEC models of single blocks show that, water columns of 1 to 2 m are optimum, however, it also depends on average block sizes. Above the optimum water column height, the pore pressure increases leading to high lift pressure, thus increase of block erosion. Below the optimum water column heights, the shear stress increases. Therefore, maintaining an optimum water column height is an important measure to reduce rock erosion.
- According to the numerical modelling the slope of the channel is a critical parameter. Both dams investigated have slope gradients that are between 3 to 5°. Channel slopes greater than 10° are seen to experience significant displacements (as per the numerical model results). Areas of the channels with steep angles must be reduced to maintain gentle slopes (less than 10°).
- The pressure developed in the rock fracture apertures are critically high when high pressure compresses the joints, causing pulsating pressures as the joint opens and closes momentarily. The phenomenon is the cause of fractures in the rock block. The waters pressures can be reduced by introducing water breakers. Slabs of concrete, anchored to the channel floor were observed at another dam site, which reduces water velocity and pressure. At Dam 2, large rock blocks located close to the plunge pool appears to break up the energy in the water.
- Plucking mechanism, where a block of rock is plucked from the groove, can be prevented through rock bolting. This particularly important in areas where pore pressure is the highest, leading to the block being forced out of the groove. If this block being plucked is a 'key block' then it will cause the rest of the blocks around it to be destabilised.
- Block sizes are critical to erosion. Smaller blocks (up to 1 m³) are easily removed and transported by the flood. At Dam 1 for example, there is a fractured zone that runs diagonally near the spillway gates to west side of the channel. The blocks in this fractured zone are smaller than 0.5 m³ in sizes. These blocks are noted to be subject to rapid erosion, leading to the fractured zone become a narrow diversion channel. Securing these smaller

blocks are difficult, however, concrete slaps can be anchored along areas like this to reinforce the smaller blocks.

- Creating channel domains according to erosion characteristic is necessary for identification of remedial measures. Upstream end of spillway channels is the most prone to erosion. Characteristics of block erosion are to be observed and evaluated to assist identifying remedial measures.

7.3 In-situ measurement of pore pressures and block displacements

During this study the LTU team also investigated the possibility to instrument rock blocks in the spillway channel to measure the hydraulic pressures and displacements in a jointed rock block. However, it was abandoned due to the complexity of the instrumentation and limitations in time and budget. Nevertheless, the field investigation is recommended.

George (2015) carried out such in-situ measurements as shown in Figure 90 and Figure 91. The pressure and displacements would measure the pressures around the block. Such measurements can be used to develop models, such as the single block 3DEC model performed in this study, to analysis the interaction between hydraulic parameters and the mechanical response of the block.

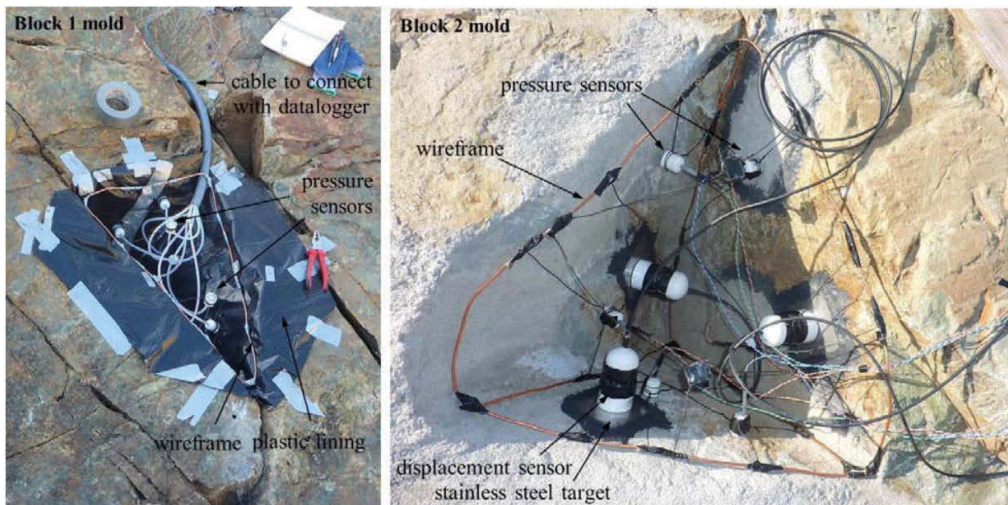


Figure 90. Installation of pressure and displacement sensors to investigate pressure and displacement around block during spillway discharge (George 2015).

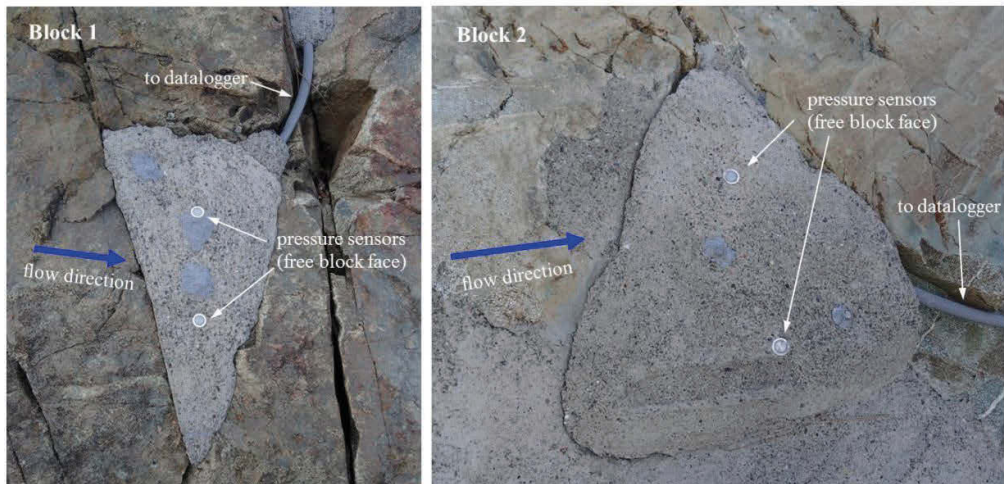


Figure 91. The instrumented block ready for measurements when water is released from the dam (George 2015).

7.4 Physical model to study block erosion

A physical model could be constructed to specifically study block erosion. The in-situ study presented above can also be conducted with a physical model, to measure water pressures, displacements, and velocities around rock blocks. The physical model test can be conducted in a controlled environment where instruments will not be easily damaged or destroyed. Several parameters can be investigated including:

- Impact of aperture sizes on hydraulic pressures and block displacement,
- Block size and shape determines how it responds to hydraulic parameters, and
- Block orientation with respect to flow.

Acoustic instrumentation can be used to study strain changes within rock block during sustain hydraulic pressure. This may help to see how fracturing initiates under sustained hydraulic pressure.

7.5 Investigation of fracture apertures

The aperture of the fractures needs special description for further investigation. It is quite clear that the aperture is an important physical parameter that controls the interaction between the hydraulic and mechanical parameters, leading to rock erosion in the spillway canals. The apertures in the spillway channels were observed to have specific characteristics. They range from less than 1 mm to well over 50 mm. They are widely open on the surface but regressively decrease into the rock. Furthermore, they are more open when facing the flow direction. The amount of water that enters the fractures will depend heavily on the apertures and their characteristics. The current study reveals that, a full-scale study is necessary to map the apertures in the spillway channels. This could include diamond drilling along the apertures to observe how they vary into the rock (Figure

92). A rebound test, using Schmidt hammer, can be used to establish strength variation along length of the aperture. This would assist in observing how fatigue, induced by pored pressures, reduces the strength of the rock and eventually forces it to fracture.

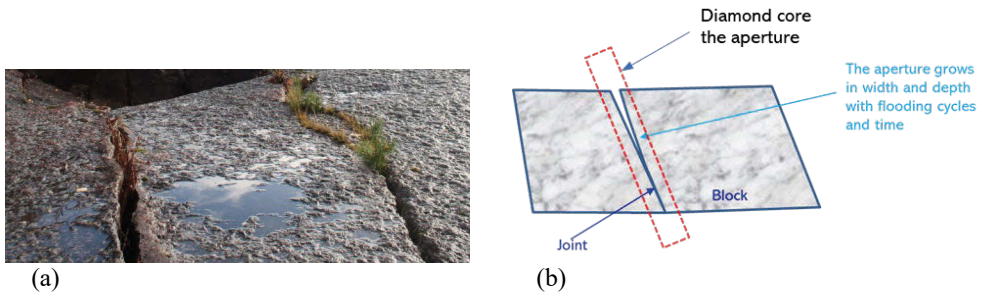


Figure 92. (a) Fracture aperture observed in spillway canals observed, (b) sketch of the aperture characteristics in a vertical section with suggestion for diamond coring for investigation.

ACKNOWLEDGEMENT

A number of people need acknowledgement.

- Sofi Bryggman and Vattenfall staff facilitated the site visit and field investigation of Dam 1.
- Carl-Oscar Nilson at Uniper facilitated the site visit and investigation of Dam 2.
- Mats Billstein at Älvkarleby facilitated the visit to the hydropower dam research facility.
- Tobias Bauer and Joel Anderson at Division of Earth Sciences and Environmental Technology at Luleå University of Technology, who flew drone to acquire the data for both dam spillways and did the initial data analyses, as well as providing continuous consultations.
- Jonas Persson of Norconsult AB was consulted during the field work campaign at Dam 2.
- Itasca Consultants AB did 3DEC modelling of Dam 1 spillway.
- SRK Consulting Oy, did drone data analyses as well as block size distribution analyses.
- Hans Åhlin at the Division of Mining and Geotechnical Engineering is acknowledged for running a few simulations using LS-DYNA to test the codes fluid dynamics capabilities.

Reference group members; Per Tengborg (BeFo), Anders Isander (Uniper), Peter Viklander (Vattenfall), Eva Hakami (Geosigma) and Fredrik Johansson (KTH).

Financial support was provided by BeFo and Energiforsk.

8. REFERENCES

- Akan, A. O. 2011. Open channel hydraulics. Elsevier.
- Akhmedov, T. K. 1988. "Calculation of the depth of scour in rock downstream of a spillway." *International Water Power & Dam Construction*, 40 (12), 25-27.
- Andersson, A. G., Hellström, J. G. I., Andreasson, P., Lundström, T. S. 2014. "Effect of spatial resolution of rough surfaces on numerically computed flow fields with application to hydraulic engineering." *Engineering Applications of Computational Fluid Mechanics*, 8 (3), 373-381.
- Andersson, L. R., Larsson, I. A. S., Hellström, J. G. I., Andreasson, P., Andersson, A. G. 2016. "Experimental Study of Head Loss over Laser scanned Rock Tunnel." In *B. Crookston & B. Tullis (Eds.), Hydraulic Structures and Water System Management. 6th IAHR International Symposium on Hydraulic Structures*, Portland, OR, 27-30 June (pp. 22-29).
- Andersson, L. R., Andersson, A. G., Andreasson, P., Hellström, J. G. I., Lundström, T. S. 2014. "Grade of geometric resolution of a rough surface required for accurate prediction of pressure and velocities in water tunnels." *Abstract of European Fluid Mechanics Conference*, Copenhagen, Denmark.
- Andersson, A. G., Andreasson, P., Hellström, J. G. I., Lundström, T. S. 2012. "Modelling and validation of flow over a wall with large surface roughness." *Abstract of European Fluid Mechanics Conference*, Rome, Italy.
- Andersson, A. G. 2013. "Modelling flow with free and rough surfaces in the vicinity of hydropower plants." *Doctoral Thesis Luleå University of Technology*. ISBN 978-91-7439-672-0
- Annandale, G. W. 2005. Scour Technology: Mechanics and Engineering Practice. New York: McGraw-Hill
- Annandale, G. W. 1995. "Erodibility." *Journal of Hydraulic Research*, 33(4), 471-494.
- Barton, N., Lien, R., & Lunde, J. 1974. "Engineering classification of rock masses for the design of tunnel support." *Rock Mechanics*, 6(4), 189-236.
- Bauer, T. and Anderson, J. Division of Exploration Geology, Luleå University of Technology, personal communication.
- Billstein, M. 2002. "Model tests Midskog power station, 2002 - adapting to the new design flows," *Report to SwedPower AB, Report number U02:52*, Waterfall Development Inc., Älvkarleby.
- Billstein, M., Carlsson, A., Johansson, N., Söder, P. E., & Lorig, L. 2003. "Midskog physical and numerical modelling." *International Water Power & Dam Construction*, 55(12), 22-26.
- Bollaert, E. 2002. "Transient water pressures in joints and formation of rock scour due to high velocity jet impact." *Communication No. 13 Laboratory of Hydraulic constructions*, Ecole Polytechnique Federale de Lausanne, Switzerland.
- Cameron, C. P., Cato, K. D., McAneny, C. C., & May, J. H. 1986. "Geotechnical aspects of rock erosion in emergency spillway channels." *Department of the Army, Waterways Experiment*

Station, Corps of Engineers, Geotechnical Laboratory.

- Chow, V.T. 1959. Open-channel hydraulics. McGraw-Hill Book Co., New York, NY.
- Dasgupta, B., Basu, D., Das, K. and Green, R. 2011. "Development of computational methodology to assess erosion damage in dam spillways." *Proc. of the 31st USSD Annual Meeting and Conf.*, San Diego, CA, April 11-15.
- Flödeskommittén. 1990. "Riktlinjer för bestämning av dimensionerande flöden för dammanläggningar," *Statens Vattenkraftverk, Svenska Kraftverksföreningen, Sveriges Meteorologiska och Hydrologiska Institut.* Stockholm.
- Frizell, K. W. 2007. "Uplift and crack flow resulting from high velocity discharges over open offset joints." *USBR Report DSO-07-07.*
- George, M. F. & N. Sitar. 2012. "Block theory application to scour assessment of unlined rock spillways." *Report No. UCB GT 12-02*, Department of Geotechnical Engineering, UC Berkeley.
- George, M. F., & Sitar, N. 2012. "Evaluation of rock scour using block theory." *In Proceedings of the 5th International Conference on Scour and Erosion (ICSE)*, Paris, France, November.
- George, M. F. 2015. "3D block erodibility: dynamics of rock-water interaction in rock scour." *Doctoral Dissertation*, UC Berkeley.
- George, M. F., Sitar, N., & Sklar, L. 2015. "Experimental evaluation of rock erosion in spillway channels." *In 49th US Rock Mechanics/Geomechanics Symposium.* American Rock Mechanics Association.
- Goodman, R. E., and Shi, G. 1985. "Block Theory and Its Application to Rock Engineering." Prentice Hall. Englewood Cliffs, N.J.
- Henderson, F.M. 1966. "Open Channel Flow." Prentice Hall. Upper Saddle River, N.J.
- Hoek, E., Kaiser, P. K., & Bawden, W. F. 2000. Support of underground excavations in hard rock. CRC Press.
- Itasca. 2019. 3DEC v.7.0
- Itasca. 2020. 3DEC v.7.0 manual. Citation link.
<http://docs.itascacg.com/3dec700/3dec/docproject/source/3dechome.html>
- Julien, Y. Pierrie. 2008. Flood Hydraulic. Lecture presentations. Colorado State University.
https://www.engr.colostate.edu/~pierre/ce_old/classes/ce717/PPT%202014/Flood%20Hydraulics-Presentation.pdf
- Karlsson, J. 2013. Kartering av erosionskador Storfinnforsen (Sweco). Internal Consulting Report.
- Kirsten, H.A.D. 1982. "Classification system for excavation in natural materials." *Civil Engineer in South Africa*, 24(7): 293–308.
- Kirsten, H.A.D. 1988. "Case histories of groundmass characterization for excavatability." *In Rock Classification Systems for Engineering Purposes*, ASTM, STP 984, L. Kirkaldie, (Ed). Pp. 102 – 120.

- Li, K. W., Pan, Y. W., & Liao, J. J. 2016. "A comprehensive mechanics-based model to describe bedrock river erosion by plucking in a jointed rock mass." *Environmental Earth Sciences*, 75(6), 517.
- Lindblom, J. 2020. "Uniform, non-uniform flows & energy dissipation." G7004b Lecture notes. Division of Mining & Geotechnical Engineering, Luleå University of Technology.
- Marinos, P., & Hoek, E. 2000. "GSI: a geologically friendly tool for rock mass strength estimation." *In ISRM international symposium*. International Society for Rock Mechanics and Rock Engineering.
- Mörén, L. 2005. "Rock Scour in Spillway Channel". *MSc Thesis*. Department of Earth Sciences, Uppsala University, Sweden. 91 pages.
- Mörén, L., & Sjöberg, J. 2007. "Rock erosion in spillway channels—A case study of the Ligga spillway." *In Proceedings of 11th Congress of the International Society for Rock Mechanics*, Lisbon, Portugal (pp. 87-90).
- Norconsult AB. 2016. Documentation of stability calculations for Storfinnforsen and Ramsele hydropower dam spillways. Report #1040471.
- Pan, Y. W., Li, K. W., & Liao, J. J. 2014. "Mechanics and response of a surface rock block subjected to pressure fluctuations: A plucking model and its application." *Engineering geology*, 171, 1-10.
- Pells, S. E. 2016. "Erosion of rock in spillways." *Doctoral dissertation*, University of New South Wales.
- Pells S., Douglas K., Pells P., Fell R., Peirson W. 2017. "Rock mass erodibility." *Journal of Hydraulic Engineering*, 143(5).
- Pitsiou, S. 1990. "The effect of discontinuities on the erodibility of rock in unlined spillways of dams." *Msc Thesis*, University of Pretoria.
- Reinius, E. 1986. "Rock erosion." *International Water Power & Dam Construction*, 38(6), 43-48.
- Richardson, K., & Carling, P. 2005. "A typology of sculpted forms in open bedrock channels." *Geological Society of America*, 39(2).
- Sklar, L. S., & Dietrich, W. E. 2004. "A mechanistic model for river incision into bedrock by saltating bed load." *Water Resources Research*, 40(6).
- Stephansson, O. 1993. "Rock stresses in the Fennoscandian shield." *In Comprehensive Rock Engineering*, J.A. Hudson, Editor. Pergamon Press. P. 445-459.
- Swedish Geology Survey (<https://www.sgu.se>)
- USACE Hydrologic Engineering Centre. 2016. HEC-RAS River Analysis System Hydraulic Reference Manual," computer program documentation Version 4.1, USACE, Hydrologic Engineering Center.
- Whipple, K. X., Hancock, G. S., & Anderson, R. S. 2000. "River incision into bedrock: Mechanics and relative efficacy of plucking, abrasion, and cavitation." *Geological Society of America Bulletin*, 112(3), 490-503.

- Wibowo, J. L., and J. S. Lin. 2009. "Stability Analysis of Spillways: Toward a Computational Approach." Power point presentation.
- Woodward, R. C. 1985. "Geological factors in spillway terminal structure design." *Engineering Geology*, 22(1), 61-70.
- Woodward, R.C. 1992. "The geology of dam spillway." *Engineering Geology*, 32, 243 - 254
- Wyllie, D.C. 1999. *Foundations on Rock*. 2nd Ed., E & FN SPON, London.
- Yang, J., Andreasson, P., Teng, P., & Xie, Q. 2019. "The past and present of discharge capacity modelling for spillways—a Swedish perspective." *Fluids*, 4(1), 10.



Box 5501
SE-114 85 Stockholm

info@befoonline.org • www.befoonline.org
Visiting address: Storgatan 19, Stockholm

ISSN 1104-1773